低速中性子を用いた原子核・素粒子物理

清　水　裕　彦

名古屋大学

理学研究科 素粒子宇宙物理学専攻 素粒子物性研究室(Φ研)

hirohiko.shimizu@nagoya-u.jp

1. Introduction
2. Lifetime
3. T-violation (CP-violation)
    EDM, n-A
4. Gravity
5. その他(B,B-L violation)

1. Introduction

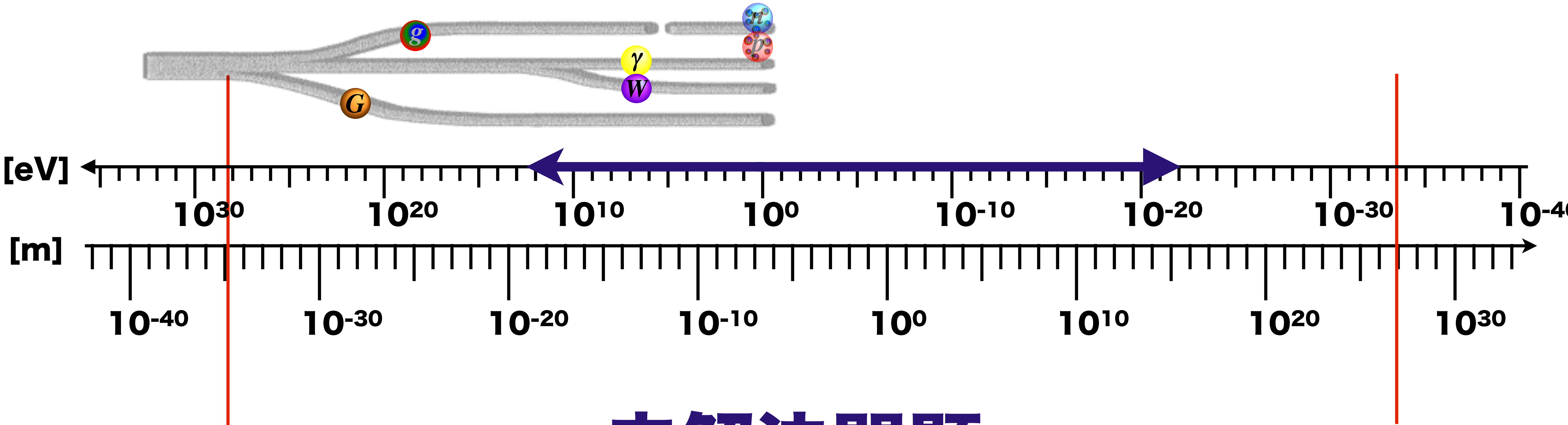

未解決問題

物質と反物質の間に対称性が成り立つのなら、この宇宙には、物質だけが観測されて、反物質がほとんど観測されないのは何故か？
Why do we observe matter and almost no antimatter if we believe there is a symmetry between the two in the universe?

暗黒物質の正体は何か？（暗黒エネルギーの正体は何か？）
What is this "dark matter" that we can't see that has visible gravitational effects in the cosmos?

素粒子標準模型が素粒子の質量を導けないのは何故か？
Why can't the Standard Model predict a particle's mass?

クォークやレプトンは”素”粒子なのか？（より基本的な粒子が存在するのか？）
Are quarks and leptons actually fundamental, or made up of even more fundamental particles?

クォークとレプトンの世代数が3である理由は何か？
Why are there exactly three generations of quarks and leptons?

重力相互作用は如何に説明されるのか？
How does gravity fit into all of this?

http://particleadventure.org/index.html

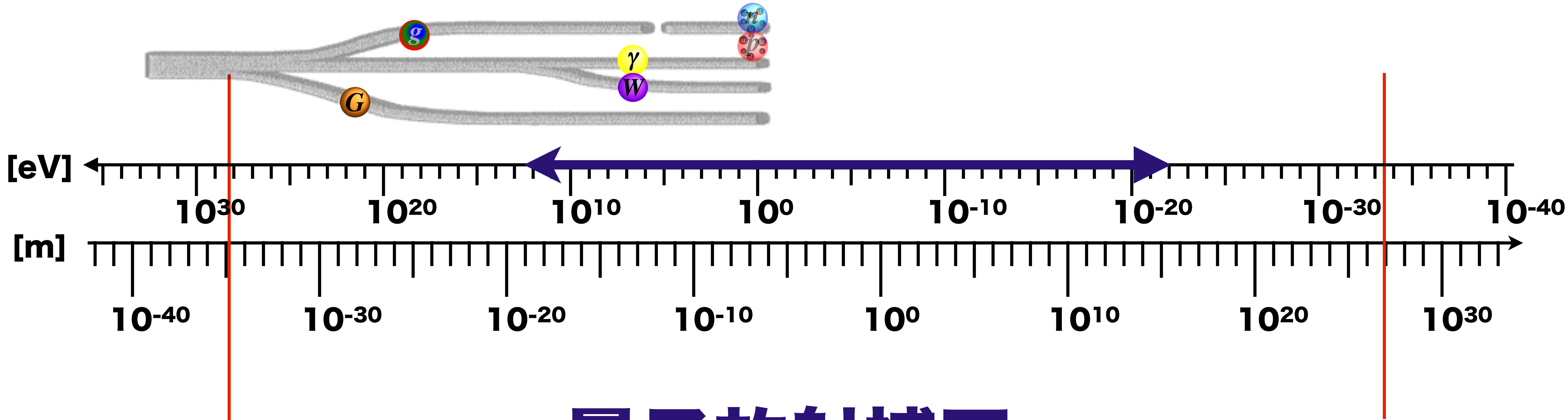

量子放射補正

$$\delta_{NEW} = \frac{\Delta O_{NEW}}{O}$$

$$\sim \frac{\alpha}{\pi}\left(\frac{M}{M'}\right)^2$$

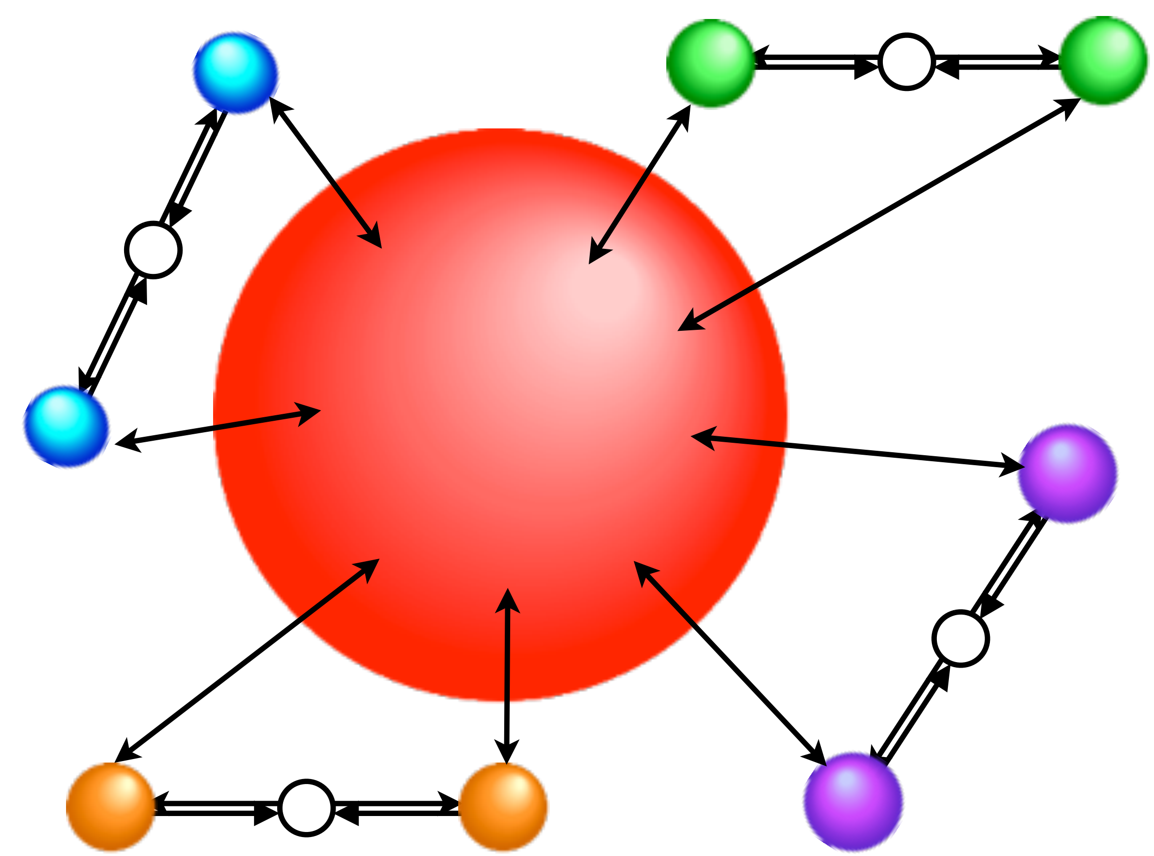

Oが正確に分かっていること

ΔO_{NEW}をいくつかの対象を比較すること

特にΔO_{NEW}が既存の枠組で禁止されているか強く抑制されている場合

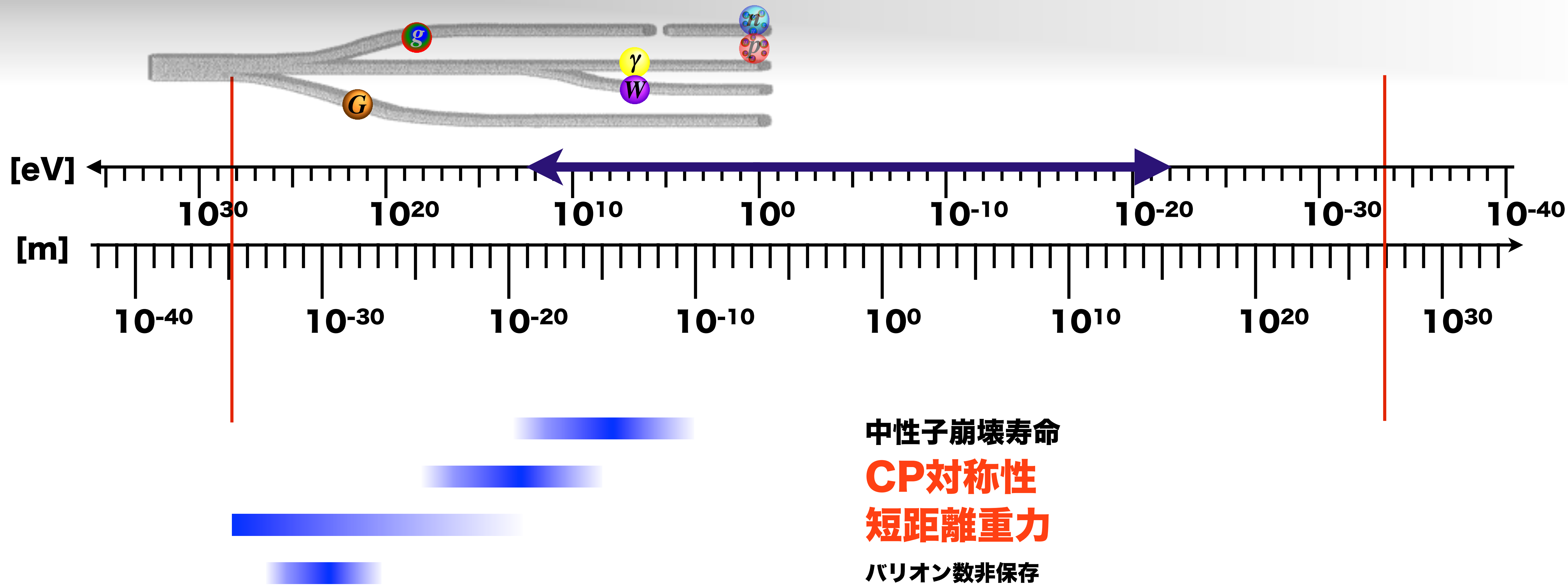

電荷を持たない　　光学的制御

量子放射補正項の精密測定

標準模型を超える新物理探索

低速中性子

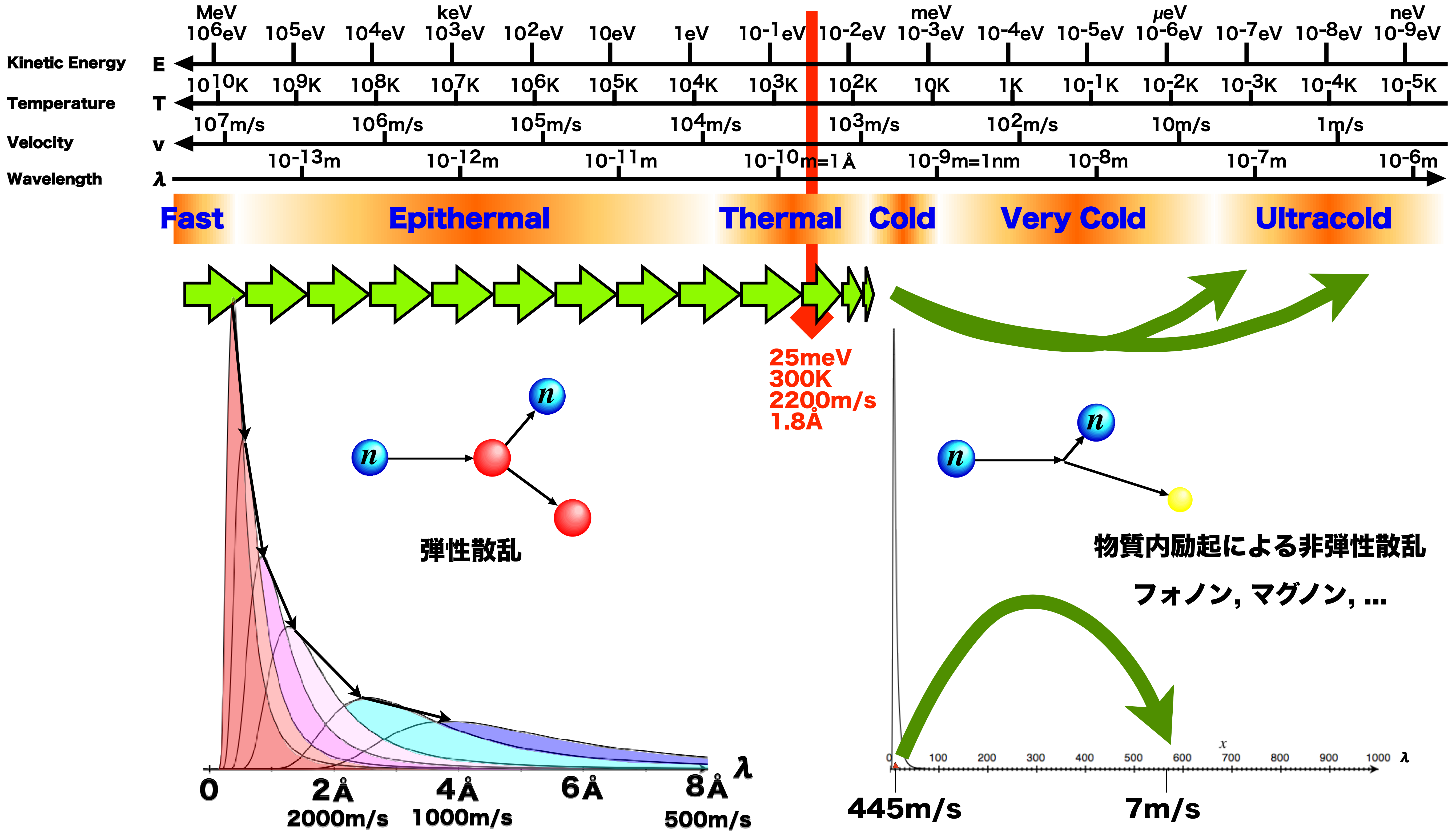

MeV keV meV μeV neV
10^6eV 10^5eV 10^4eV 10^3eV 10^2eV 10eV 1eV 10^{-1}eV 10^{-2}eV 10^{-3}eV 10^{-4}eV 10^{-5}eV 10^{-6}eV 10^{-7}eV 10^{-8}eV 10^{-9}eV
Kinetic Energy E
10^{10}K 10^9K 10^8K 10^7K 10^6K 10^5K 10^4K 10^3K 10^2K 10K 1K 10^{-1}K 10^{-2}K 10^{-3}K 10^{-4}K 10^{-5}K
Temperature T
10^7m/s 10^6m/s 10^5m/s 10^4m/s 10^3m/s 10^2m/s 10m/s 1m/s
Velocity v
10^{-13}m 10^{-12}m 10^{-11}m 10^{-10}m=1Å 10^{-9}m=1nm 10^{-8}m 10^{-7}m 10^{-6}m
Wavelength λ
Fast
Epithermal
Thermal
Cold
Very Cold
Ultracold
25meV
300K
2200m/s
1.8Å
n
弾性散乱
物質内励起による非弾性散乱
フォノン, マグノン, ...
λ
0
2Å
2000m/s
4Å
1000m/s
6Å
8Å
500m/s
100 200 300 400 500 600 700 800 900 1000
445m/s
7m/s

Neutron

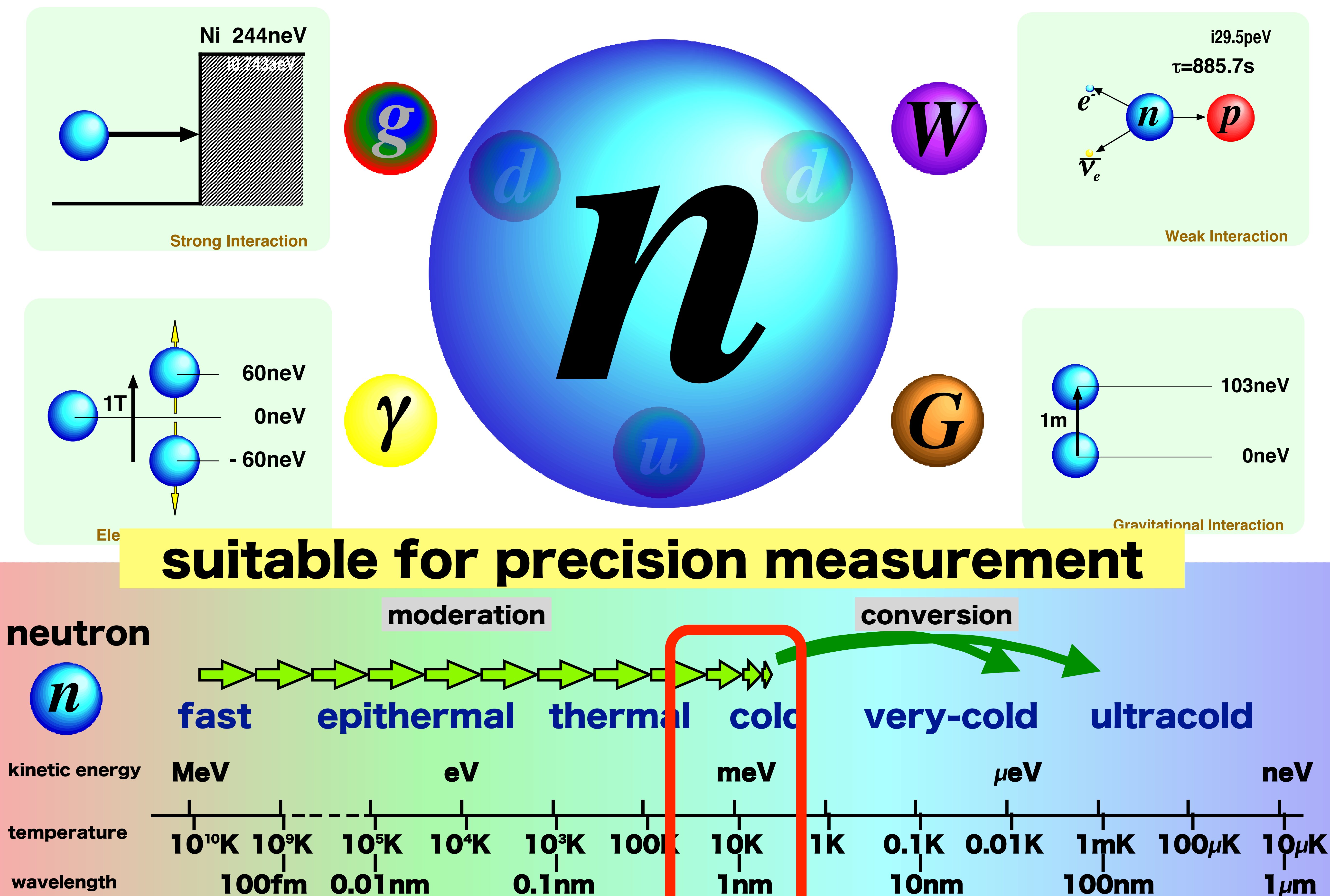

Ni 244neV
Strong Interaction
i29.5peV
τ=885.7s
e
n
p
$\bar{\nu}_e$
Weak Interaction
g
W
d
d
n
u
γ
G
60neV
1T
0neV
- 60neV
Ele
1m
103neV
0neV
Gravitational Interaction
suitable for precision measurement
moderation
conversion
neutron
n
fast
epithermal
thermal
cold
very-cold
ultracold
kinetic energy
MeV
eV
meV
μeV
neV
temperature
10¹⁰K
10⁹K
10⁵K
10⁴K
10³K
100K
10K
1K
0.1K
0.01K
1mK
100μK
10μK
wavelength
100fm
0.01nm
0.1nm
1nm
10nm
100nm
1μm

2. Lifetime

超冷中性子閉込め

Storage experiments with UCN

"counting the surviving neutrons"

"UCN bottle"

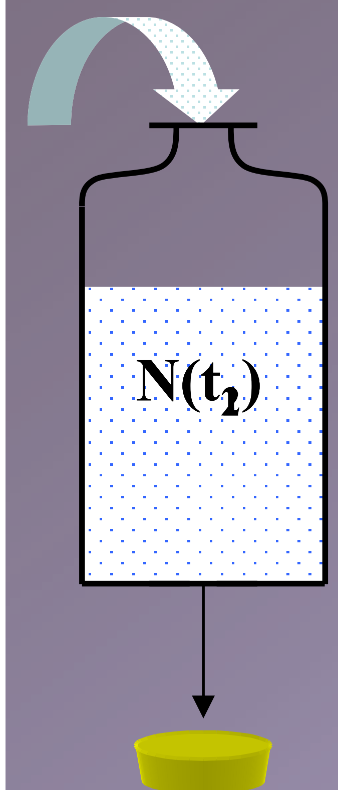

中性子数の減少

τ_m $t_2 - t_1$ $N(t_2)$

$$\frac{1}{\tau_m} = \frac{1}{\tau_B} + \frac{1}{\tau_{wall}} + \frac{1}{\tau_{leak}} + \frac{1}{\tau_{vacuum}} + \ldots$$

→ 0 (experiment)

$$\frac{1}{\tau_{wall}} = M \cdot V_{eff}$$ → 0 (extrapolation)

閉込めの不完全性の補正不定性

τ_m — τ_B

Two relative measurements

冷中性子ビーム

Beam experiments with cold neutrons

"counting the dead neutrons"

崩壊数/入射中性子数

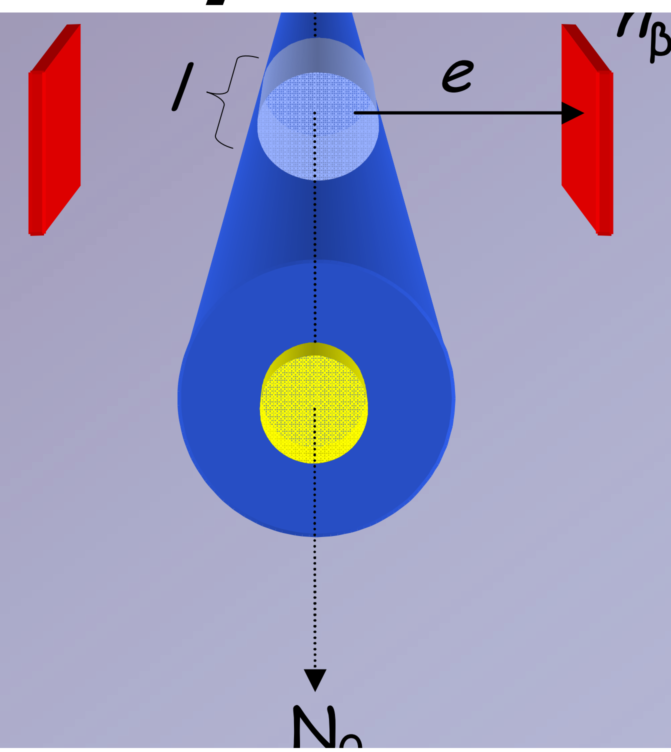

検出効率の較正不定性

$$n_B = \frac{dN}{dt} = -\frac{N_0}{\tau_n} e^{v \cdot \tau_n}$$

Two absolute measurements

Lifetime

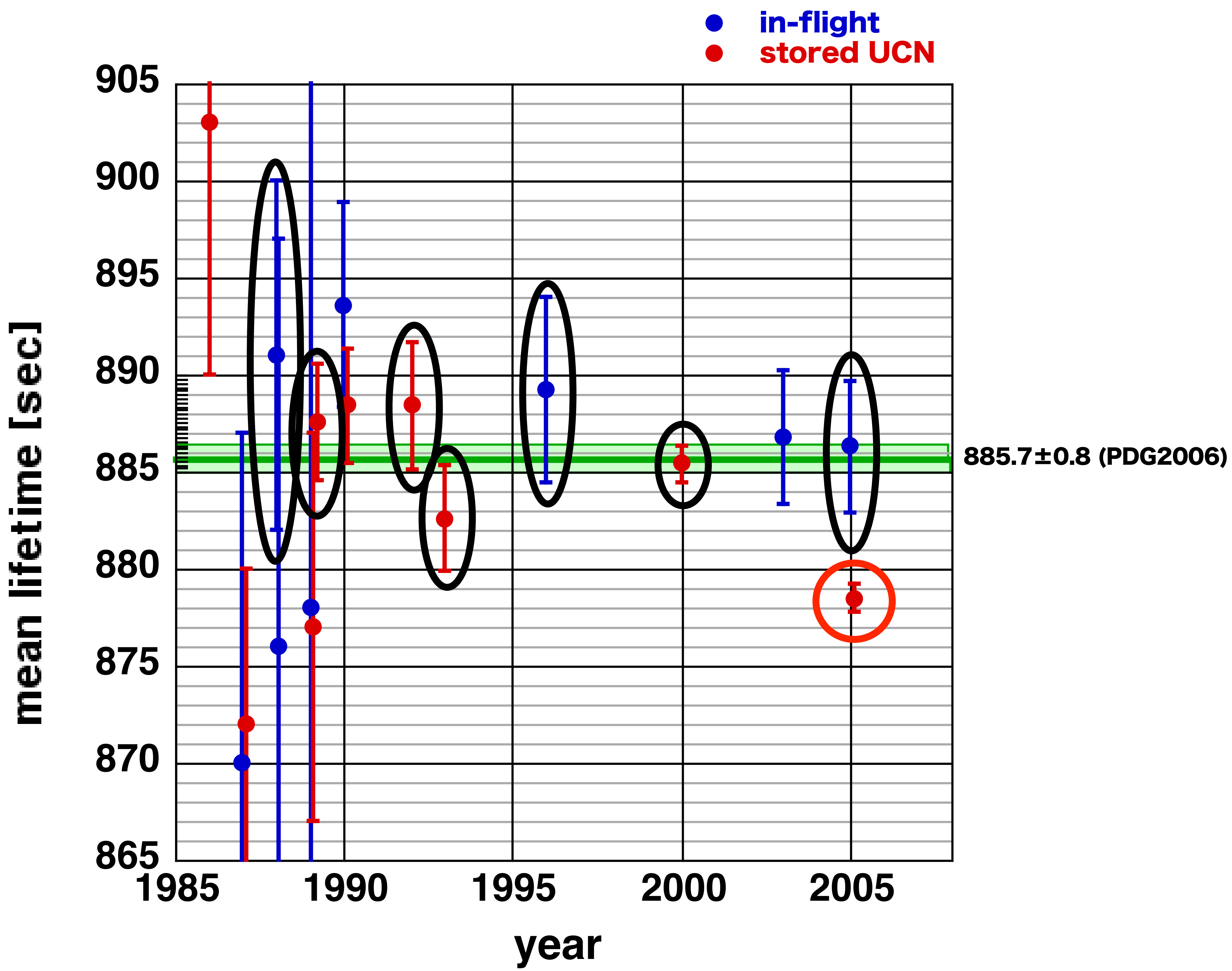
in-flight
stored UCN
905
900
895
890
885
880
875
870
865
1985
1990
1995
2000
2005
year
mean lifetime [sec]
885.7±0.8 (PDG2006)

Lifetime

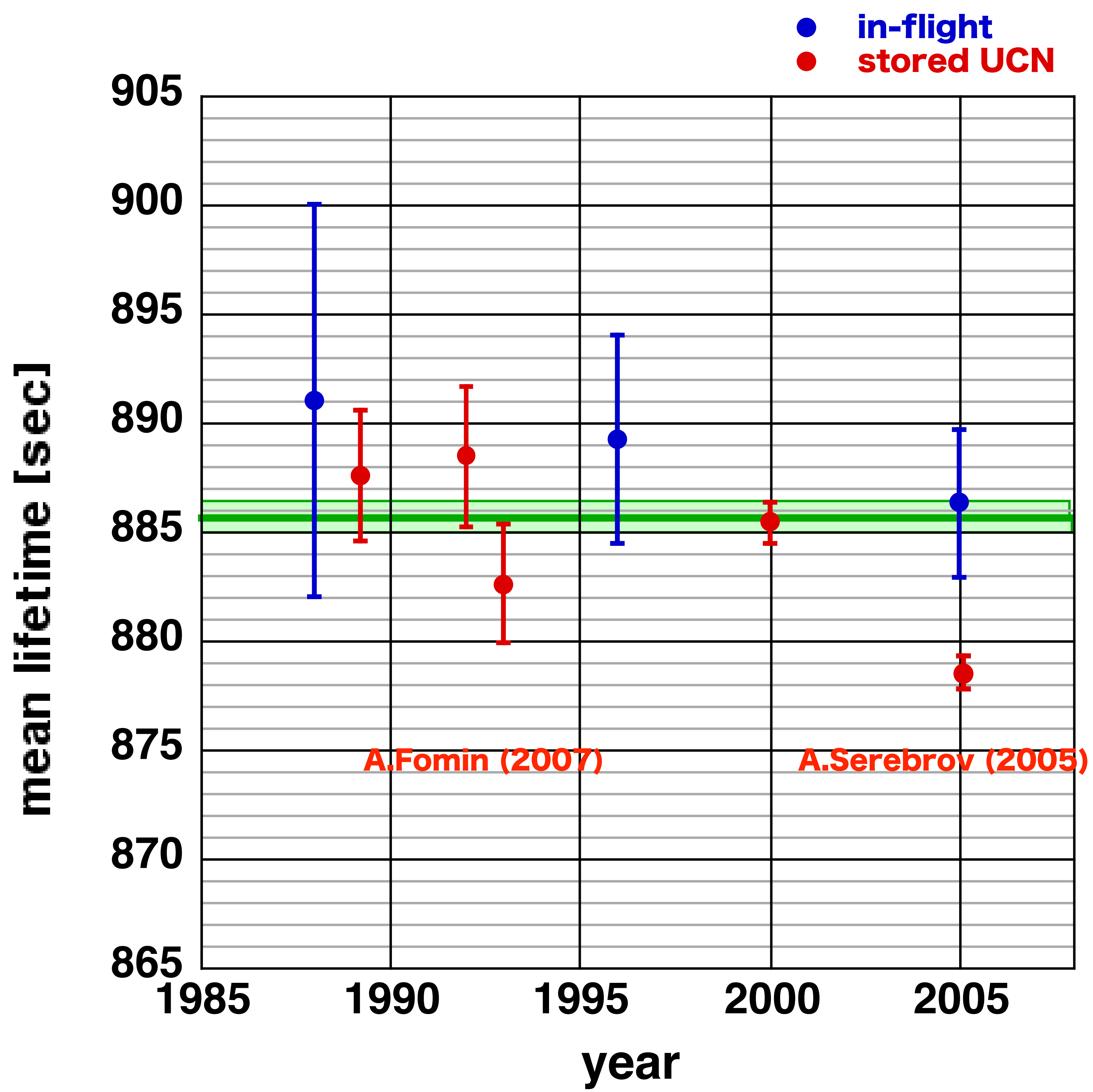

in-flight
stored UCN
905
900
895
890
885
880
875
870
865
mean lifetime [sec]
A.Fomin (2007)
A.Serebrov (2005)
1985
1990
1995
2000
2005
year

Lifetime

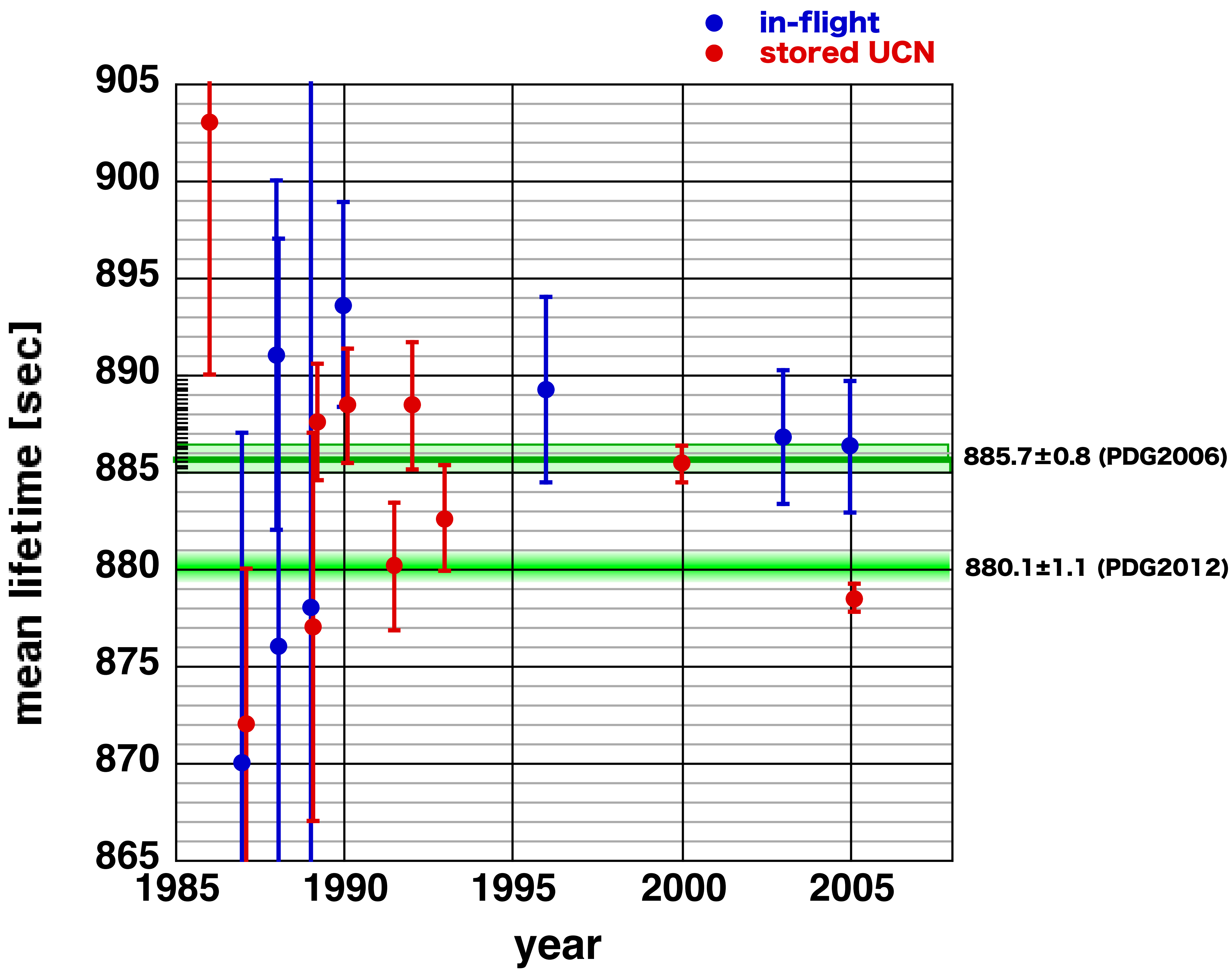

in-flight
stored UCN
905
900
895
890
885
880
875
870
865
mean lifetime [sec]
1985
1990
1995
2000
2005
year
885.7±0.8 (PDG2006)
880.1±1.1 (PDG2012)

Experiments for neutron lifetime

Method	Beam	Penning trap	Gravitational trap	Magnetic trap
Neutron source	reactor	reactor	reactor	reactor
Energy	Cold neutron	Cold neutron	UCN	UCN
Detection particle	**Electron**	Proton	Neutron	Neutron
Challenge	high background	flux monitor	wall effect	depolarization
Result	878 ± 27 ± 14 (1989)	886.6 ± 1.2 ± 3.2 (2005)	878.5 ± 0.7 ± 0.3 (2008)	878 ± 1.9 (2009)

Neutron lifetime is measured by in-beam and storage methods.
Our experiment is in-beam method.
We are using pulsed neutrons from separation neutron source.

We are trying for O(0.1%) with In−beam method.

単一の検出器

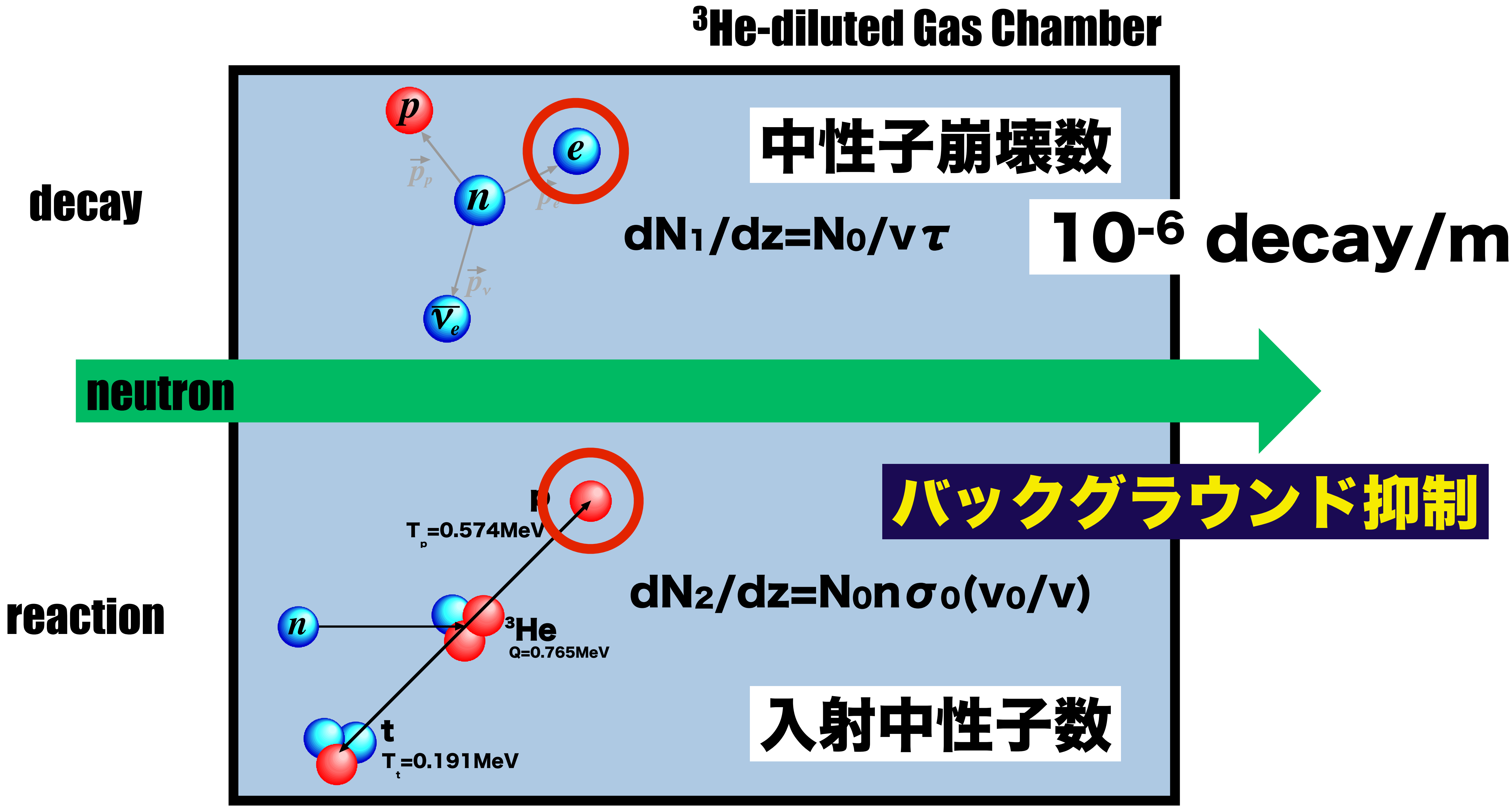

$$N_1/N_2=1/(\tau n \sigma_0 v_0)$$

Spin Flip Chopper

高周波印加で中性子スピンの向きを制御することで 中性子ビームを高速に振分け

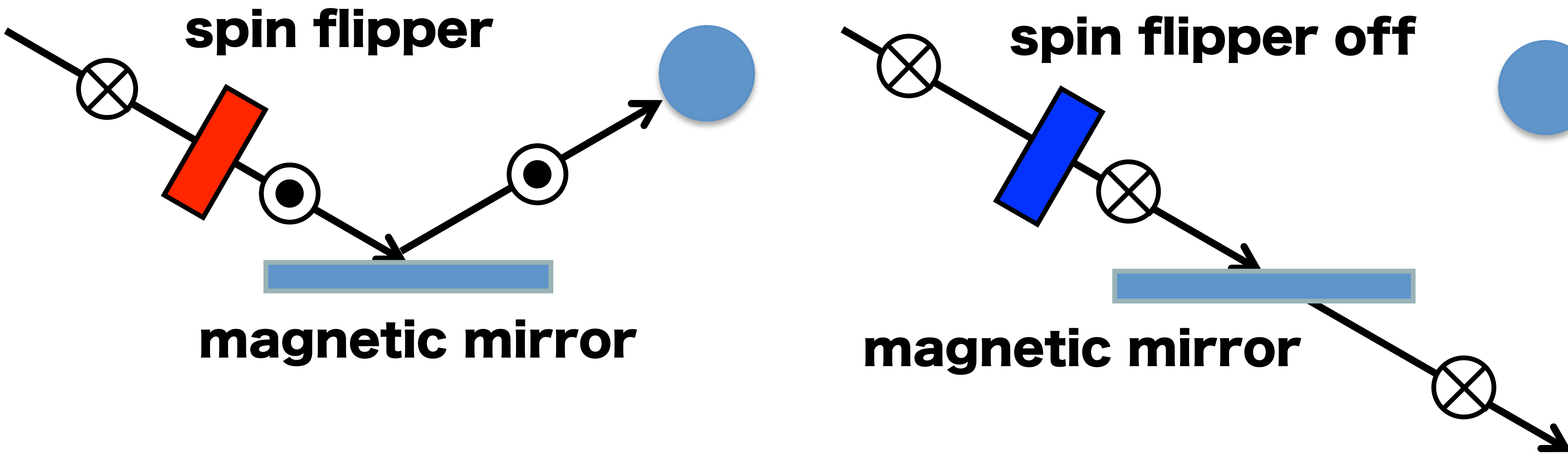

速度の揃った中性子ビームバンチを検出器に導く

中性子起因のバックグラウンドを抑制

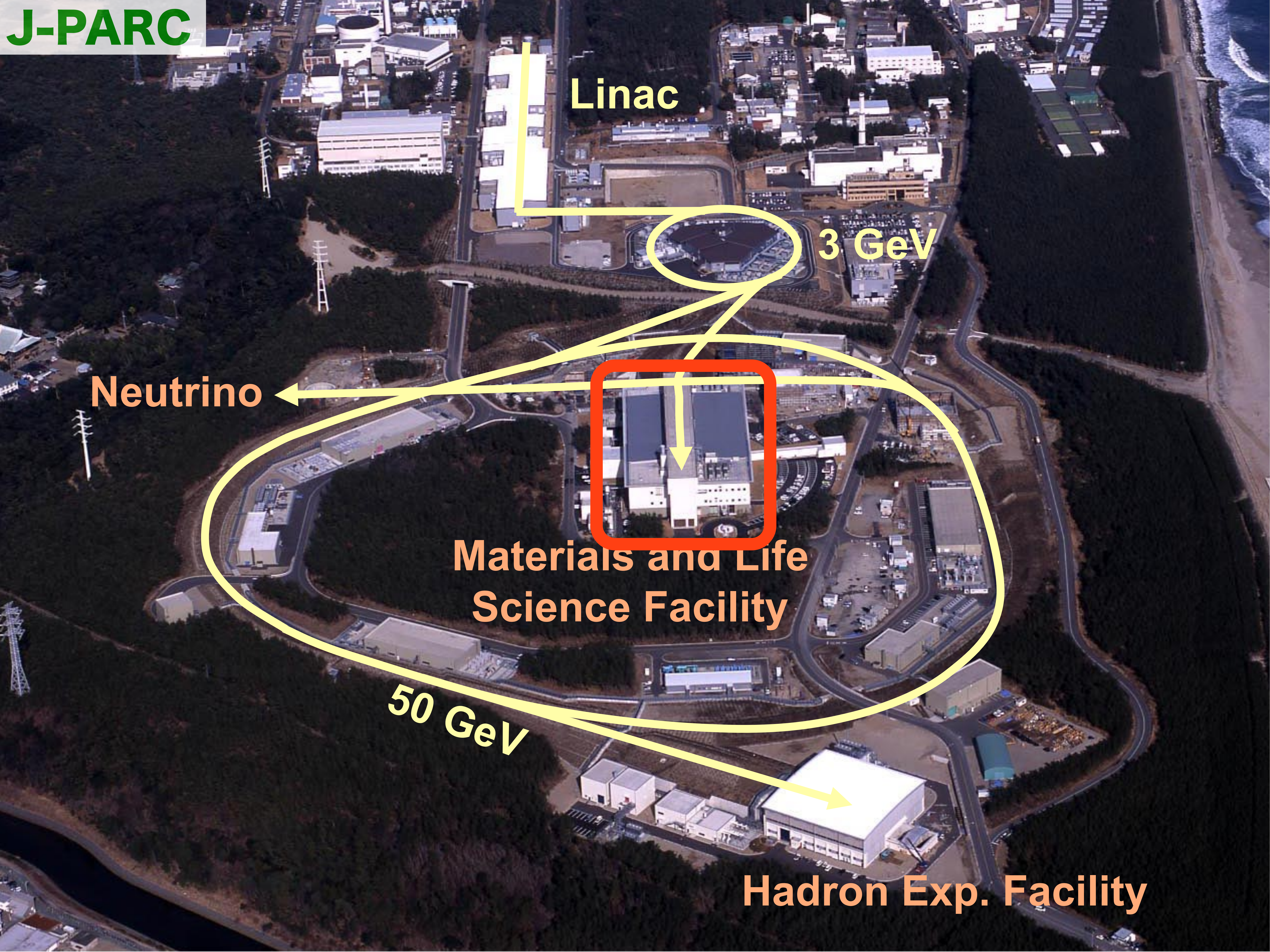
J-PARC
Linac
3 GeV
Neutrino
Materials and Life
Science Facility
50 GeV
Hadron Exp. Facility

J-PARC Pulsed Neutron source

BL05, Polarization beam branch

Repetition rate	25Hz
Moderator	Coupled （20 K）
Beam size	10 cm x 4 cm
Flux	8.6 x 10^6 s-1 cm-2 (1MW)
Polarization	96%
Energy	1 〜 20 meV
wavelength	0.2 〜 1 nm
Velocity	500 〜 2000 m/s

→ Experimental apparatus is installed at 20 m distance

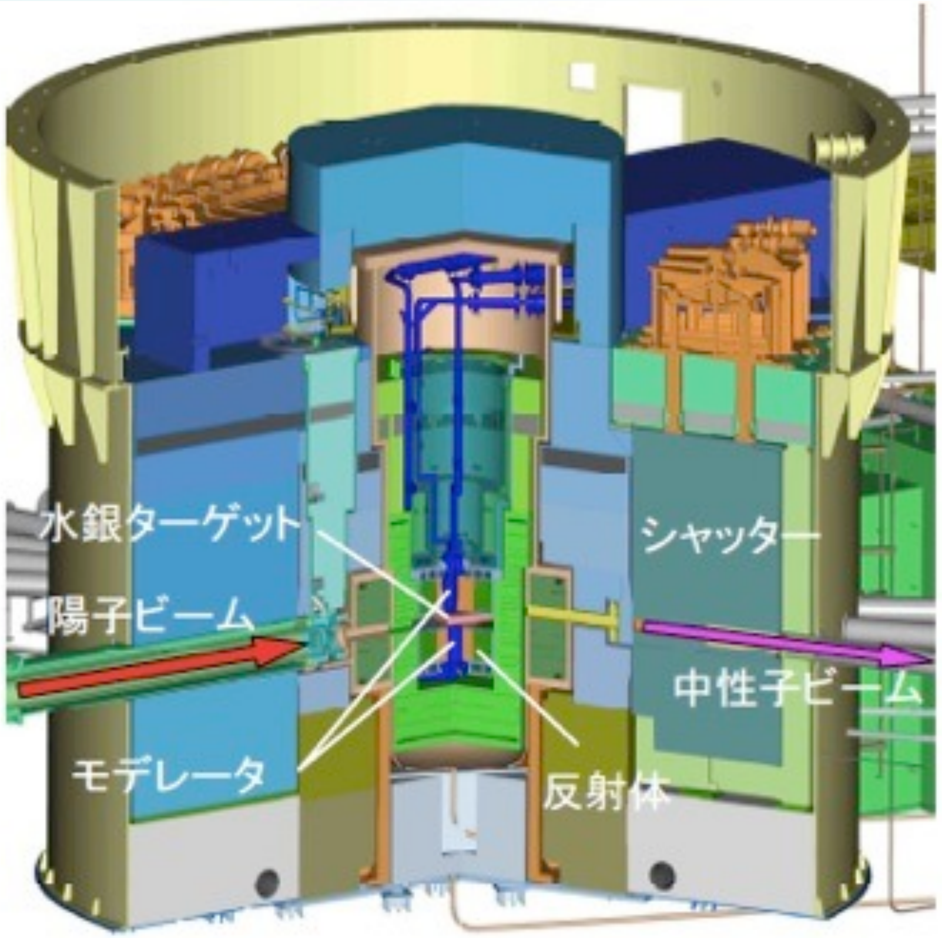

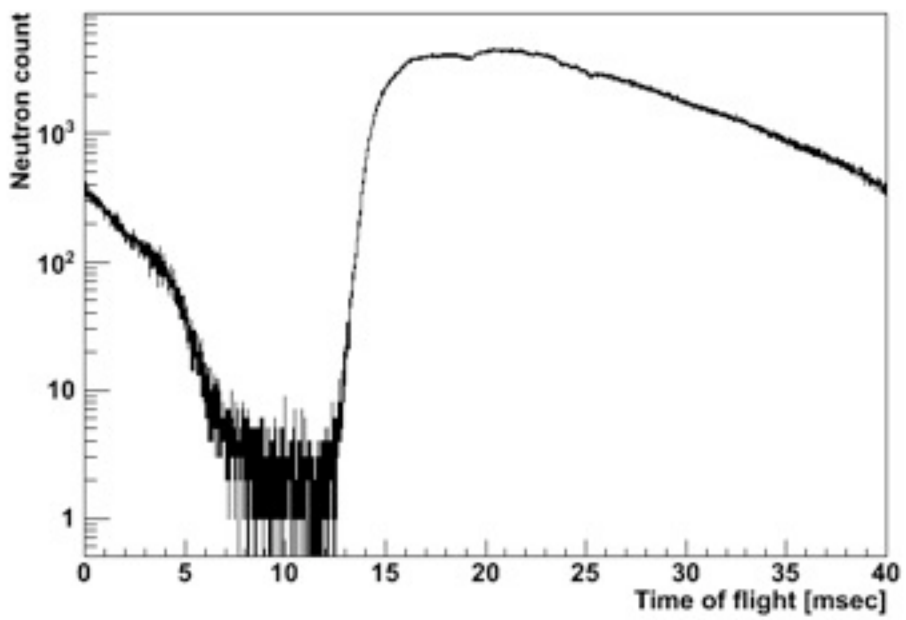

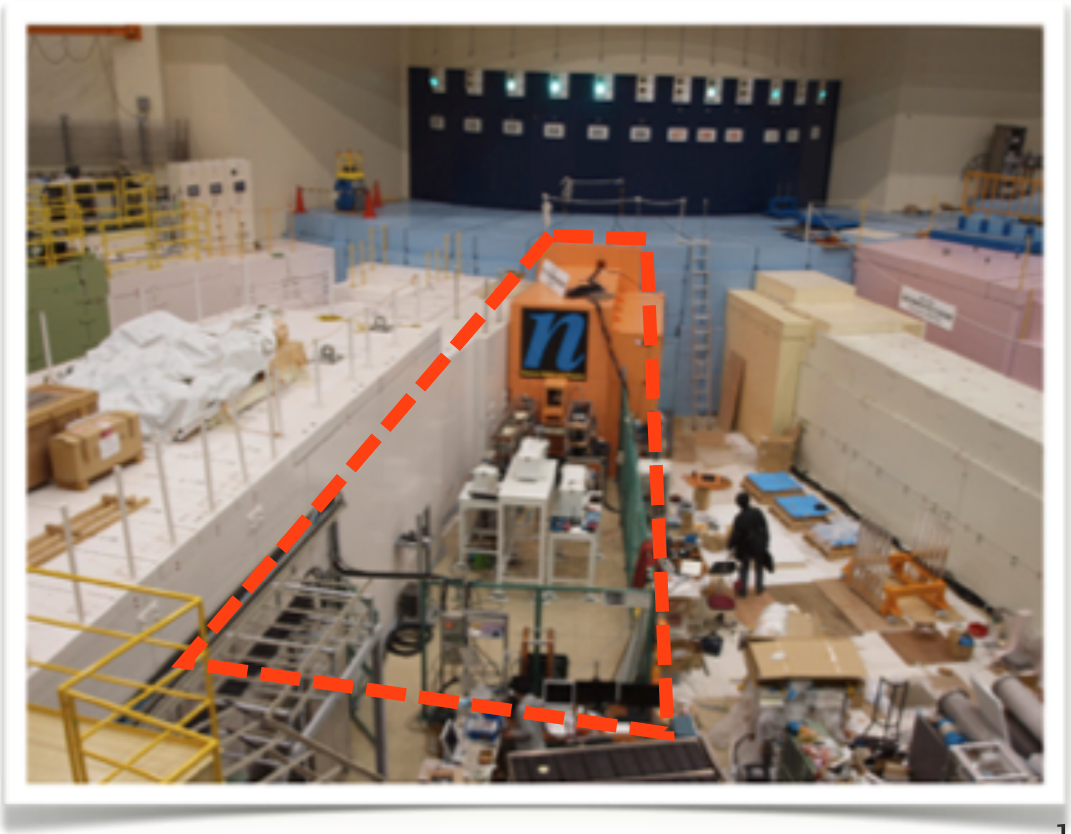

Supermirror Benders in Assembly

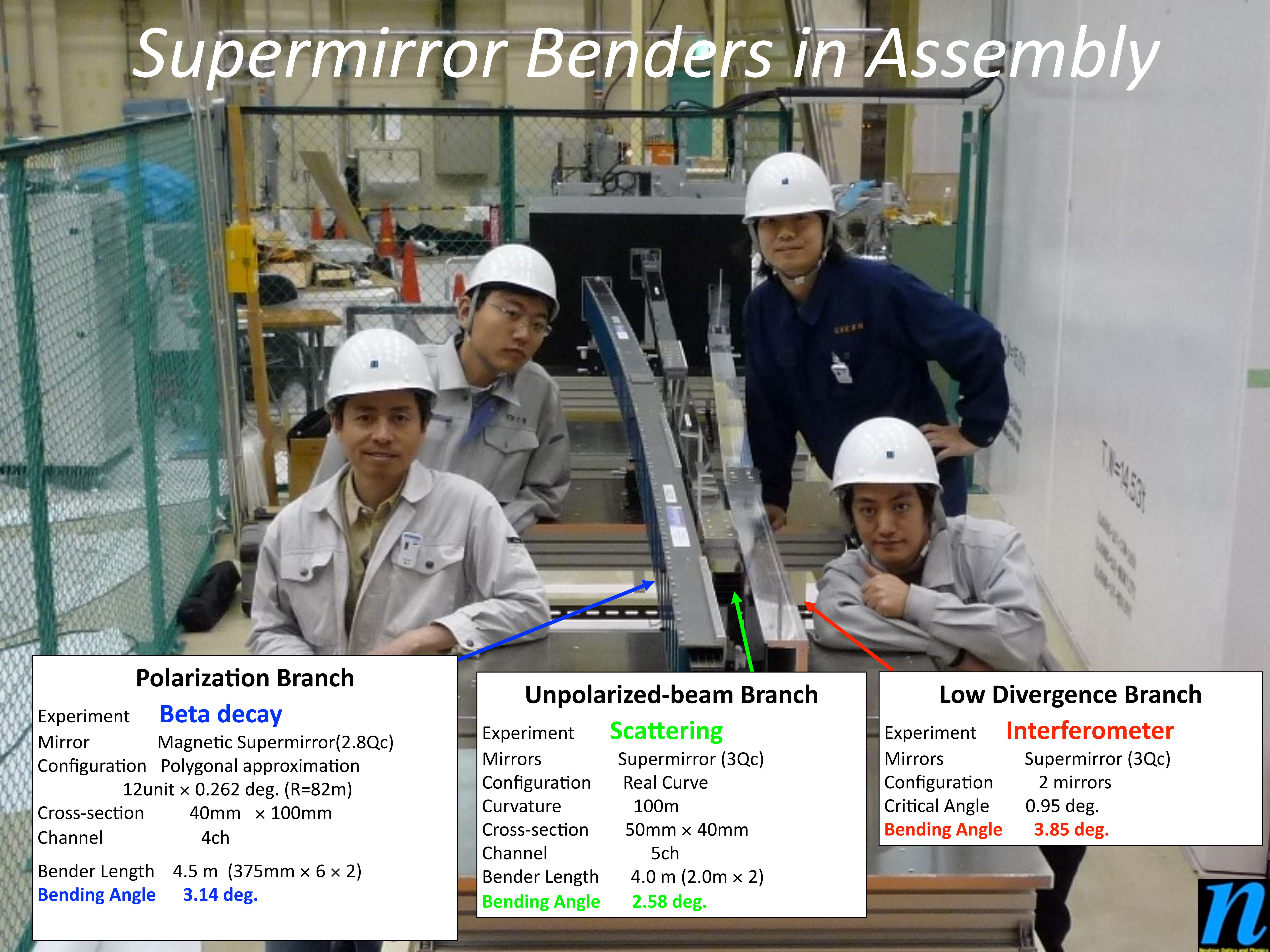

Polarization Branch

Experiment **Beta decay**
Mirror Magnetic Supermirror(2.8Qc)
Configuration Polygonal approximation
12unit × 0.262 deg. (R=82m)
Cross-section 40mm × 100mm
Channel 4ch

Bender Length 4.5 m (375mm × 6 × 2)
Bending Angle 3.14 deg.

Unpolarized-beam Branch

Experiment **Scattering**
Mirrors Supermirror (3Qc)
Configuration Real Curve
Curvature 100m
Cross-section 50mm × 40mm
Channel 5ch
Bender Length 4.0 m (2.0m × 2)
Bending Angle 2.58 deg.

Low Divergence Branch

Experiment **Interferometer**
Mirrors Supermirror (3Qc)
Configuration 2 mirrors
Critical Angle 0.95 deg.
Bending Angle 3.85 deg.

J-PARC/MLF BL05 (NOP: Neutron Optics and Physics)

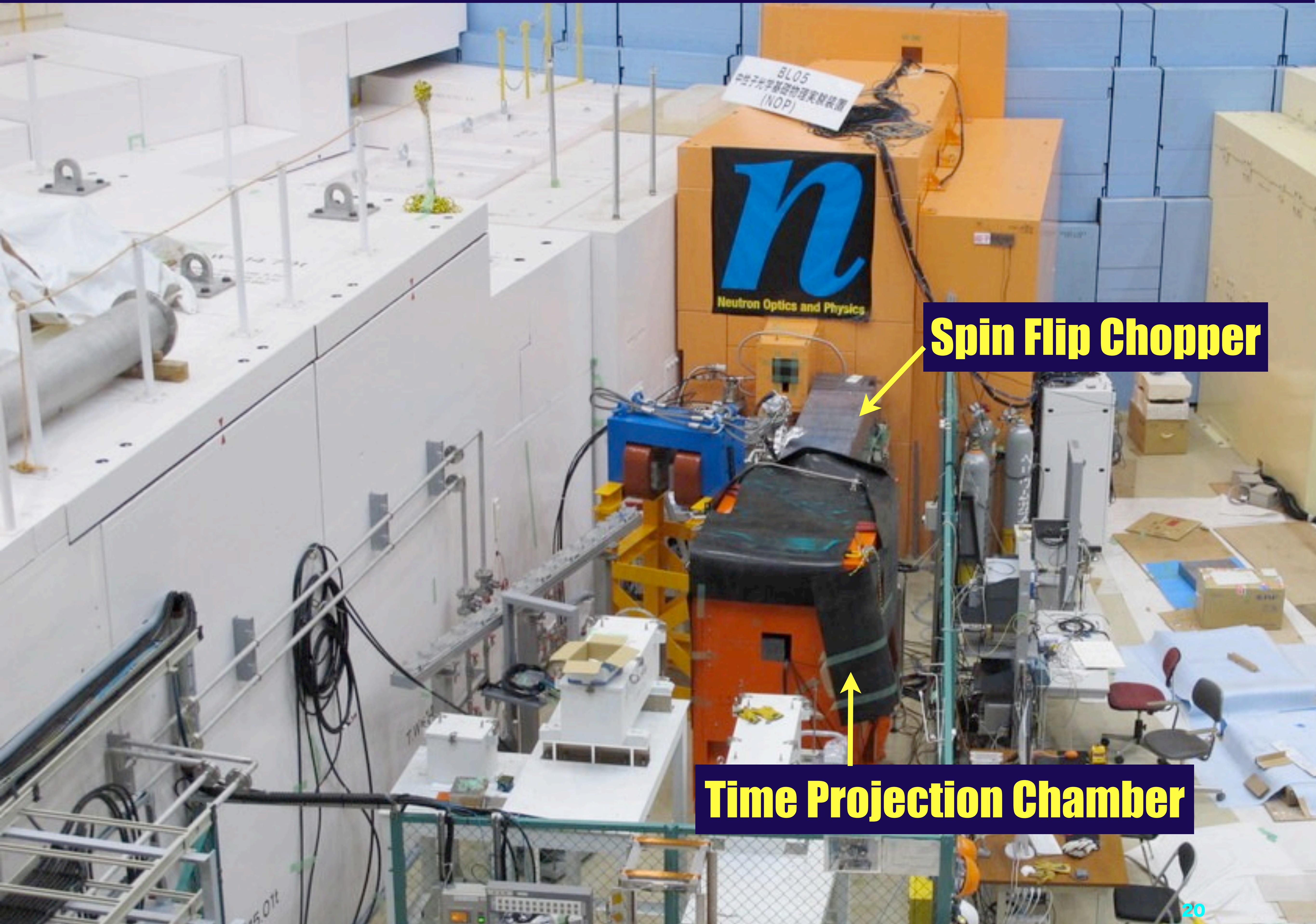

In flight β−decay

Beta decay

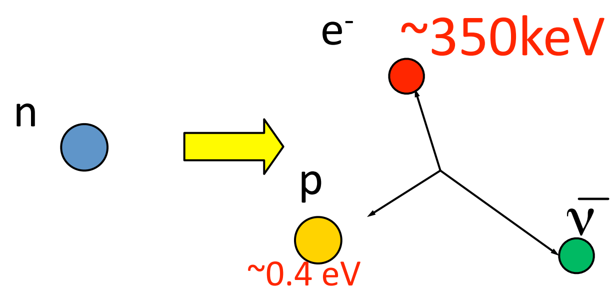

$$N_e = \frac{\varepsilon_e t \rho_n}{\tau_n}$$

~10^{-6} decay in 1m

Neutron decays into electron, proton and neutrino.

β-decay is 3-body decay, so energy spectrum has a low energy tail.

99.9% of β-decay electrons have >4 keV energy.

Energy spectrum of electron

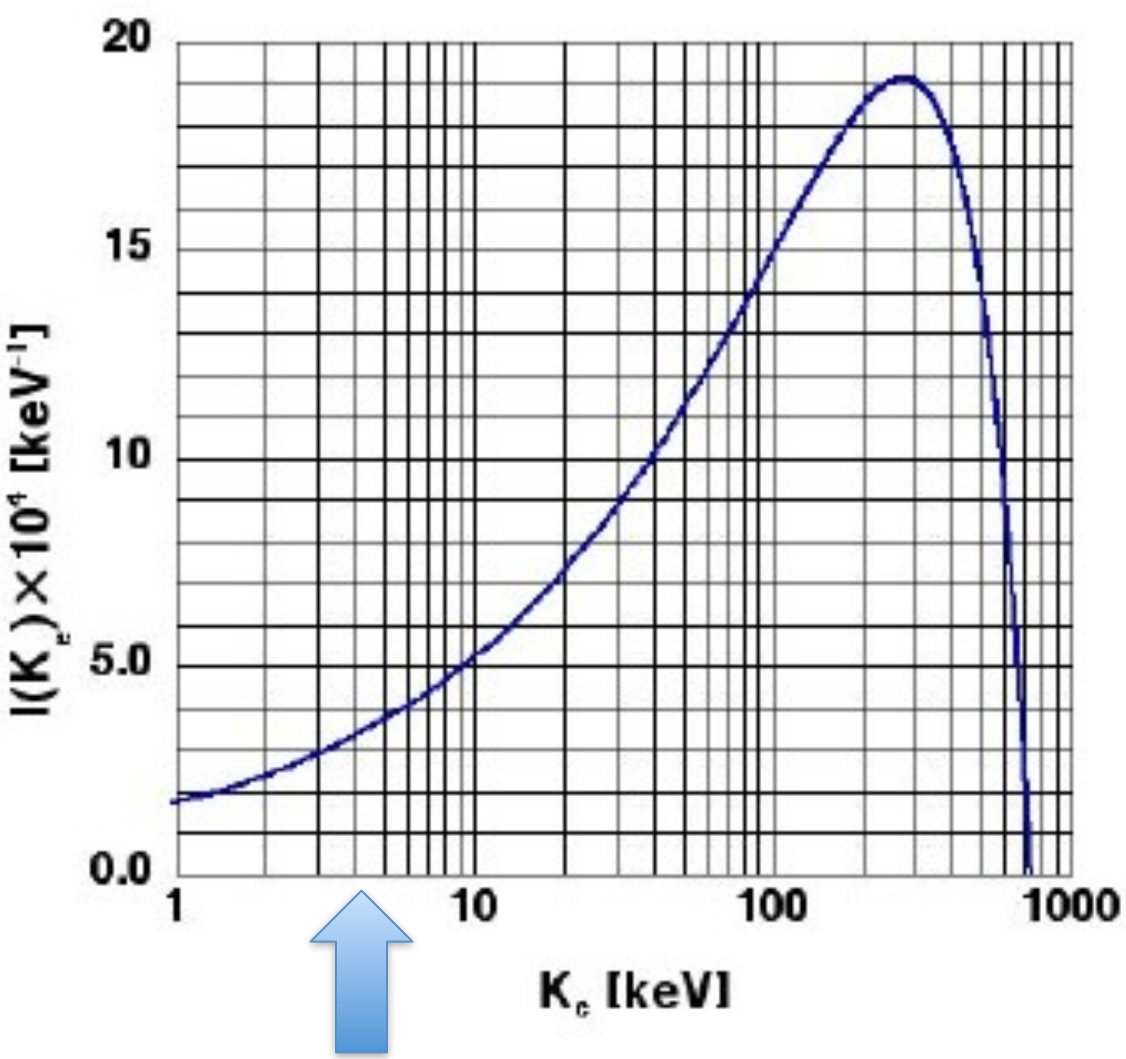

Neutron flux

$^3He(n,p)^3H$

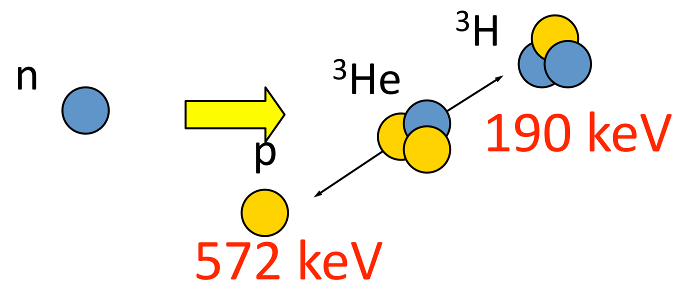

$$N_p = \varepsilon_p t \rho_n \rho_{^3He} \sigma_{^3He}(v_n)$$

$$\sigma_{3He}(v_n)\, v_n = \sigma_{3He}(v_0)\, v_0$$

Reaction rate is proportional to $1/v$

β *decay ~3.6mPa* ^{3}He

The difficulty of in-beam method is determination of the beam flux.

By adding a small amount of ^{3}He, we can measure the neutron flux via the $^3He(n,p)^3H$ reaction.

4mPa of ^{3}He gives same event rate with beta decay.

Both of the event rates are proportional to 1/v, so the velocity dependence is canceled by taking the ratio.

Spin Flip Chopper(SFC)

Resonance flippers flip the neutron spin.

Magnetic supermirror reflects only non-flipped neutrons.

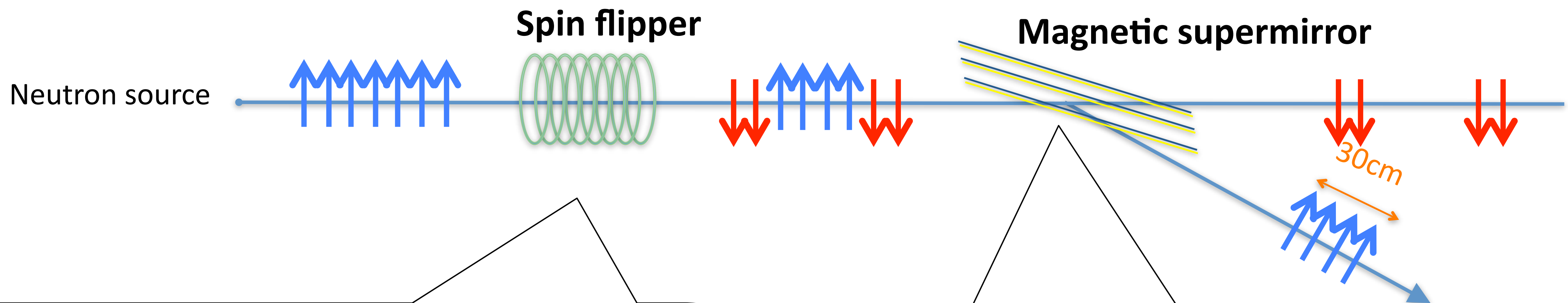

Guide field B_y and oscillating field $B_z \sin(\omega t)$

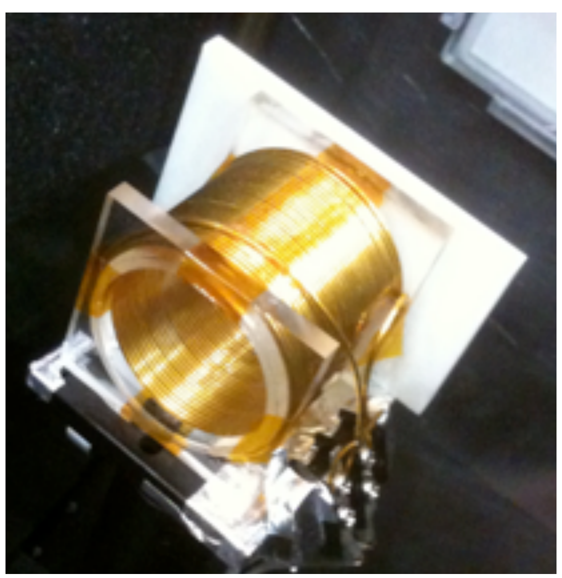

Diameter	50 mm
Length	40 mm
RF frequency	29 kHz
RF field B_z	0.3 mT
Guiding field B_y	1 mT

$$P = \frac{B_z^2}{B_z^2 + (B_y - \frac{\hbar}{2|\mu_n|}\omega)^2} \sin^2\left(\sqrt{B_z^2 + \left(B_y - \frac{\hbar}{2|\mu_n|}\omega\right)^2}\, t\right)$$

Multilayer of Ferromagnetic and Paramagnetic materials

Ferromagnetic	Fe
Paramagnetic	$SiGe_3$
Magnetizing field	35 mT
Length	140 mm
Height	35 mm
number of	5
Critical angle	m=5

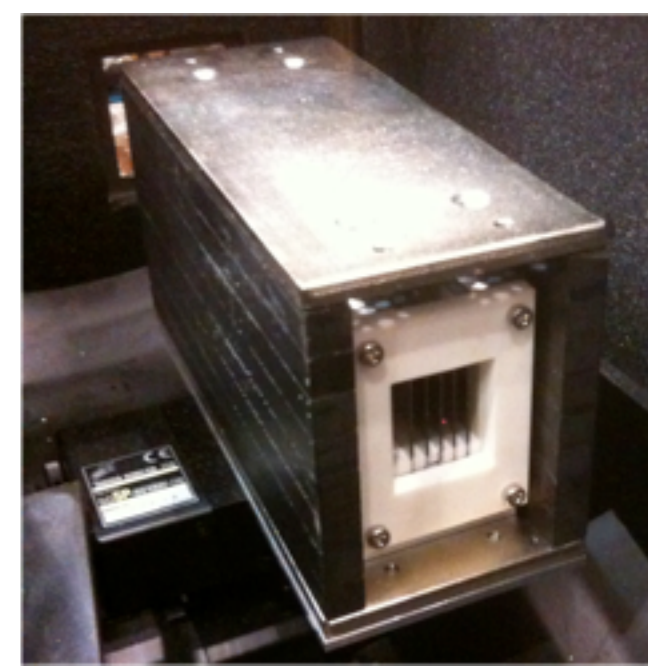

Neutron of 1300m/s can reflect with 1.5°

Depolarization makes the contrast worse.

SFC performance

With 2 flipper and 3 mirror sets

- Optimized to give good contrast

Beam size	3 cm x 2 cm
Minimum bunch length	15 cm
Rising length	5 cm
Flux (flipper on)	1.2 x 10^6 neutron/sec
Flux (flipper off)	0.3 x 10^4 neutron/sec
Contrast	400
Flux with 5 bunches	1.7 x 10^5 neutron/sec
Decay rate	0.1 decay/sec
Fiducial Time	2.8 ms / beam cycle

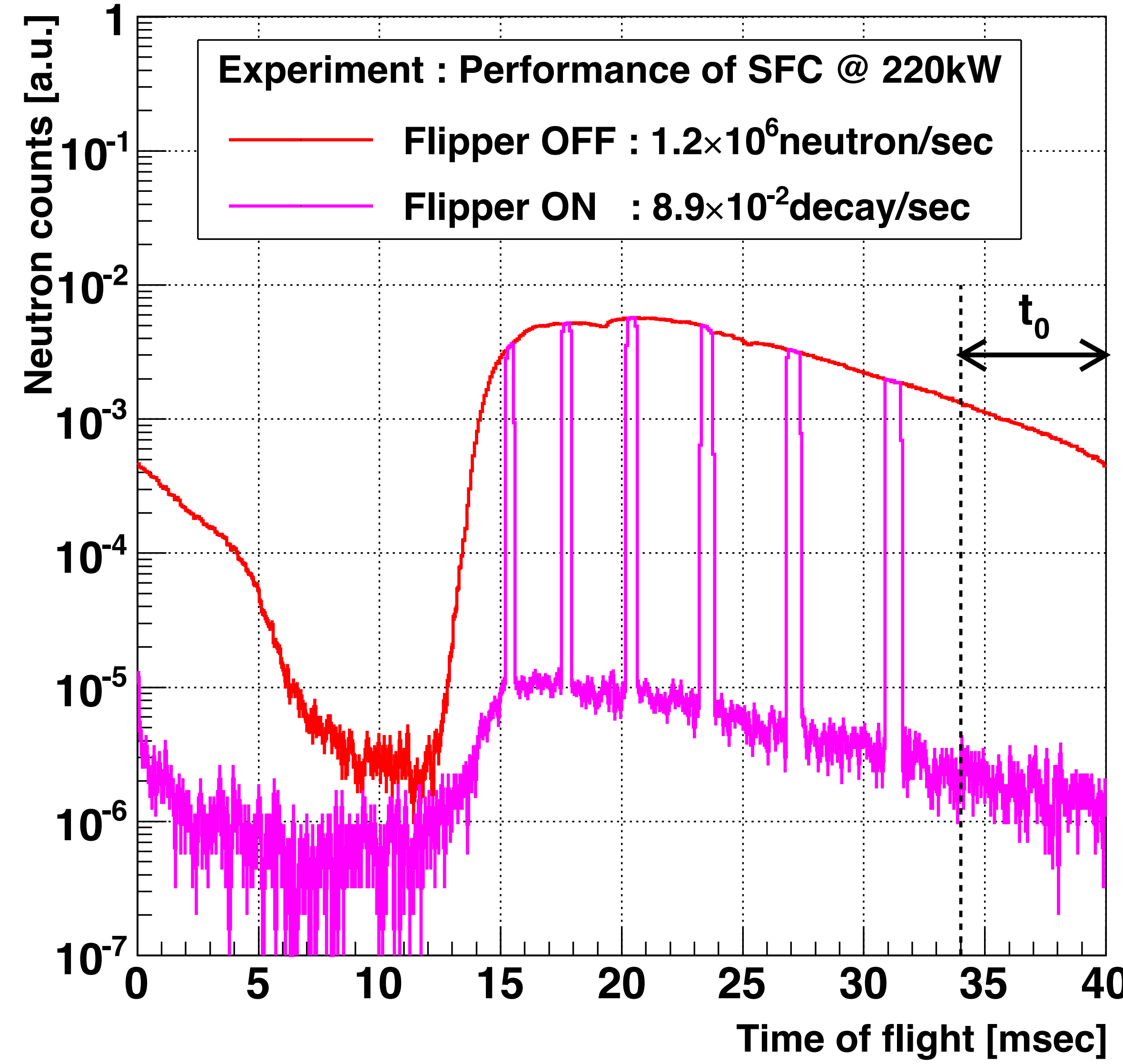

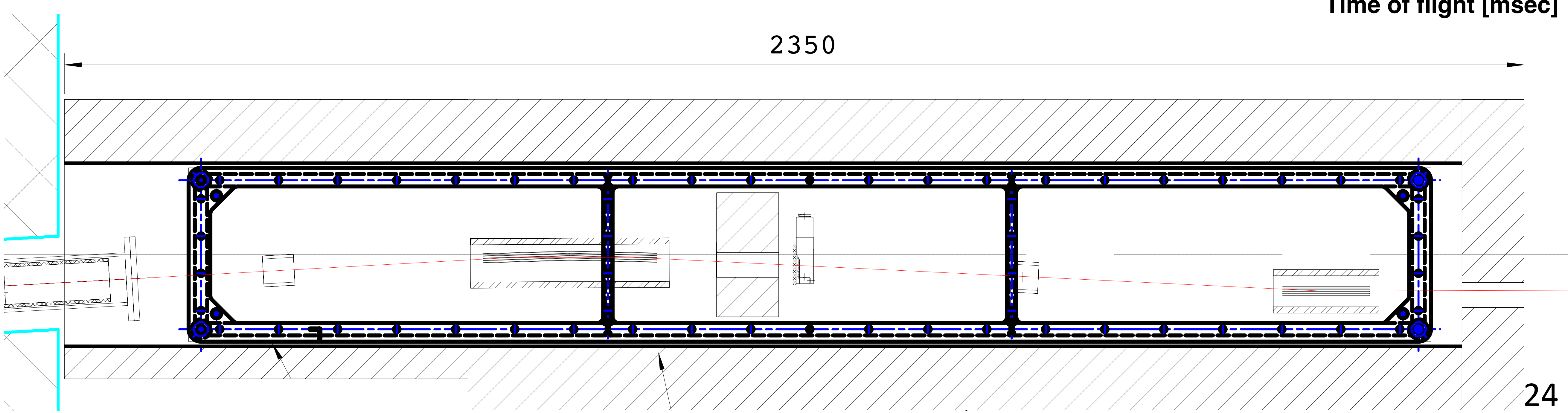

Time Projection Chamber

Efficiency of cosmic ray is 97 %/wire

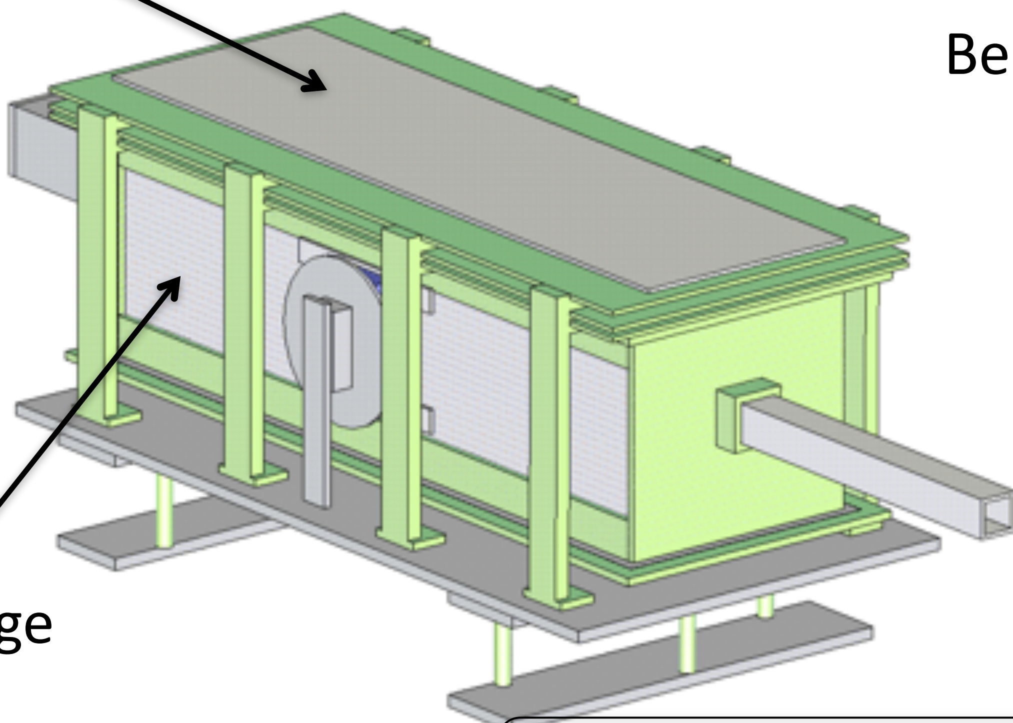

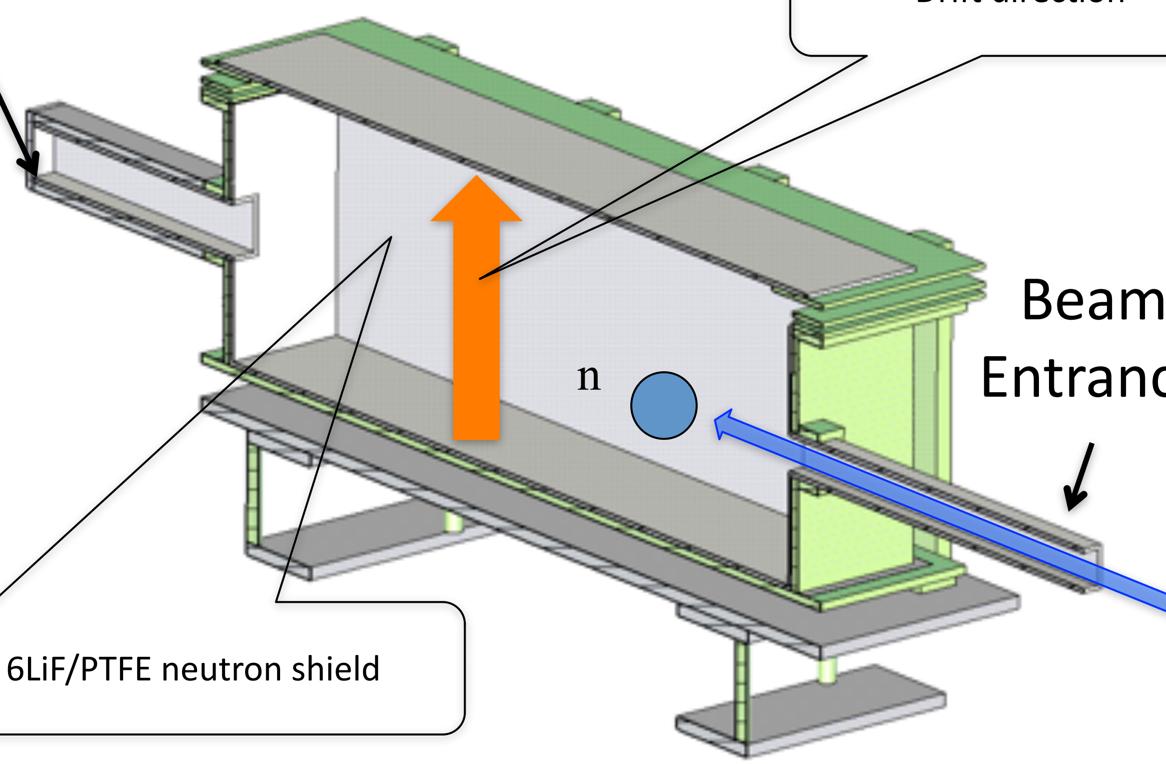

Voltage of MWPC (12 mm pitch)

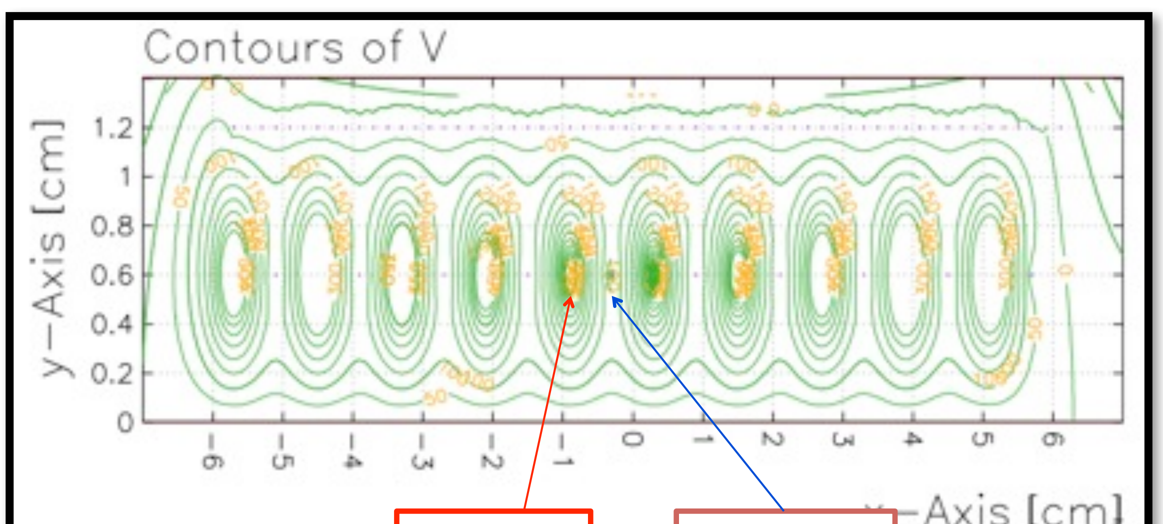

Anode wire	29 of W-Au wires(+1780V)
Field wire	28 of Be-Cu (0V)
Cathode wire	120 of Be-Cu (0V)
Drift length	30 cm (-9000V)
Gas mixture	He:CO_2=85kPa:15kPa
TPC size(mm)	300,300,970

Low background TPC (inside)

PEEK (Poly-Ether-Ether-Ketone) *: used in gas detector for the first time*

Feature : Chemically made from organic materials → small impurity

Pros : easily machinable, weldable,

1m material can be made to accuracy of 100μm

Cons : Small elasticity, need pre-tention to set up wires

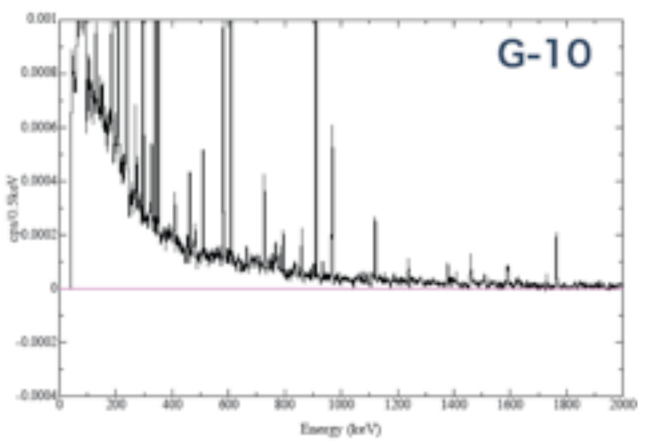

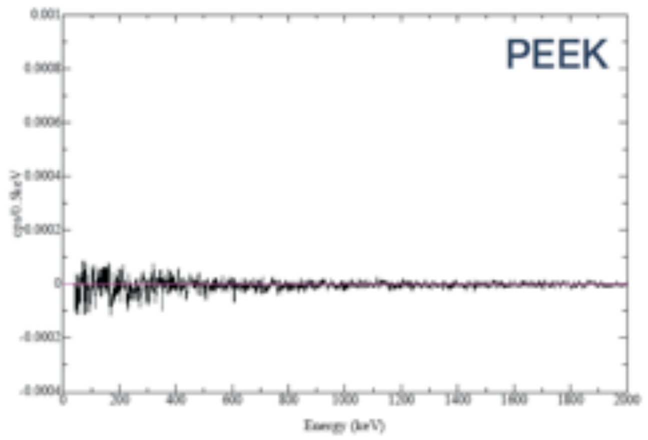

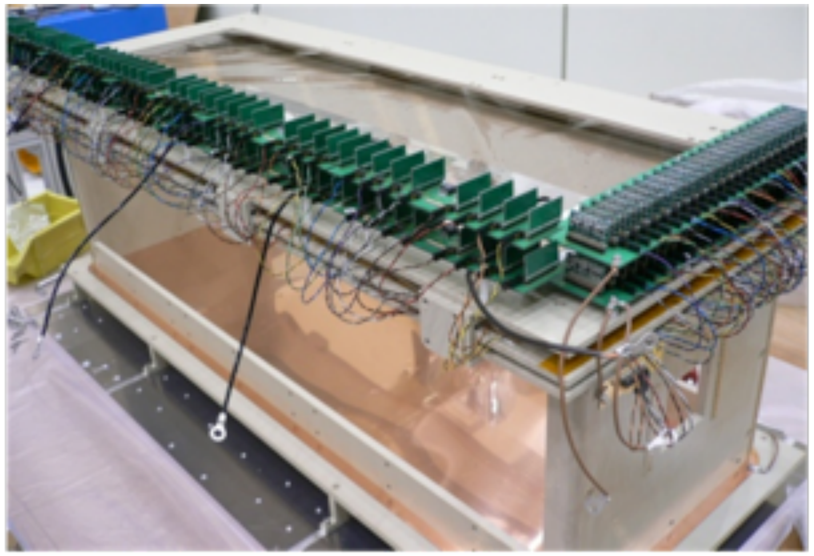

Backgrounds caused by prompt γ rays

from capture reactions of scattered neutrons by gas

^{6}LiF board: sintered 95% enriched ^{6}LiF and PTFE

（LiF : PTFE=30wt% : 70wt%）

All inner surface covered with ^{6}LiF board

- Relative permittivity is ϵ=3.0
- Position of electrodes were optimized by simulation.
- Uniformity of the drift velocities was less than 1%

^{6}Li + neutron → α + ^{3}H
Absorption length is 500μm

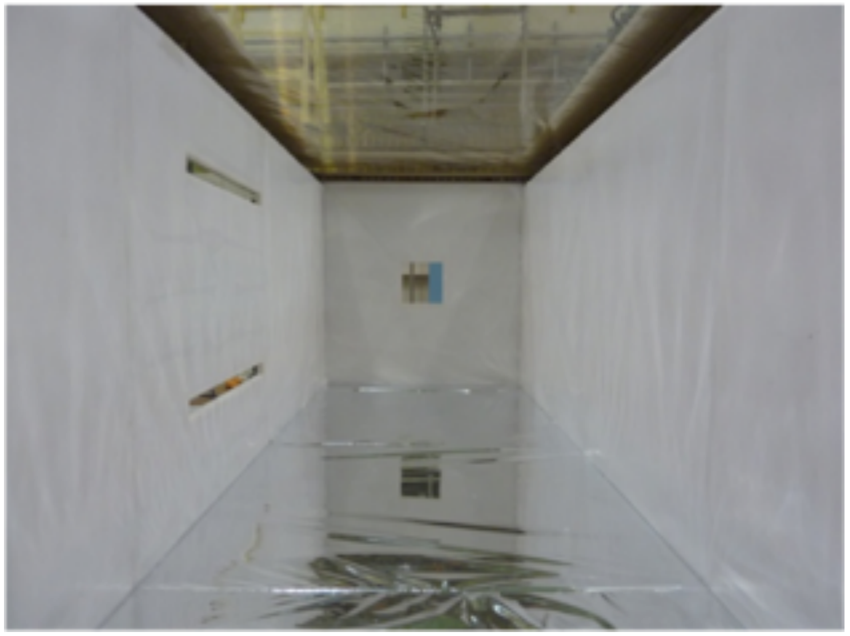

Low background TPC (outside)

- Lead shielding and Cosmic ray Veto

Energy cut

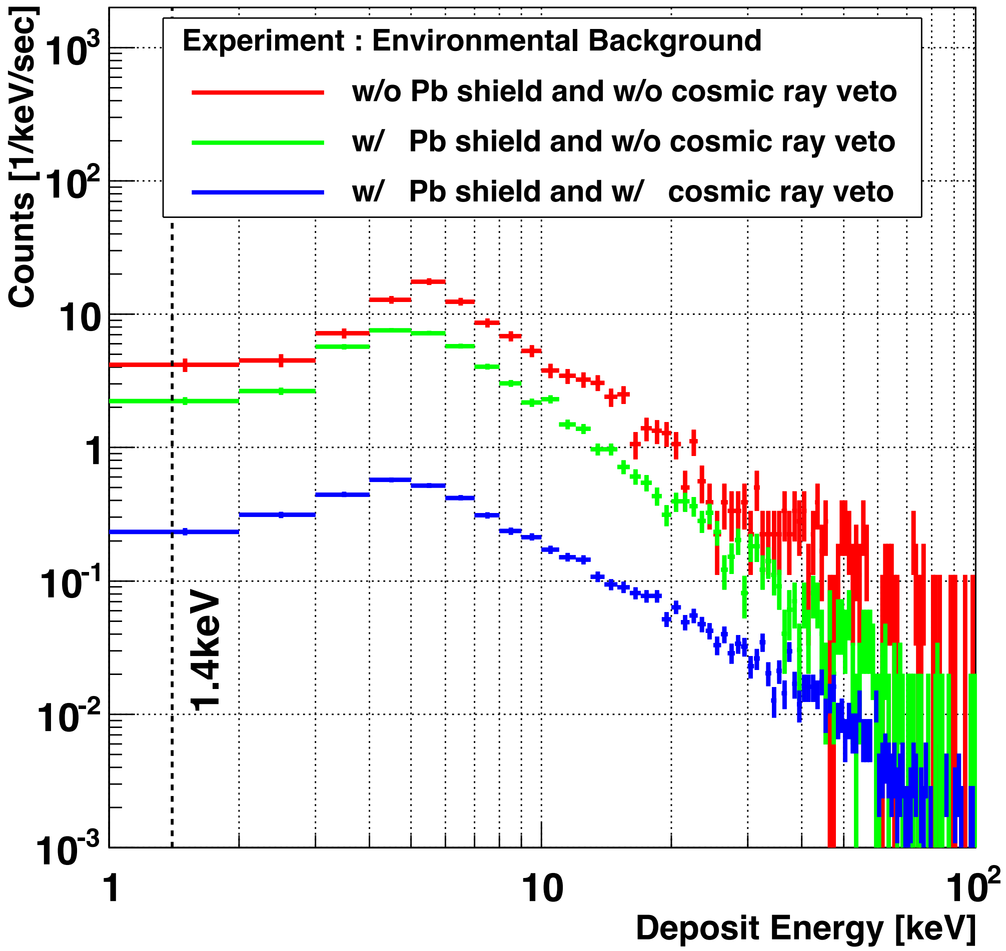

- Event Selection
  - Energy cut : Energy deposit over 1.4keV
  - Fiducial cut : Hit on Beam region

	Total count [cps]	With Energy cut [cps]	With Fiducial cut [cps]
No shielding or veto	123.7	100.1	30.7
+With Lead	58.4	44.2	13.9
+With Veto	7.7	4.3	1.4

→

Environmental radiation : 0.8 cps
Cosmic ray : 0.5 cps
Radioactives in TPC : 0.1 cps

S/N increased to 0.9

Estimation of statistical error

The decay rate is 0.1cps for beam power of 220 kW.

S/N of 0.9 achieved in present condition.

- J-PARC beam power

  will be 400 kW (about twice) at 2014.

- Spin flip chopper
  - The intensity is limited by mirror size.
  - Present beam size is 3 x 2 cm.
  - Large mirrors make the beam size to 10 x 4 cm.
  - Beam Intensity will be 16 times

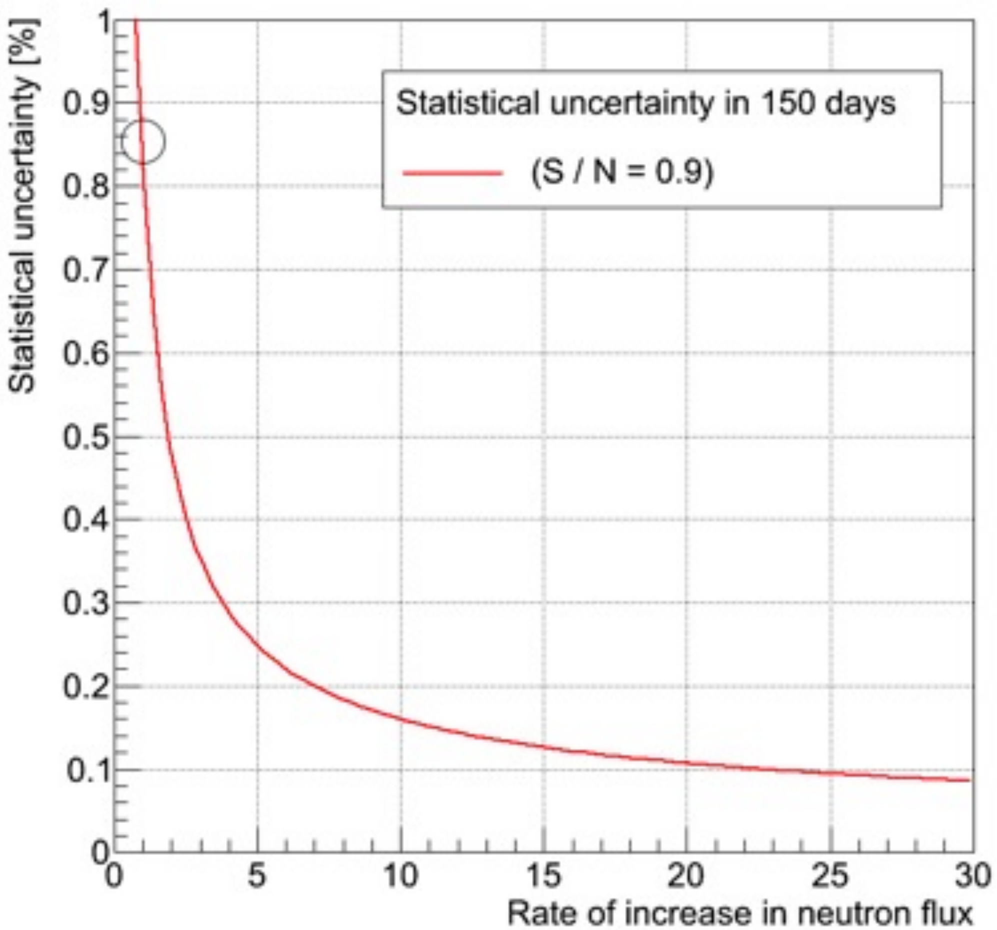

⇨ Beam intensity will be 32 times at 2014.
Statistical error is estimated to achieve 0.1 % in 150 days.

Number density of ^{3}He atoms

TPC gas is prepared by mixing natural He and ^{3}He(>99.9%)

We determine

1) Absolute pressure of mixed He ~80 kPa
2) ^{3}He/^{4}He for abundance of 10^{-6} with accuracy of 10^{-3}

- Pressure can be measured to 10^{-4} precision at 100 kPa with a piezo-drive transducer.

- Partical pressure of ^{3}He dopant is controlled by a baratron gauge and volume expansion method.
  It provide $\Delta P(^3\mathrm{He})/P$ ~ 0.2%.

- Temperature can be measured with ΔT ~0.1 K.

- Natural He contents ^{3}He of ~0.1 ppm. It will be determined by a mass spectroscopy. Present limit is 1%.

Present uncertainty of ^{3}He density is ~0.2%

Cross section of $^3He(n,p)^3H$

Transmission of ^{3}He was measured.

Present σ_{np} is 5333 ± 7 barn (0.13%)

C. D. KEITH *et al.* PHYSICAL REVIEW C 69, 034005 (2004)

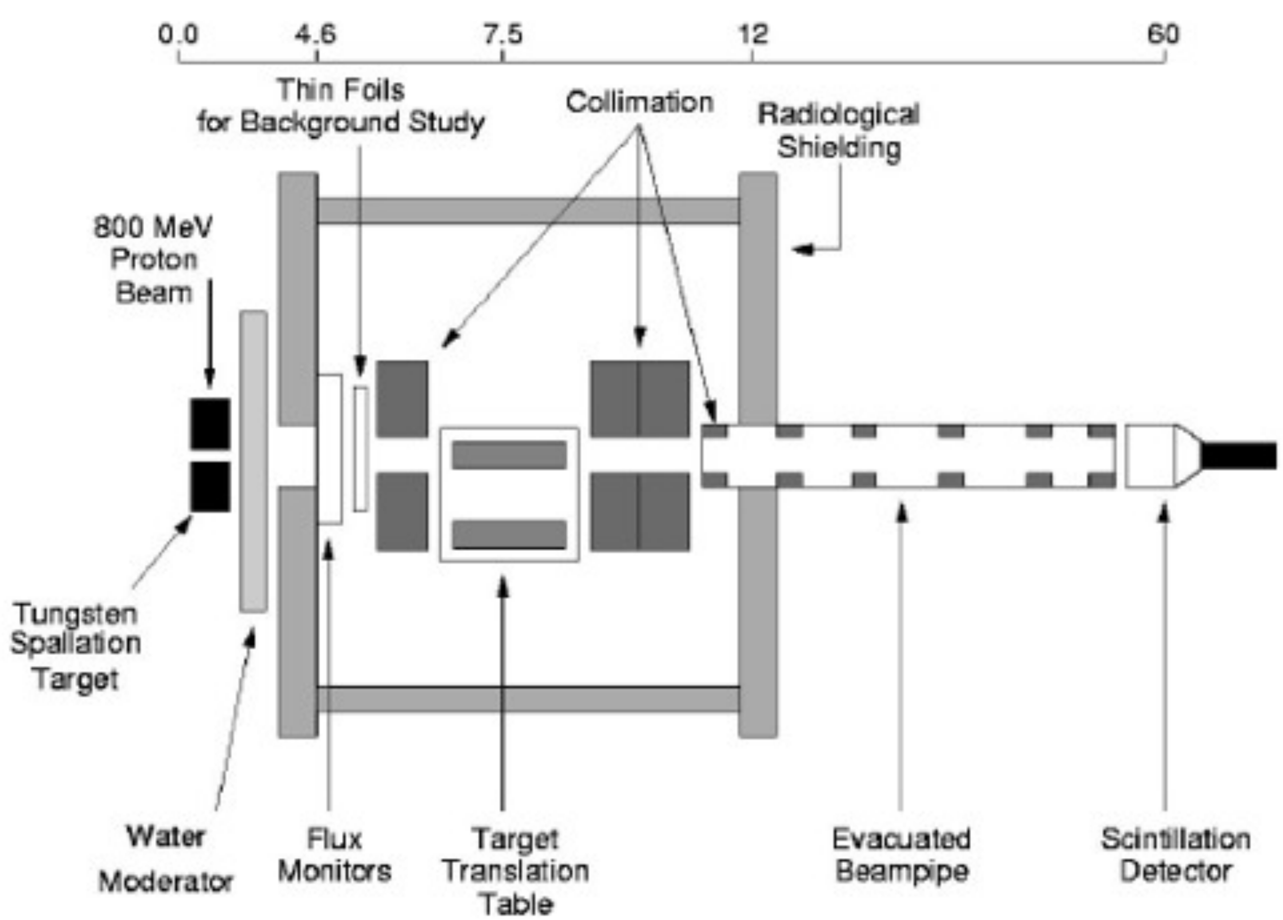

More precise measurement can be done at J-PARC (e.g. 100m beamline).

Uncertainties

$$\tau_n^{-1} = \frac{N_e / \varepsilon_e}{N_p / \varepsilon_p} \rho_{^3He} \sigma_{np}(v_0) v_0$$

- Statistical uncertainty: ~0.1% by measurement of 150 days.
- Determination of N_e and N_p : $\varepsilon_\beta > 99.9\%$(4keV), ε_p=100%

  Background of

  ~1% of simultaneous background

  ~35% of time dependent background

  ~110% of time independent background

  Should be subtracted correctly.

- Density of ^3He atoms → ~0.2%
- $^3He(n,p)^3H$ cross section → 0.13%.

Timeline of this experiment

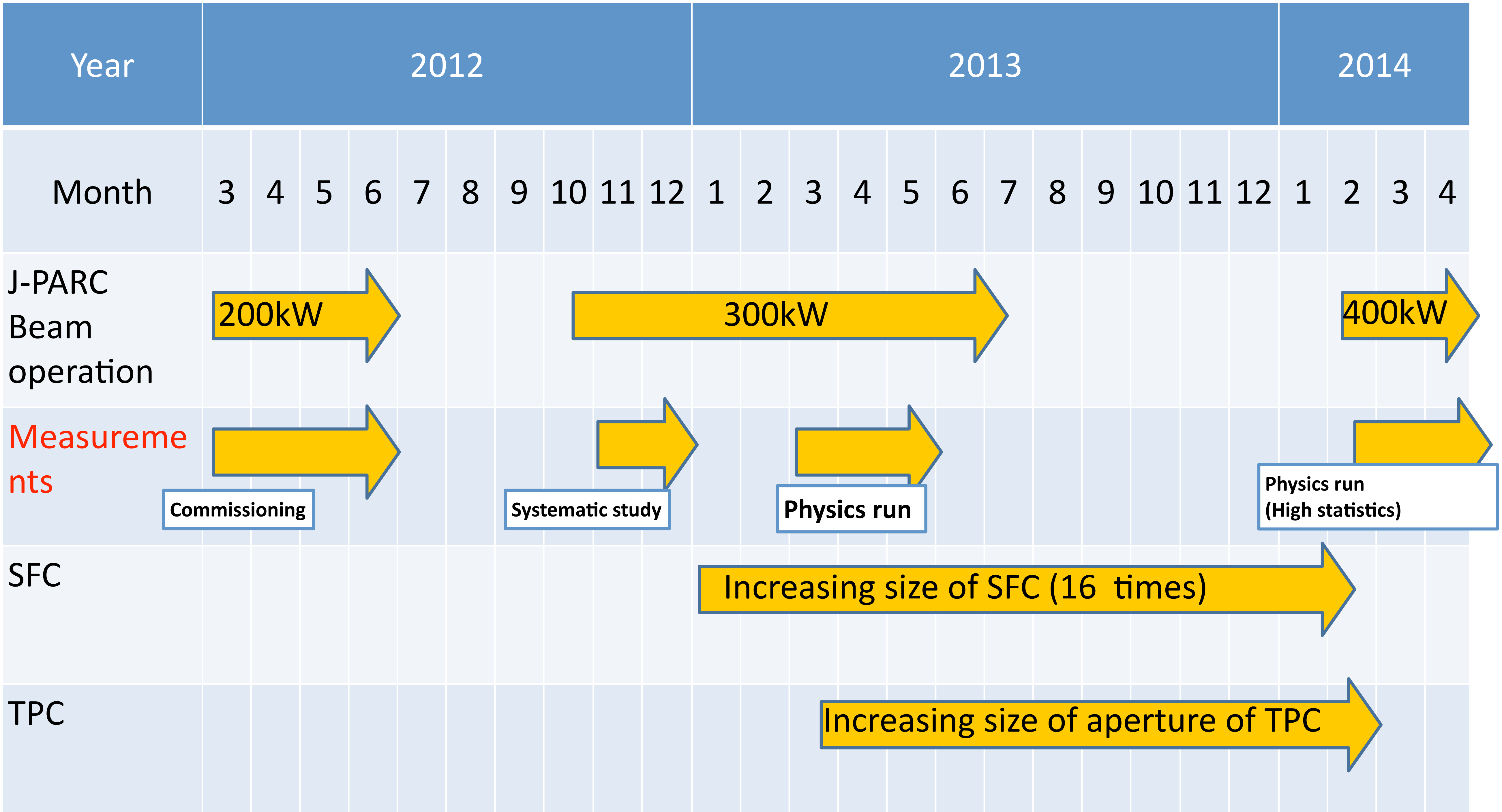

Correlation Terms at the Lowest Order

$$\frac{d\Gamma}{dE_e d\Omega_e d\Omega_\nu} = \frac{(G_\mu V_{\mathrm{ud}})^2}{(2\pi)^5}(1+3\lambda^2)p_e E_e E_\nu^{\,2} \times \left[1 + a\frac{\vec{p}_e \cdot \vec{p}_\nu}{E_e E_\nu} + \frac{\langle\vec{J}\rangle}{J} \cdot \left[A\frac{\vec{p}_e}{E_e} + B\frac{\vec{p}_\nu}{E_\nu}\right]\right]$$

$$a = \frac{1-\lambda^2}{1+3\lambda^2}$$

$$A = -2\frac{\lambda(\lambda+1)}{1+3\lambda^2}$$

$$B = 2\frac{\lambda(\lambda-1)}{1+3\lambda^2}$$

Correlation Terms at the Next-Lowest Order

$$\frac{d\Gamma}{dE_e d\Omega_{\hat{p}_e} d\Omega_{\hat{p}_\nu}} = \frac{(G_F V_{ud})^2}{(2\pi)^5} \frac{F(Z,E_e)\,|\vec{p}_e|\,E_\nu}{m_n\,[E_p + E_\nu + E_e\,(\vec{\beta}\cdot\hat{p}_\nu)]}|M|^2.$$

$$|M|^2 = m_n m_p E_e E_\nu \left(1 + \frac{\alpha}{2\pi}\,e_V^R\right)\left(1 + \frac{\alpha}{2\pi}\,\delta_\alpha^{(1)}\right)$$
$$\times C_0(E_e)(1+3\tilde{g}_A^2)\left\{1 + \left(1 + \frac{\alpha}{2\pi}\,\delta_\alpha^{(2)}\right) C_1(E_e)\vec{\beta}\cdot\hat{p}_\nu\right.$$
$$\left. + \left(1 + \frac{\alpha}{2\pi}\,\delta_\alpha^{(2)}\right)[C_2(E_e) + C_3(E_e)\vec{\beta}\cdot\hat{p}_\nu]\hat{n}\cdot\vec{\beta} + [C_4(E_e) + C_5(E_e)\vec{\beta}\cdot\hat{p}_\nu]\hat{n}\cdot\hat{p}_\nu\right\}$$

$$\delta_\alpha^{(1)} = 3\ln\left(\frac{m_N}{m_e}\right) + \frac{1}{2} + \frac{1+\beta^2}{\beta}\ln\left(\frac{1+\beta}{1-\beta}\right) - \frac{1}{\beta}\ln^2\left(\frac{1+\beta}{1-\beta}\right) + \frac{4}{\beta}L\left(\frac{2\beta}{1+\beta}\right)$$
$$+4\left[\frac{1}{2\beta}\ln\left(\frac{1+\beta}{1-\beta}\right) - 1\right]\left[\ln\left(\frac{2(E_e^{max}-E_e)}{m_e}\right) + \frac{1}{3}\left(\frac{E_e^{max}-E_e}{E_e}\right) - \frac{3}{2}\right]$$
$$+\left(\frac{E_e^{max}-E_e}{E_e}\right)^2 \frac{1}{12\beta}\ln\left(\frac{1+\beta}{1-\beta}\right),$$

$$\delta_\alpha^{(2)} = \frac{1-\beta^2}{\beta}\ln\left(\frac{1+\beta}{1-\beta}\right) + \left(\frac{E_e^{max}-E_e}{E_e}\right)\frac{4(1-\beta^2)}{3\beta^2}\left[\frac{1}{2\beta}\ln\left(\frac{1+\beta}{1-\beta}\right) - 1\right]$$
$$+\left(\frac{E_e^{max}-E_e}{E_e}\right)^2 \frac{1}{6\beta^2}\left[\frac{1-\beta^2}{2\beta}\ln\left(\frac{1+\beta}{1-\beta}\right) - 1\right].$$

$$L(z) = \int_0^z \frac{dt}{t}\ln(1-t)$$

$$C_0(E_e) = 1 + \frac{1}{m_N(1+3\tilde{g}_A^2)}\left\{(\tilde{g}_A^2 - 2\mu_V\tilde{g}_A + 1)E_e^{max} - \frac{m_e^2}{E_e}(1+\tilde{g}_A^2) + 2\mu_V\tilde{g}_A(\beta^2+1)E_e\right\}$$

$$C_1(E_e) = \tilde{a}\left\{1 + \frac{1}{m_N}\left[\frac{(\tilde{g}_A^2 + 2\mu_V\tilde{g}_A + 1)}{1+3\tilde{g}_A^2}\frac{m_e^2}{E_e} + \frac{(\tilde{g}_A^2+1)[8\mu_V\tilde{g}_A E_e - 4E_e^{max}\tilde{g}_A(\tilde{g}_A+\mu_V)]}{(\tilde{g}_A^2-1)(1+3\tilde{g}_A^2)}\right]\right\}$$

$$C_2(E_e) = \tilde{A}\left\{1 + \frac{1}{m_N}\left[\frac{(\tilde{g}_A^2-1)(\tilde{g}_A+\mu_V)}{2\tilde{g}_A(1+3\tilde{g}_A^2)}(E_e^{max}-E_e) + \frac{E_e(\mu_V-1)}{\tilde{g}_A-1} - \beta^2 E_e\frac{\tilde{g}_A^2 + 2\tilde{g}_A\mu_V + 1}{1+3\tilde{g}_A^2}\right]\right\}$$

$$C_3(E_e) = \tilde{A}\frac{E_e(\tilde{g}_A-\mu_V)}{2m_N\tilde{g}_A}$$

$$C_4(E_e) = \tilde{B}\left\{1 + \frac{1}{m_N}\left[\frac{E_e\beta^2(\tilde{g}_A^2-1)(\tilde{g}_A-\mu_V)}{2\tilde{g}_A(1+3\tilde{g}_A^2)} + \frac{(\tilde{g}_A+\mu_V)(\tilde{g}_A-1)^2}{(\tilde{g}_A+1)(1+3\tilde{g}_A^2)}(E_e - E_e^{max})\right]\right\}$$

$$C_5(E_e) = \tilde{B}\frac{(\tilde{g}_A+\mu_V)}{2m_N\tilde{g}_A}(E_e^{max}-E_e)$$

Correlation Terms at the Next-Lowest Order

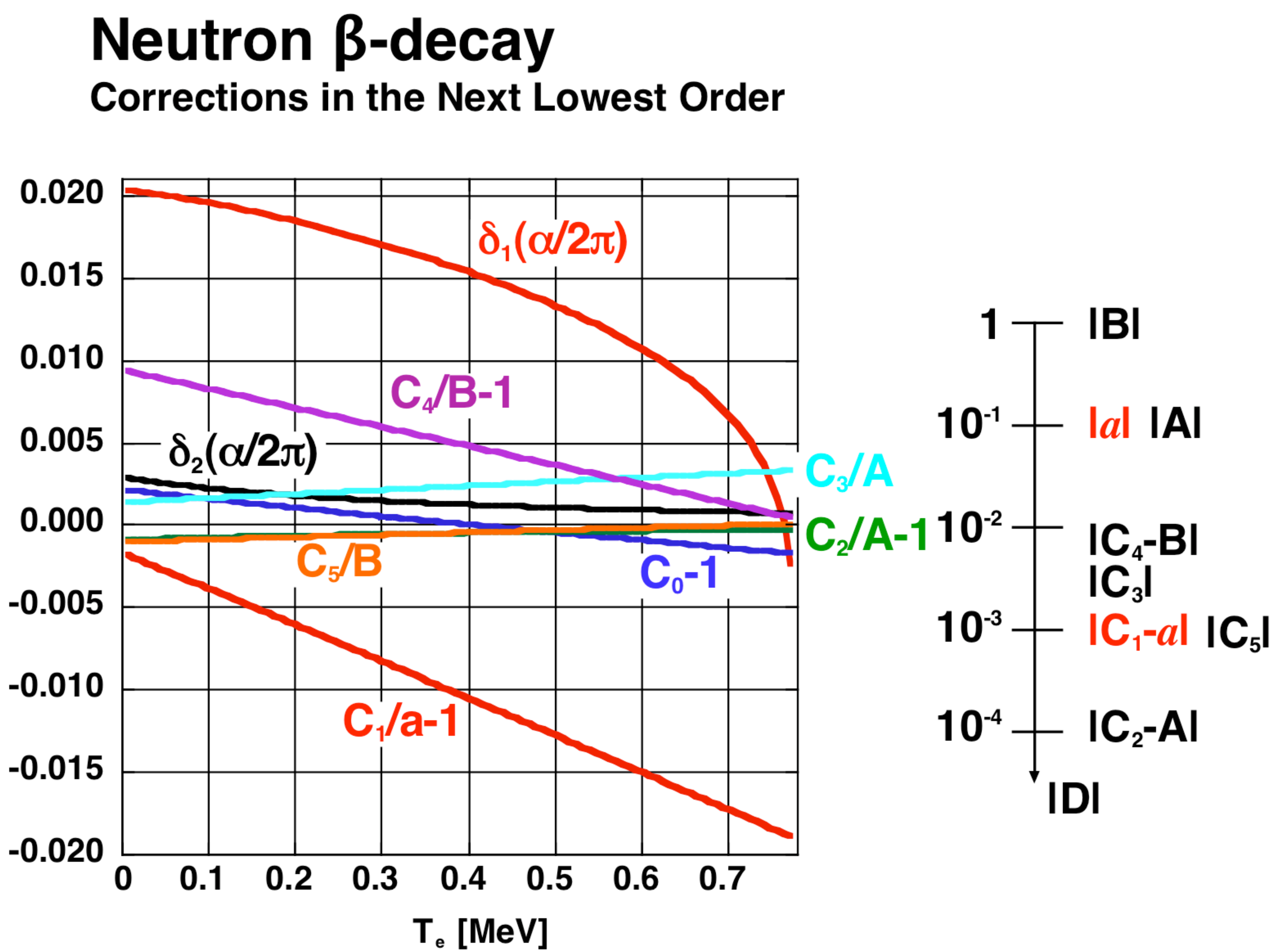

A Possible Sensitivity to SUSY

$$L^{\beta-\mathrm{decay}} = -\frac{4G_\mu}{\sqrt{2}} \sum_{\gamma,\varepsilon,\delta} a^{\gamma}_{\varepsilon\delta}\, \bar{e}_\varepsilon \Gamma^\gamma \nu_e\, \bar{u} \Gamma_\gamma d_\delta$$

$$\Delta B = -2\frac{m}{E}\frac{\lambda}{1+3\lambda^2}\mathrm{Re}\left[2(2\lambda+1)\frac{g_T}{g_A}\left(\frac{a^T_{RL}}{a^V_{LL}}\right)^* - \frac{g_S}{g_V}\left(\frac{a^S_{RL}+a^S_{RR}}{a^V_{LL}}\right)^*\right]$$

β-energy dependence in neutrino asymmetry coefficient B

$\Delta B \leq 10^{-3}$ (maximal LR-mixing)

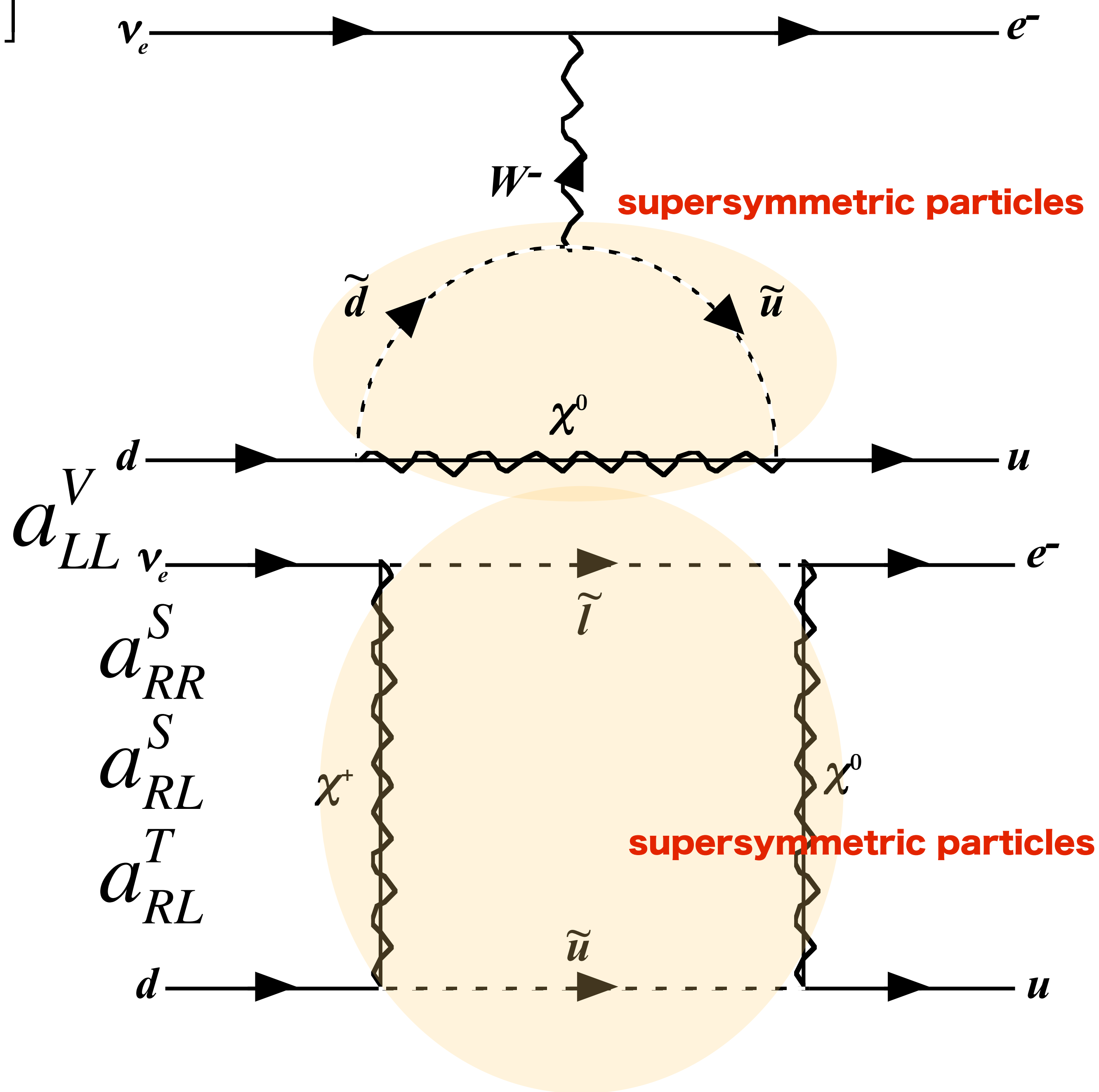

10^{-4}-level accuracy may probe SUSY

Ramsey-Musolf&Su, PhysRep456(2008)1

3. T-violation

電気双極子能率

$U = -\mathbf{d}\cdot\mathbf{E} \quad \neq \quad U = \mathbf{d}\cdot\mathbf{E}$

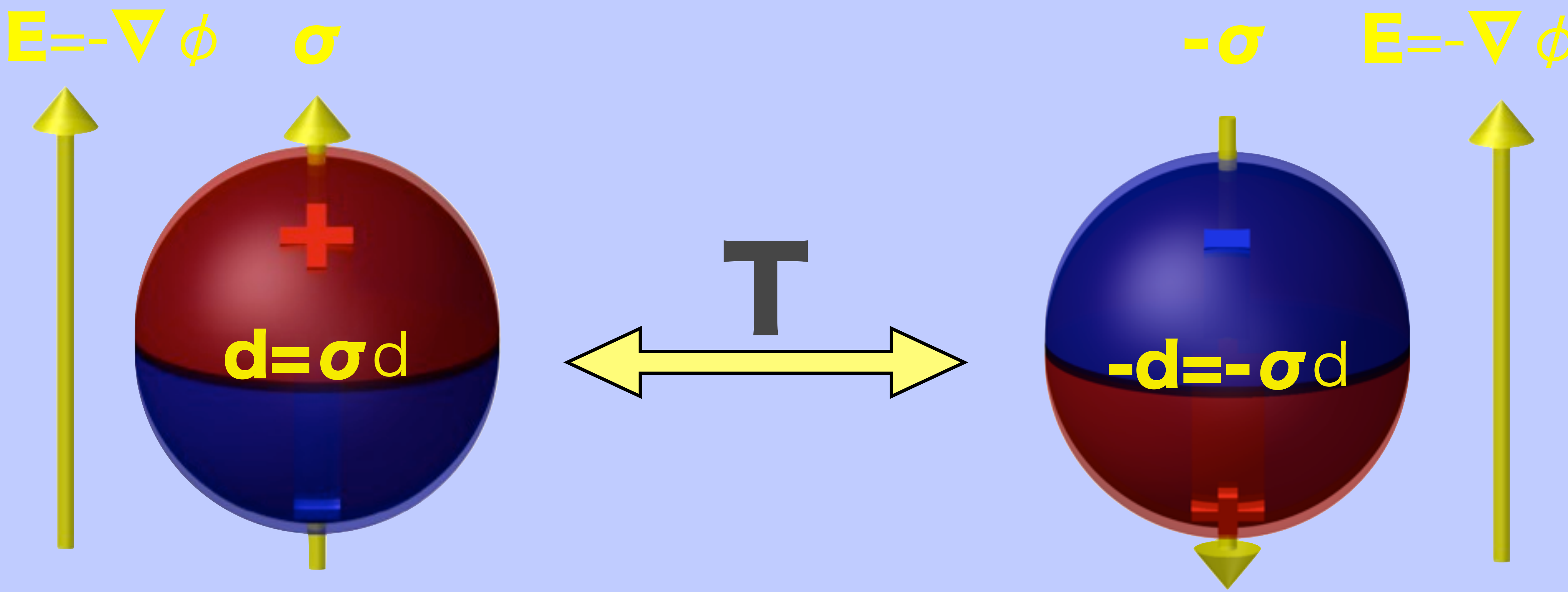

d≠0ならば時間反転対称性が破れる

TeV新物理→EDM

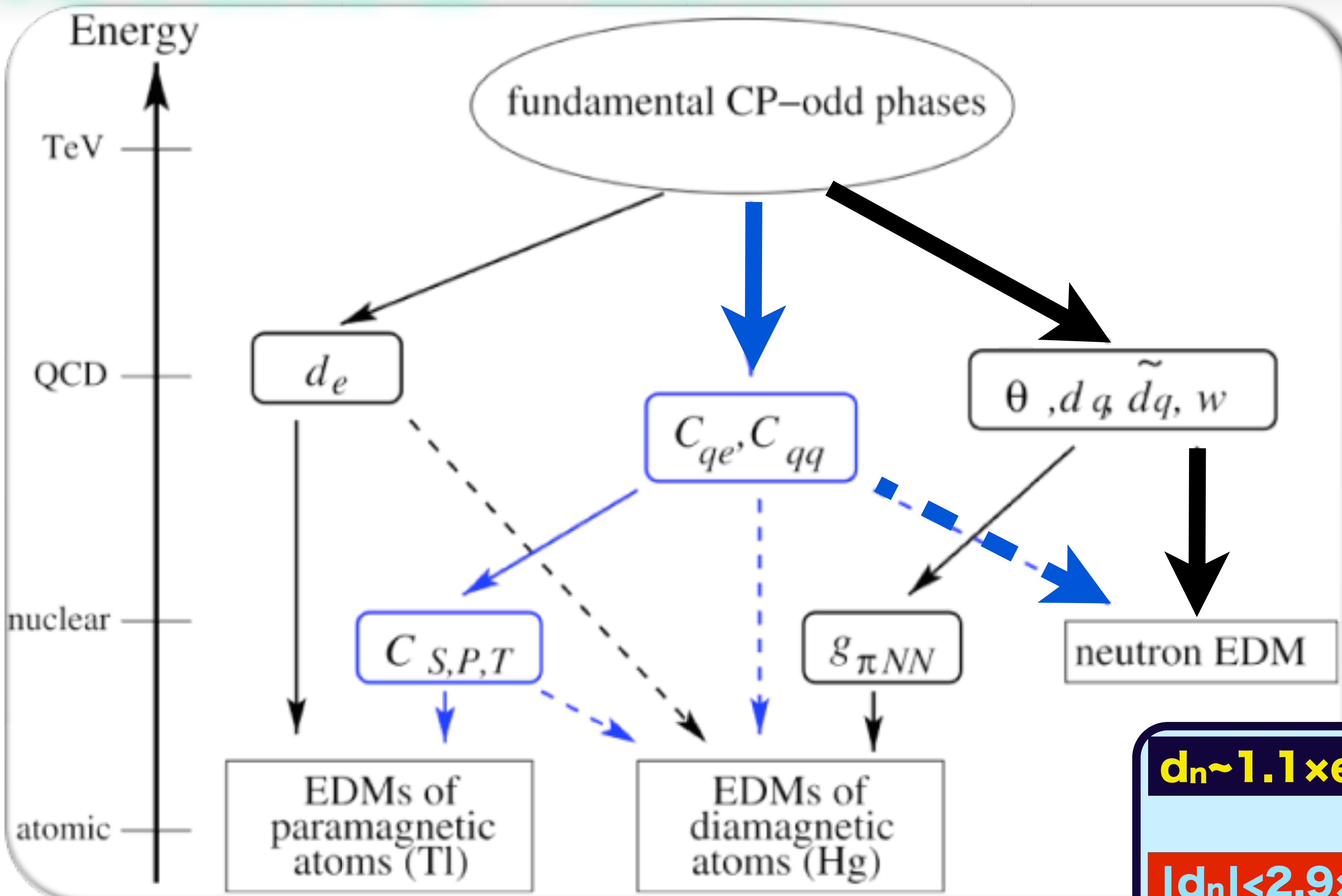

$d_n \sim 1.1\times e(0.5 d_u^c + d_d^c) + 1.4\times(-0.25 d_u + d_d)$

valence quark contribution

$|d_n| < 2.9\times10^{-26}$ e cm

SM: $|d_e| \sim 10^{-32}$ e cm

$d_{Tl} \sim -585 d_e - e\ 43\mathrm{GeV}\times(C_S^{(0)} - 0.2 C_S^{(1)})$

relativistic effect

$|d_{Tl}| < 9\times10^{-25}$ e cm

$|d_e| < 1.7\times10^{-27}$ e cm

SM: $|d_e| <\sim 10^{-40}$ e cm

$d_{Hg} \sim 7\times10^{-3}\times e(0.5 d_u^c + d_d^c)$

$|d_{Hg}| < 3.1\times10^{-29}$ e cm

via pion-nucleon interaction

$d_D \sim (d_u + d_d) - 0.2e(d_u^c + d_d^c) + 6e(d_d^c - d_u^c)$

constituent particle EDMs　　pion exchange

$|d_D| \Rightarrow 10^{-29}$ e cm

	Current limit [e·cm]	Future goal	Neutron equivalent
Neutron	$<1.6\times10^{-26}$	$\sim10^{-28}$	10^{-28}
^{199}Hg atom	$<2\times10^{-28}$	$\sim2\times10^{-29}$	10^{-25} - 10^{-26}
^{129}Xe atom	$<6\times10^{-27}$	$\sim10^{-30}$ - 10^{-33}	10^{-26} - 10^{-29}
Deuteron nucleus		$\sim10^{-29}$	3×10^{-29} - 5×10^{-31}

3.1. Electric Dipole Moment

Measurement Procedure

search for the phase change when the electric field is reversed

$$\frac{\omega_\pm}{2\pi} = 3\times10^{1}\,\frac{B}{1\,\mu T} \pm 5\times10^{-8}\,\frac{d_n}{10^{-26}\ e\ cm}\,\frac{E}{10kV/cm}$$

magnetic — electric

$\hbar\omega_+ = 2\mu_n B + 2d_n E$ B E

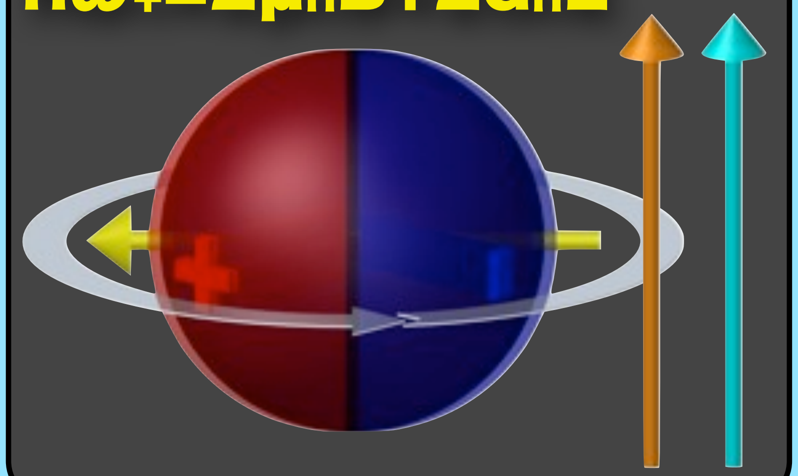

$\hbar\omega_- = 2\mu_n B - 2d_n E$ B E

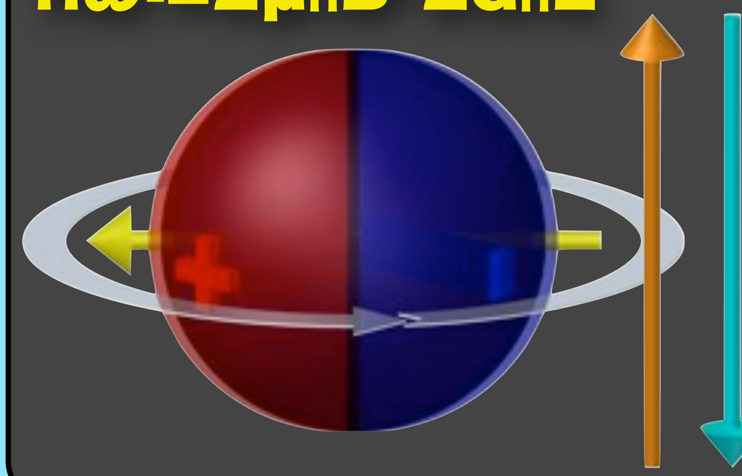

$$\Delta\phi = \int(\omega_+ - \omega_-)dt = \frac{2d_n ET}{\hbar}$$

$$\Delta d_n = \frac{\hbar/2}{ET\,N^{1/2}}$$

$ET = 10^6$ s kV/cm

$E = 10^4$ V/cm, $T = 100$s

Confined Ultracold Neutron Spin Precession Freq.

$ET = 10^6$ s kV/cm

$E = 10^9$ V/cm, $T = 1$ms

$|d_n| < 2.9\times10^{-26}$ e cm (90%CL)

Cold Neutron Diffraction in Single Crystal

$2d_n E = 6\times10^{-22}$ eV

中性子電気双極子能率の測定

$$\frac{\omega_\pm}{2\pi} = 30\,\frac{B}{1\mu T} \pm 50\times10^{-9}\,\frac{d_n}{10^{-26}\,e\,cm}\,\frac{E}{10kV/cm}$$

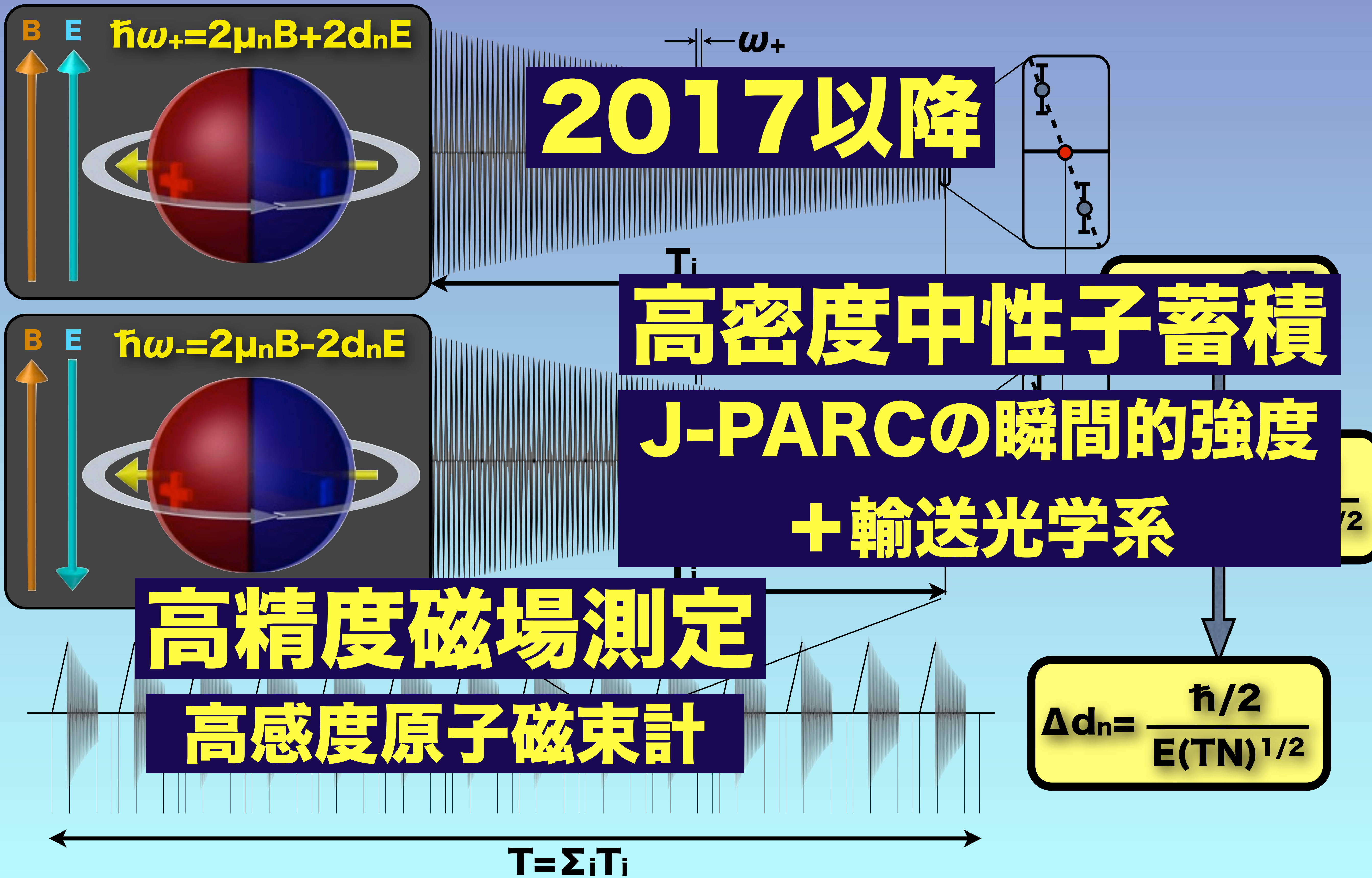

2017以降

高密度中性子蓄積

J-PARCの瞬間的強度
＋輸送光学系

高精度磁場測定

高感度原子磁束計

Magnetometer

Rb NMOR magnetometer

in progress for the atomic EDM research at T.I.T. and RIKEN as a Grant-in-Aid Program.

Goal sensitivity = 100 aT (=0.1fT)

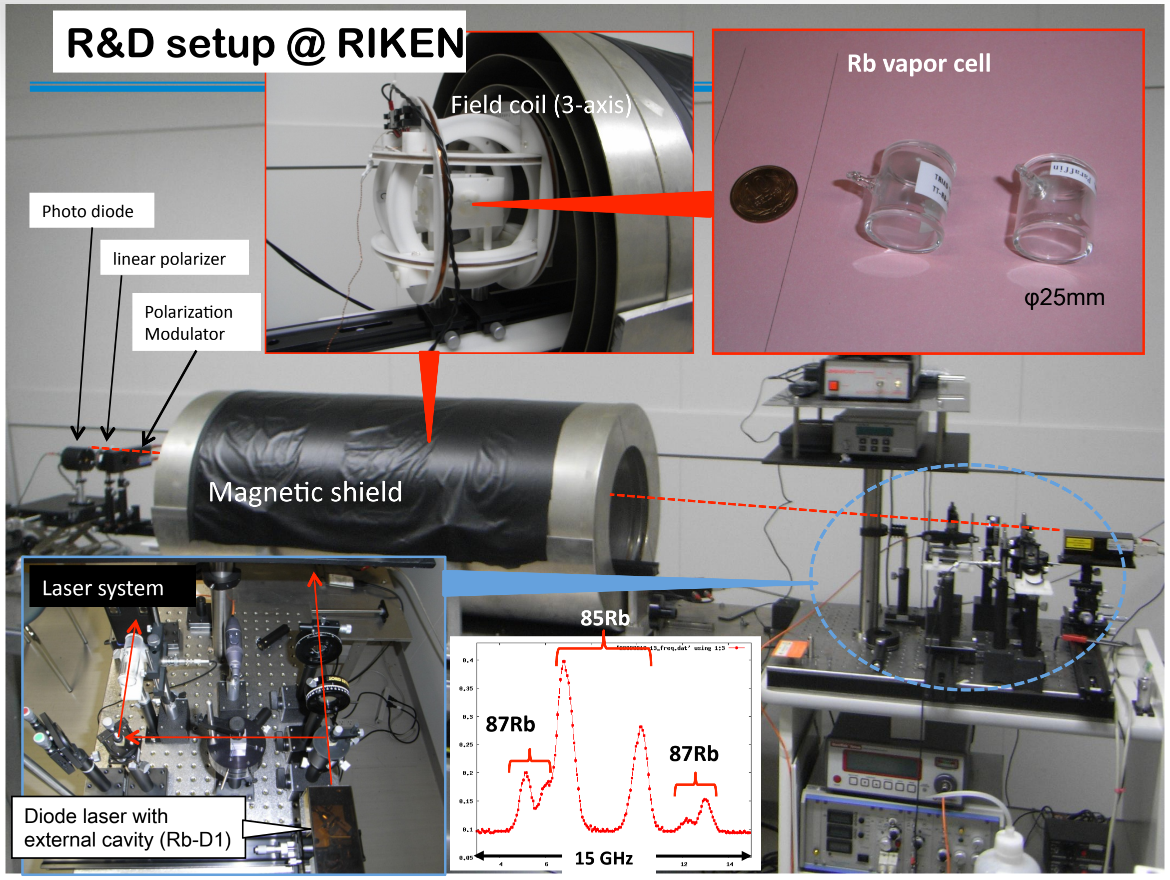

Hg Co-magnetometer

We start the study with a Hg lamp using the infrastructure of the ^{3}He nuclear polarization R&D station at the KEK/IMSS.

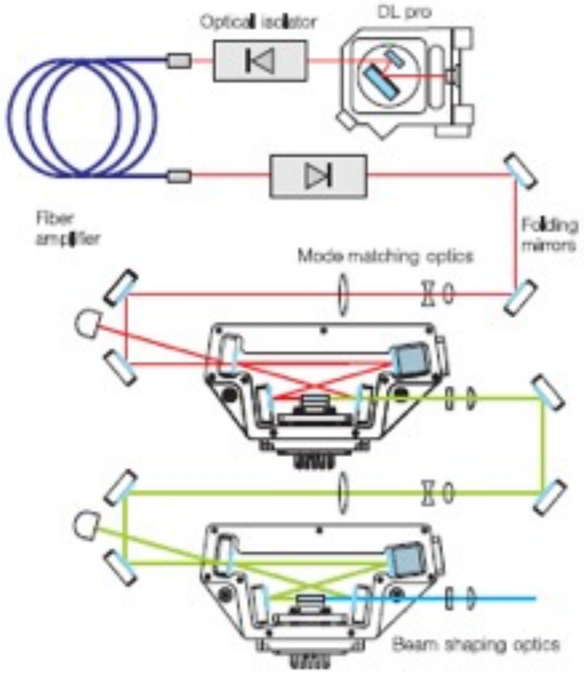

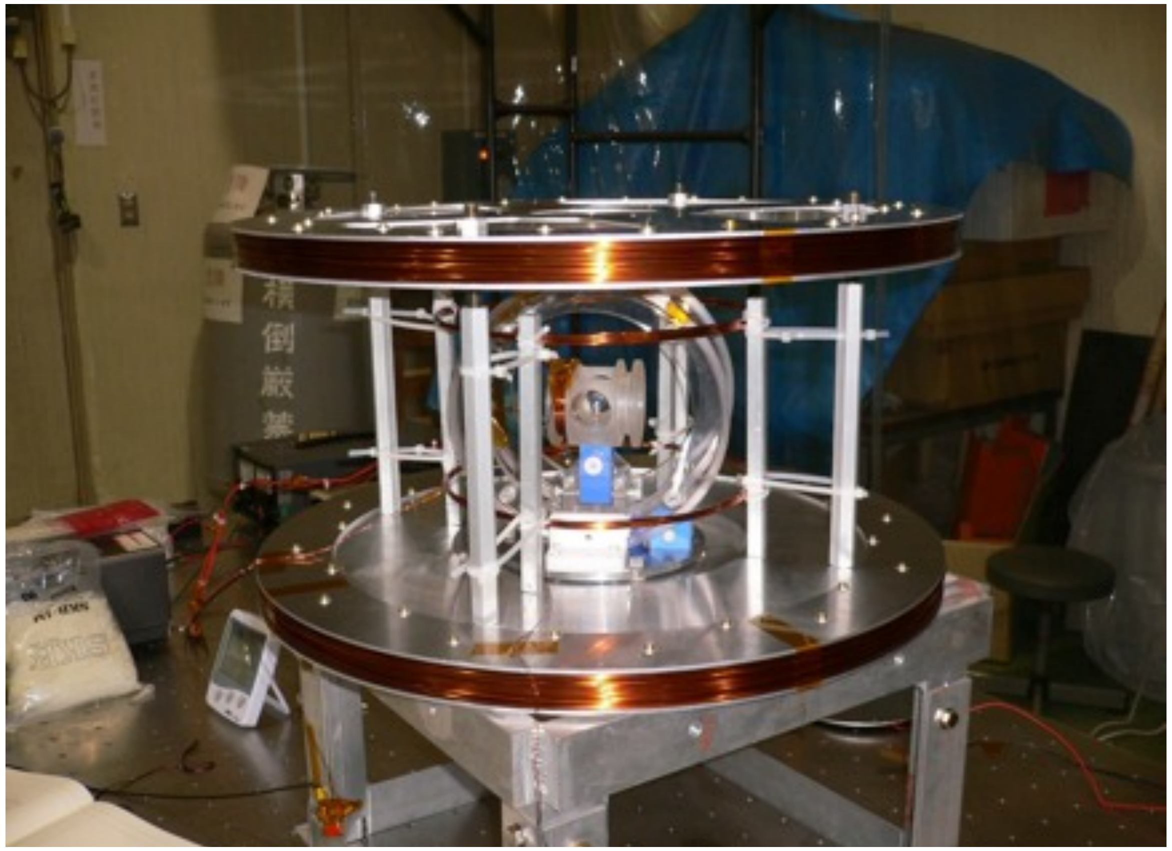

Magnetometer

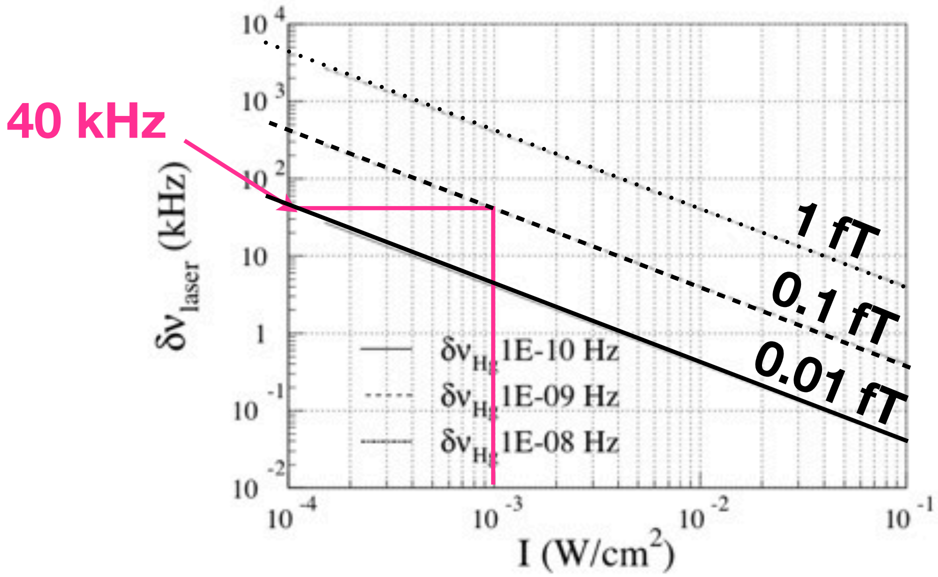

Fig. 11. 入射レーザ強度 (I) と許容強度変動量 ($\delta\nu_{laser}$) の関係. 各直線はそれぞれ目標とする ^{199}Hg ラーマー周波数測定精度 ($\delta\nu_{Hg}$) が異なる.

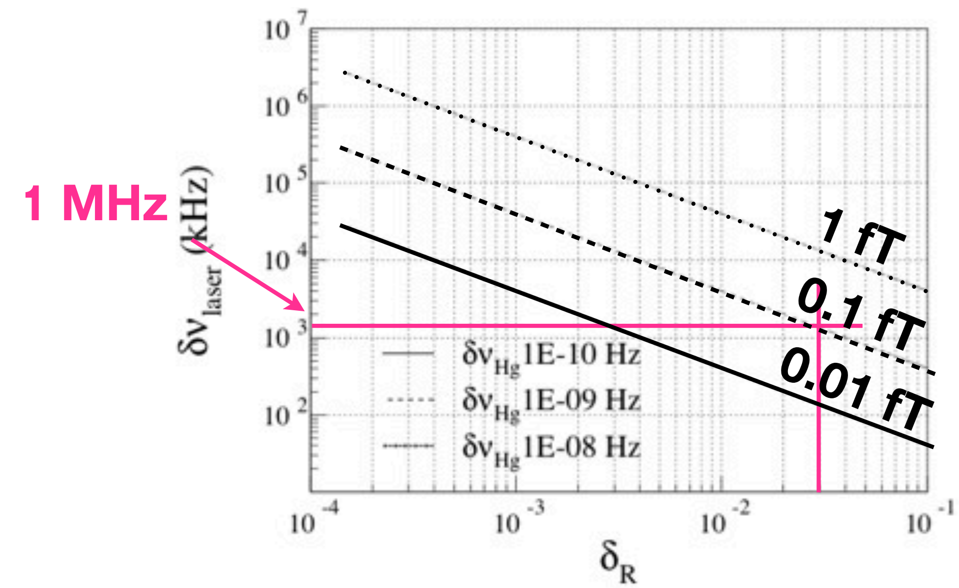

Fig. 13. 強度変動量 (δ_R) と周波数絶対精度 ($\delta\nu_{laser}$) の関係。各直線はそれぞれ目標とする ^{199}Hg ラーマー周波数測定精度 ($\delta\nu_{Hg}$) が異なる。

Frequency stability < 40 kHz
→ Laser power 1mW / cm^2

Absolute accuracy < 1 MHz
→ Power stability < 3%

Laser setup and Cell test is on-going...

単結晶を用いたEDM測定

測定感度

$$\sigma_D = \frac{(\hbar/2)}{\alpha E t N^{1/2}}$$

UCN

ultracold neutron

$E \sim 10^4$ V cm^{-1}

$t \sim 10^3$ s

$Et \sim 10^7$ V s cm^{-1}

$Et \sim 10^6$ V s cm^{-1}

Diffraction

cold neutron

$E \sim 10^8 - 10^9$ V cm^{-1}

$t \sim 10^{-2}$ s

$Et \sim 10^6 - 10^7$ V s cm^{-1}

$$f(\boldsymbol{q}) = f_0 + f_{\rm Schw}(\boldsymbol{q}) + f_{\rm EDM}(\boldsymbol{q})$$

$$f_0 = a$$

$$f_{\rm Schw}(\boldsymbol{q}) = i\frac{2e\mu_n}{\hbar c}(Z - F(q))\frac{\boldsymbol{\sigma}\cdot(\boldsymbol{k}\times\boldsymbol{q})}{q^2}$$

$$f_{\rm EDM}(\boldsymbol{q}) = i\frac{2med_n}{\hbar^2}(Z - F(q))\frac{\boldsymbol{\sigma}\cdot\boldsymbol{q}}{q^2}$$

$$F(\boldsymbol{q}) = \int \rho(\boldsymbol{q}) e^{i\boldsymbol{q}\cdot\boldsymbol{r}} d^3 r$$

結晶の回折によるEDM探索

nEDM測定精度

$$(\Delta d_n)_{\rm stat} = \frac{\hbar/2}{\alpha E T\sqrt{N}},$$

非中心対称性結晶内電場での回折の際のスピン回転を精密測定

$E\sim10^9$ V/cm ⇒ UCN蓄積

$T\sim10^{-3\sim-2}$ s

$E\sim10^4$ V/cm

$T\sim10^3$ s

***ET* は同程度**

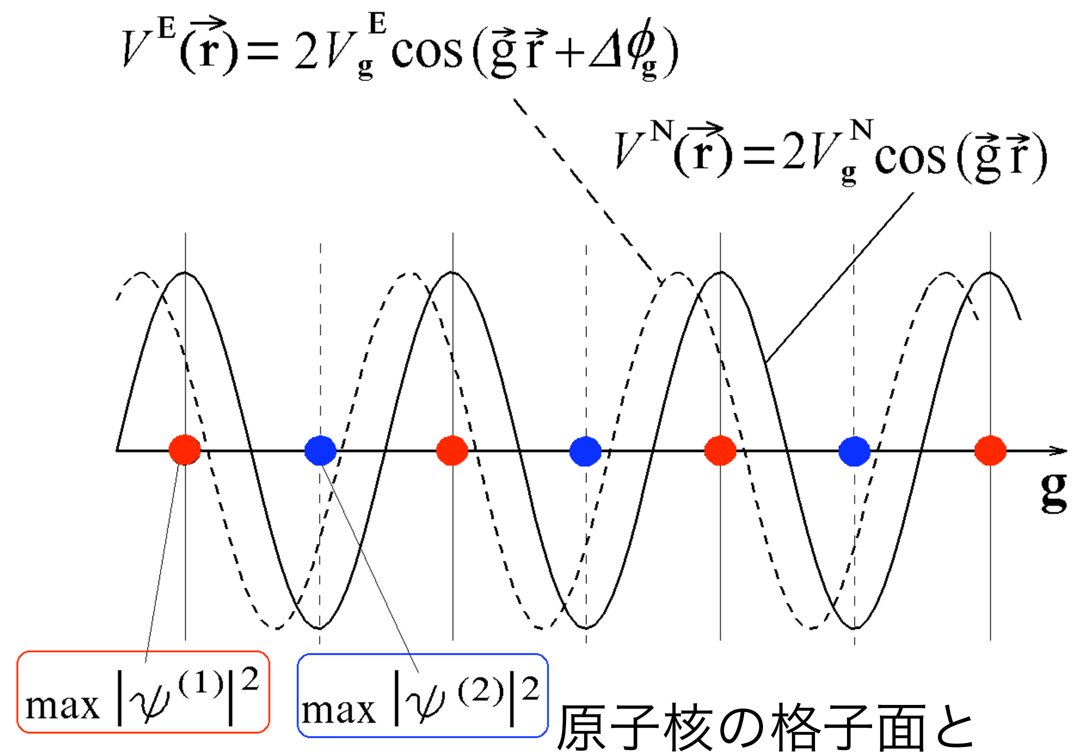

原子核の格子面と電場の格子面がズレている

⇒ Bragg近傍での散乱で強い電場を感じる

スピン回転

90度入射でゼロ

$$\varphi = \varphi_S + \varphi_{\rm EDM} = \frac{2E\mu_n L v_{\parallel}}{c\hbar v_{\perp}} + \frac{2E d_n L}{\hbar v_{\perp}}$$

Schwinger effect

電場内を磁気モーメントが動くので磁場を感じてスピン回転

EDM

入射エネルギー依存性で分離可能

$$\psi(\mathbf r) = e^{-i\,\mathbf{kr}} + a\cdot e^{-i(\mathbf k+\mathbf g)\mathbf r}$$

$$\mathbf E = \mathbf E_{\mathbf g}\cdot\frac{|V_{\mathbf g}|}{E_{\mathbf k}-E_{\mathbf k_{\mathbf g}}}$$

$$\mathbf E_g = \mathbf g\cdot V_g^E \sin\Delta\phi_g$$

⇒ **UCN以外での10^{-26} ecmの検証、新物理探索**

結晶の回折によるEDM探索

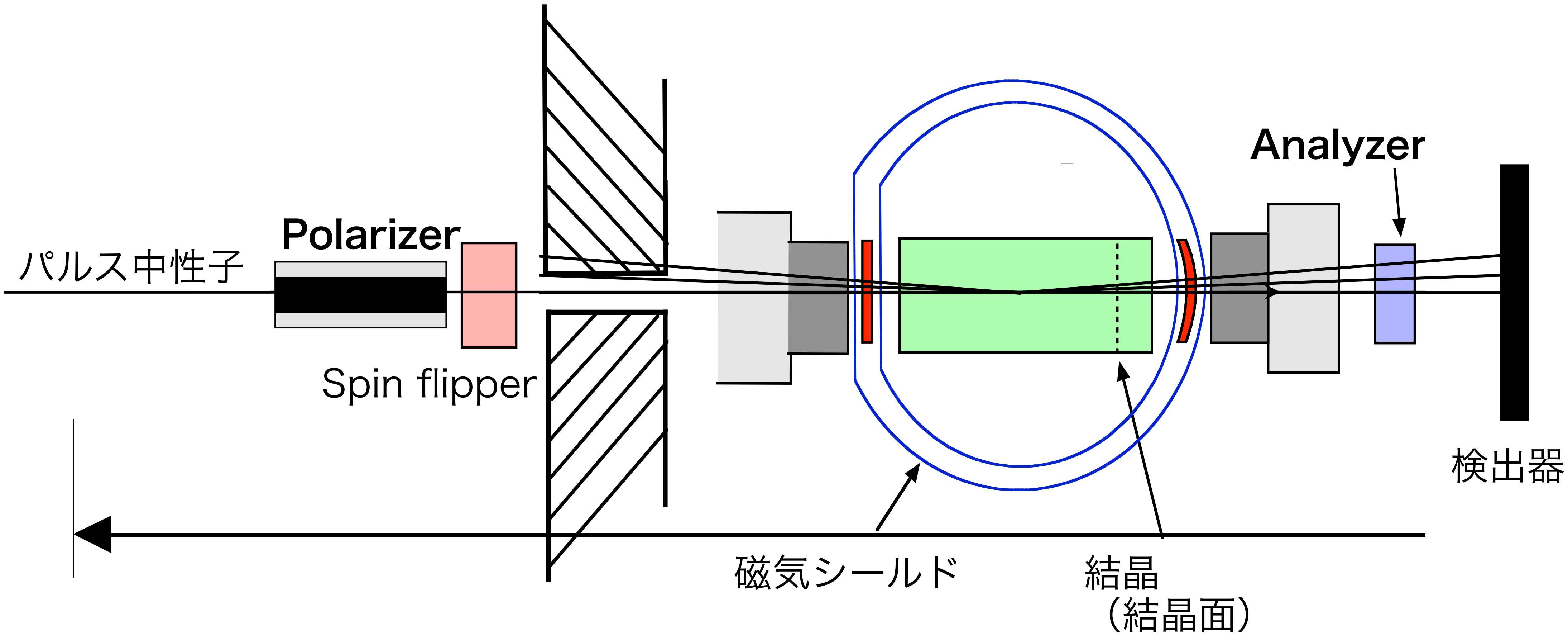

統計誤差 $(\Delta d_n)_{\rm stat} = \dfrac{\hbar/2}{\alpha E T \sqrt{N}},$ 現状、統計が制限

$\boldsymbol{E}$：**より高電場を持つ結晶の探索** SiO_2 → BGO → BSO

$\boldsymbol{T}$：**より大きな（長い）結晶の作成** 1cc → 1L

$\boldsymbol{N}$：**より大きな（断面積）結晶の作成**

⇒ 10^{-26} ecm/ yr

系統誤差

残留磁場	10^{-4} Gauss
磁場変動	10^{-5} Gauss/h
スピン解析誤差	10^{-3} rad
結晶アラインメント精度	0.02 deg
結晶温度制御	0.01 deg

⇒ ～6×10^{-27} ecm

3.2. T-violation in Compound Nuclei

nA反応におけるT-violation

隣接するs波共鳴とp波共鳴の干渉領域では、非対称度が増幅する

P-violation では 増幅率〜10^6 の核種が知られている

$$\Delta\sigma_{\mathrm{P}}^{nA} \leq \Delta\sigma_{\mathrm{P}}^{NN} \times 10^6$$

T-violation でも同様の増幅効果

meson交換によるEDM（chromo-EDM）のみ着目

$$\left|\Delta\sigma_{\mathrm{T}}^{nA}\right| \leq 10^6 \times \kappa(J) \left[\bar{g}_\pi^{(0)} + 0.26\bar{g}_\pi^{(1)} - 0.0012\bar{g}_\eta^{(0)} + 0.0034\bar{g}_\eta^{(1)} - 0.0071\bar{g}_\rho^{(0)} + 0.0035\bar{g}_\rho^{(1)} + 0.0019\bar{g}_\omega^{(0)} - 0.00063\bar{g}_\omega^{(1)}\right]$$

$$\simeq 10^5[\mathrm{b}] \times \kappa(J) \times \bar{g}_\pi^{(0)}$$

nEDMの上限値　$|d_n| < 2.9 \times 10^{-26}[\mathrm{e\ cm}]$ は　$\bar{g}_\pi^{(0)} < 2.5 \times 10^{-10}$ に対応

$$\Rightarrow \quad \left|\Delta\sigma_{\mathrm{T}}^{nA}\right| < 2.5 \times 10^{-4}[\mathrm{b}] \times \kappa(J)$$

$0.25[\mathrm{mb}] \times \kappa(J)$ より高い精度で測定すると、
nEDMより高感度で新物理探索

κ (J)が大きい方が実験に有利

κ (J)は標的核スピン(I)、複合核スピン(J)、
p波部分波間の混合角(θ)の関数で、オーダーで変化する

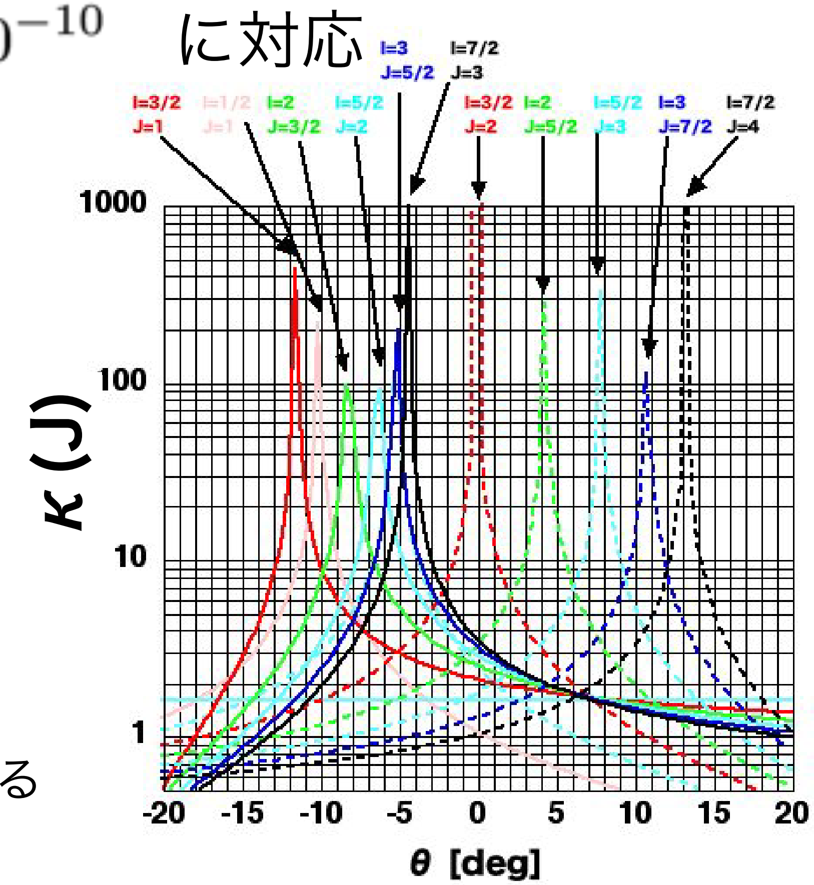

複合核共鳴におけるT-violation

$$f = A' + B'\,\sigma\bullet I + C'\,\sigma\bullet k + D'\,\sigma\bullet(I\times k)$$

$$\sigma\cdot(k\times I)$$

neutron spin (σ), *neutron momentum* (k), *target spin* (I)

$$\Delta\sigma_{CP} = \sigma^{+} - \sigma^{-}$$

σ^{+} = *p-wave resonance cross section in*

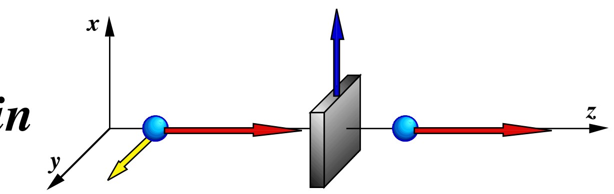

σ^{-} = *p-wave resonance cross section in*

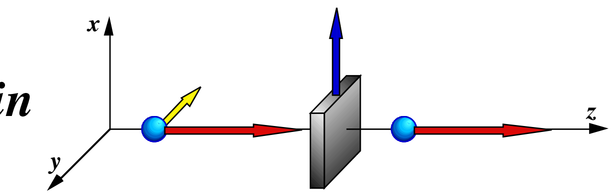

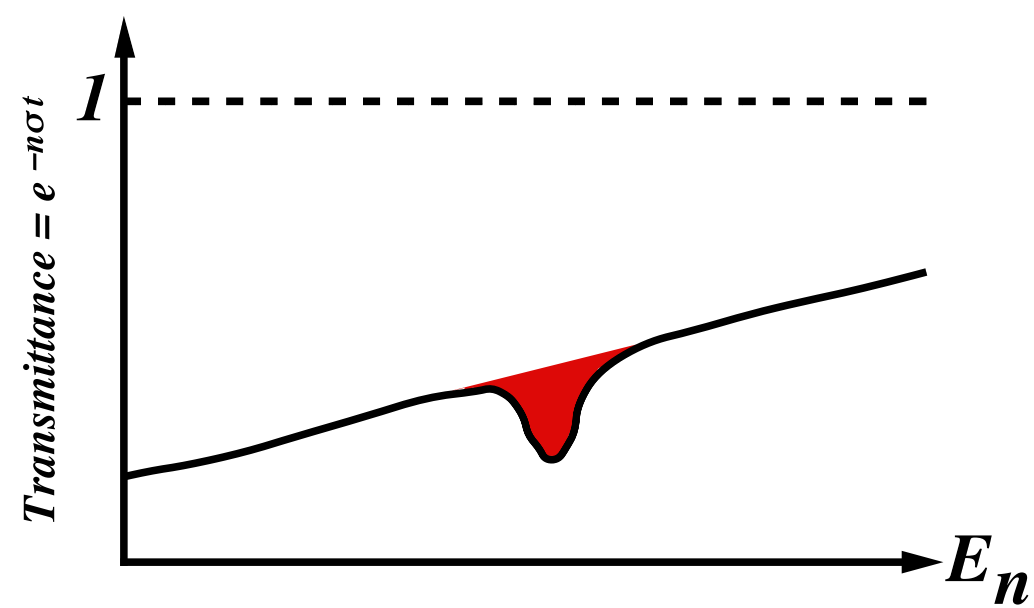

Gudkov, Phys. Rep. 212 (1992) 77

$$\Delta\sigma_{\rm CP} = \kappa(J)\frac{w}{v}\Delta\sigma_{\rm P}$$

T-violation

測定すべき非対称度

g_{CP}/g_P **10^{-3}**

P-violation **$10^{-2}\sigma_{\rm tot}$**

$$\kappa(J=I+\frac{1}{2}) = \frac{3}{2\sqrt{2}}\left(\frac{2I+1}{2I+3}\right)\frac{\sqrt{2I+1}(2\sqrt{I}x-\sqrt{2I+3}y)}{(2I-3)\sqrt{2I+3}x-(2I+9)\sqrt{I}y}$$

$$\kappa(J=I-\frac{1}{2}) = -\frac{3}{2\sqrt{2}}\left(\frac{(2I+1)\sqrt{I}}{\sqrt{(I+1)(2I-1)}}\right)\frac{2\sqrt{I+1}x+\sqrt{2I-1}y}{(I+3)\sqrt{2I-1}x+(4I-3)\sqrt{I+1}y}$$

$$x^2 = \frac{\Gamma^n_{p,1/2}}{\Gamma^n_p} \qquad y^2 = \frac{\Gamma^n_{p,3/2}}{\Gamma^n_p}$$

$$x^2+y^2=1$$

$$x=\cos\phi \qquad y=\sin\phi$$

Candidate Resonances for the T-violation Experiment

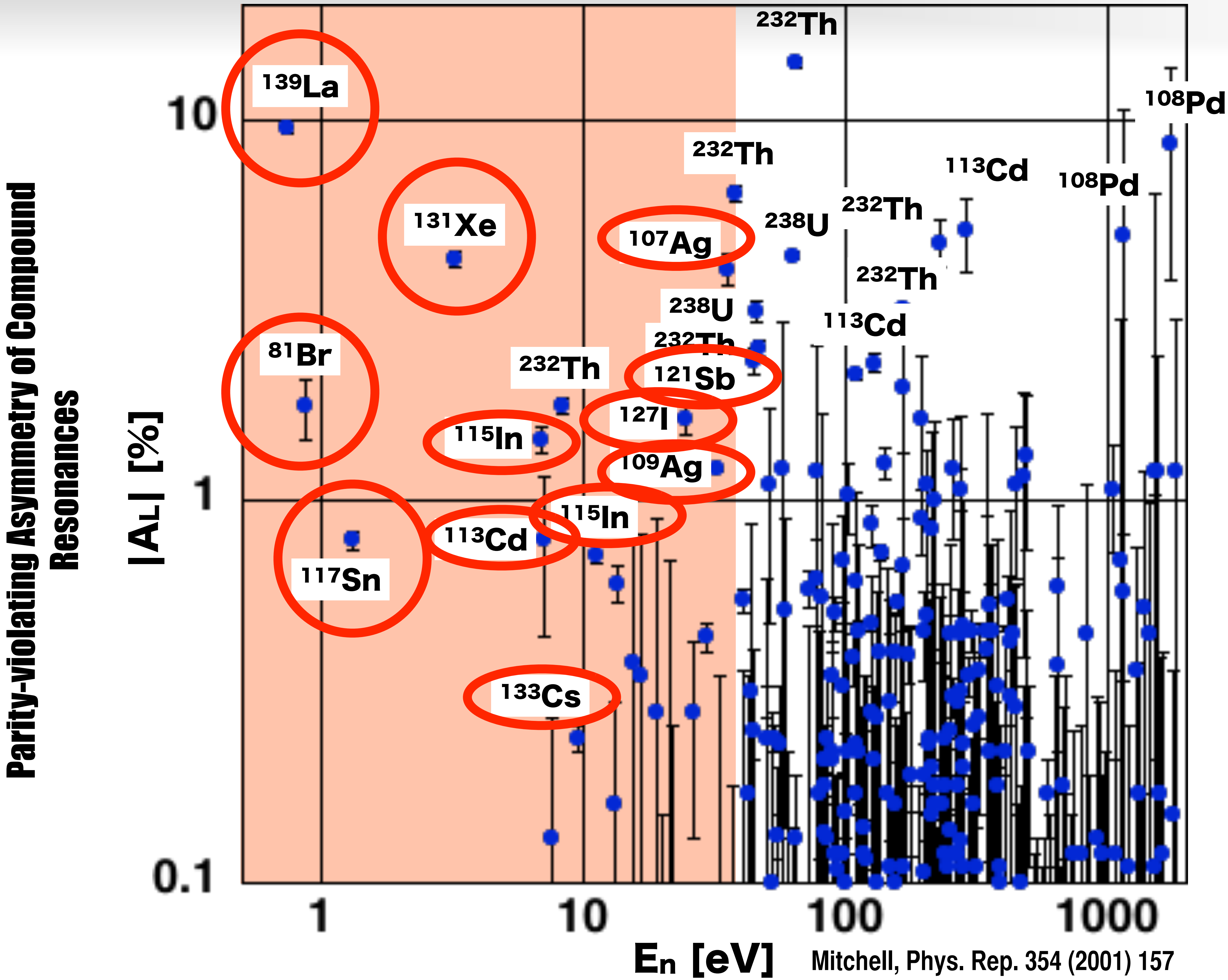

Mitchell, Phys. Rep. 354 (2001) 157

Y.-H.Song et al., Phys. Rev. C83 (2011) 065503

$$
\begin{aligned}
V_{\mathrm{PT}} = & \left[-\frac{\bar{g}_\eta^{(0)} g_\eta}{2m_N} \frac{m_\eta^2}{4\pi} Y_1(x_\eta) + \frac{\bar{g}_\omega^{(0)} g_\omega}{2m_N} \frac{m_\omega^2}{4\pi} Y_1(x_\omega) \right] \boldsymbol{\sigma}_- \cdot \hat{\boldsymbol{r}} \\
& + \left[-\frac{\bar{g}_\pi^{(0)} g_\pi}{2m_N} \frac{m_\pi^2}{4\pi} Y_1(x_\pi) + \frac{\bar{g}_\rho^{(0)} g_\rho}{2m_N} \frac{m_\rho^2}{4\pi} Y_1(x_\rho) \right] \boldsymbol{\tau}_1 \cdot \boldsymbol{\tau}_2 \boldsymbol{\sigma}_- \cdot \hat{\boldsymbol{r}} \\
& + \left[-\frac{\bar{g}_\pi^{(2)} g_\pi}{2m_N} \frac{m_\pi^2}{4\pi} Y_1(x_\pi) + \frac{\bar{g}_\rho^{(2)} g_\rho}{2m_N} \frac{m_\rho^2}{4\pi} Y_1(x_\rho) \right] T_{12}^z \boldsymbol{\sigma}_- \cdot \hat{\boldsymbol{r}} \\
& + \left[-\frac{\bar{g}_\pi^{(1)} g_\pi}{2m_N} \frac{m_\pi^2}{4\pi} Y_1(x_\pi) + \frac{\bar{g}_\eta^{(1)} g_\eta}{2m_N} \frac{m_\eta^2}{4\pi} Y_1(x_\eta) + \frac{\bar{g}_\rho^{(1)} g_\rho}{2m_N} \frac{m_\rho^2}{4\pi} Y_1(x_\rho) + \frac{\bar{g}_\omega^{(1)} g_\omega}{2m_N} \frac{m_\omega^2}{4\pi} Y_1(x_\omega) \right] \tau_+ \boldsymbol{\sigma}_- \cdot \hat{\boldsymbol{r}} \\
& + \left[-\frac{\bar{g}_\pi^{(1)} g_\pi}{2m_N} \frac{m_\pi^2}{4\pi} Y_1(x_\pi) - \frac{\bar{g}_\eta^{(1)} g_\eta}{2m_N} \frac{m_\eta^2}{4\pi} Y_1(x_\eta) - \frac{\bar{g}_\rho^{(1)} g_\rho}{2m_N} \frac{m_\rho^2}{4\pi} Y_1(x_\rho) + \frac{\bar{g}_\omega^{(1)} g_\omega}{2m_N} \frac{m_\omega^2}{4\pi} Y_1(x_\omega) \right] \tau_+ \boldsymbol{\sigma}_+ \cdot \hat{\boldsymbol{r}}
\end{aligned}
$$

$$
\boldsymbol{\sigma}_\pm = \boldsymbol{\sigma}_1 \pm \boldsymbol{\sigma}_2 \qquad \boldsymbol{r} = \boldsymbol{r}_1 - \boldsymbol{r}_2 \qquad x_a = m_a r
$$

$$
T_{12}^z = 3\tau_1^z \tau_2^z - \boldsymbol{\tau}_1 \cdot \boldsymbol{\tau}_2 \qquad Y_1(x) = \left(1 + \frac{1}{x}\right) \frac{e^{-x}}{x}
$$

$$
g_\pi = 13.07, \quad g_\eta = 2.24, \quad g_\rho = 2.75, \quad g_\omega = 8.25
$$

$$d_n = \frac{e}{m_N}\frac{g_\pi(\bar{g}_\pi^{(0)} - \bar{g}_\pi^{(2)})}{4\pi^2}\ln\frac{m_N}{m_\pi} \simeq 0.14(\bar{g}_\pi^{(0)} - \bar{g}_\pi^{(2)})$$

$$|d_n| < 2.9\times 10^{-26}\,\mathrm{e\,cm} \rightarrow \bar{g}_\pi^{(0)} < 2.5\times 10^{-10}$$

$$\left|d(^{199}\mathrm{Hg})\right| < 2.1\times 10^{-28}\,\mathrm{e\,cm} \rightarrow \bar{g}_\pi^{(1)} < 0.5\times 10^{-11}$$

$$\frac{\Delta\sigma_{\mathrm{PT}}}{2\sigma_{\mathrm{tot}}} = \frac{-0.185\mathrm{b}}{2\sigma_{\mathrm{tot}}}\left[\bar{g}_\pi^{(0)} + 0.26\bar{g}_\pi^{(1)} - 0.0012\bar{g}_\eta^{(0)} + 0.0034\bar{g}_\eta^{(1)}\right.$$
$$\left.-0.0071\bar{g}_\rho^{(0)} + 0.0035\bar{g}_\rho^{(1)} + 0.0019\bar{g}_\omega^{(0)} - 0.00063\bar{g}_\omega^{(1)}\right]$$

10^6 10^2

0.5×10^{-10}[b] ⇒ 0.5×10^{-4}[b] ⇒ 0.5×10^{-2}[b]

実験の概念図

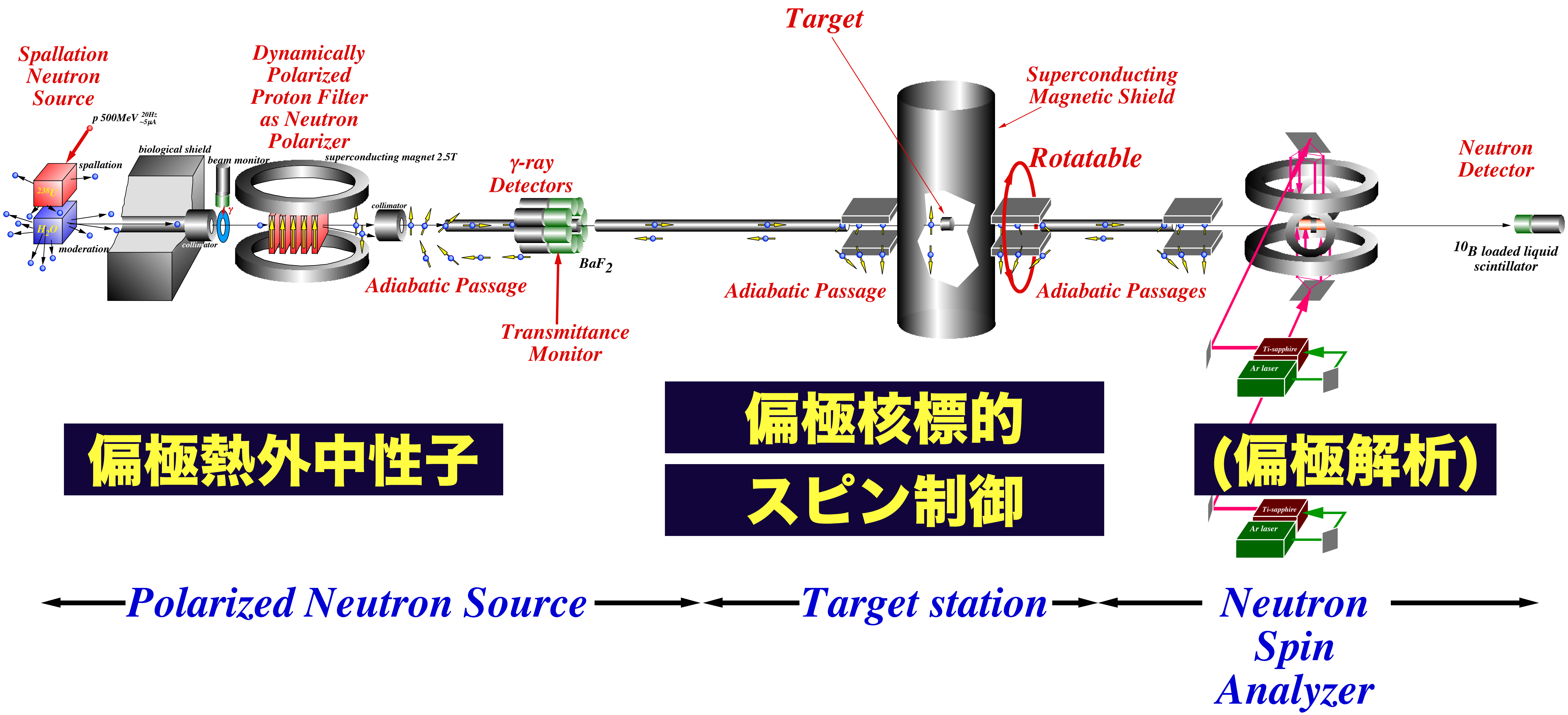
Spallation Neutron Source
p 500MeV
biological shield
beam monitor
spallation
moderation
collimator
Dynamically Polarized Proton Filter as Neutron Polarizer
superconducting magnet 2.5T
collimator
γ-ray Detectors
BaF2
Adiabatic Passage
Transmittance Monitor
Target
Superconducting Magnetic Shield
Rotatable
Adiabatic Passage
Adiabatic Passages
Neutron Detector
10B loaded liquid scintillator
偏極熱外中性子
偏極核標的
スピン制御
(偏極解析)
Polarized Neutron Source
Target station
Neutron Spin Analyzer

(n,γ)測定

xの決定 → Weak行列要素の決定 → 統計的扱いの妥当性

→ 核力に含まれる対称性の破れ

κの大きな共鳴

← New Physics の各モデルの計算

← 偏極子　標的核偏極　Spin制御

← 光学的記述の妥当性範囲の実験的検証

↓

時間反転対称性の破れ　　New Physicsの発見

3. Gravity

-Medium Range Force Search-

Gravity

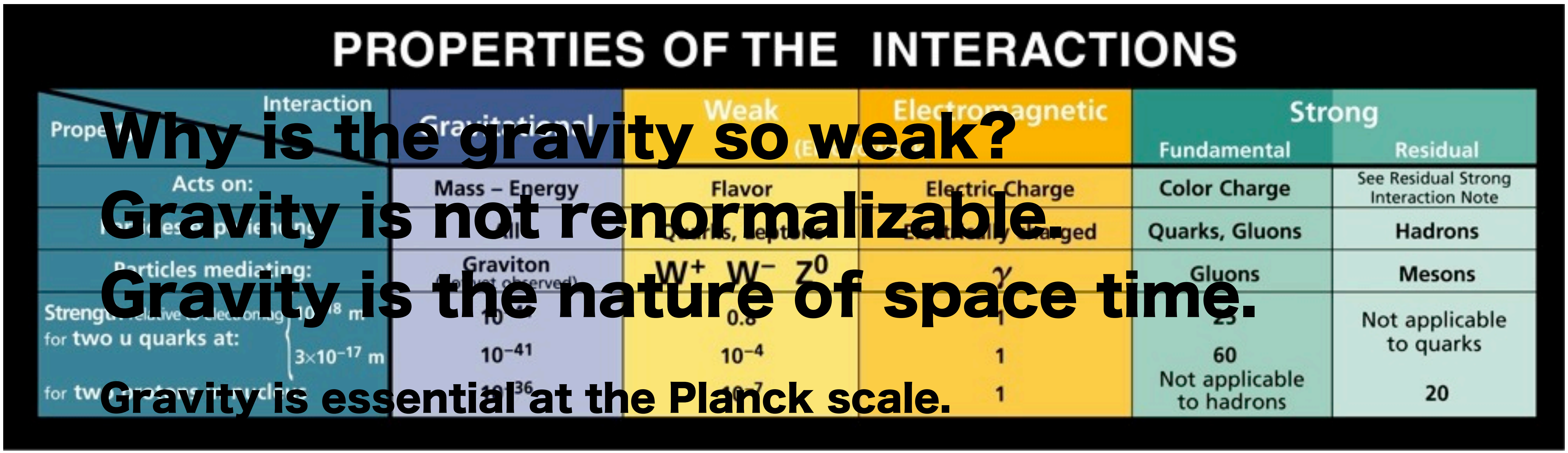

PROPERTIES OF THE INTERACTIONS

Property \ Interaction	Gravitational	Weak (Electroweak)	Electromagnetic	Strong: Fundamental	Strong: Residual
Acts on:	Mass – Energy	Flavor	Electric Charge	Color Charge	See Residual Strong Interaction Note
Particles experiencing:	All	Quarks, Leptons	Electrically Charged	Quarks, Gluons	Hadrons
Particles mediating:	Graviton (not yet observed)	W^+ W^- Z^0	γ	Gluons	Mesons
Strength relative to electromag for two u quarks at: 10^{-18} m	10^{-41}	0.8	1	25	Not applicable to quarks
3×10^{-17} m	10^{-41}	10^{-4}	1	60	
for two protons in nucleus	10^{-36}	10^{-7}	1	Not applicable to hadrons	20

Why is the gravity so weak?

Gravity is not renormalizable.

Gravity is the nature of space time.

Gravity is essential at the Planck scale.

"hierarchy problem": M_{GUT}~10^{24}eV ⇔ $M_{SU(2)\times U(1)}$~10^{11}eV

Phenomena out of the standard model is existing.

Neutrino Oscillation, Dark Energy, Dark Matter

Super-K, SNO, KamLAND WMAP

Gravity

3-dim. Gravity

$$F_3(r) = G_3 \frac{m_1 m_2}{r^2}$$

N-dim. Gravity

$$F_N(r) = G_N \frac{m_1 m_2}{r^{N-1}}$$

continuity at r=R*

$$\frac{G_3}{R^{*2}} = \frac{G_N}{R^{*N-1}} \Rightarrow G_3 = \frac{G_N}{R^{*N-3}}$$

If R* is longer than the Planck's length, G_3 becomes smaller.

Parametrization: $V(r)=-(GM/r)(1+\alpha e^{-r/\lambda})$

KK-graviton, which is emitted off our brane with the momentum (q_1, q_2, ...,q_n) along the extradimension, looks having the mass |q|.

momentum is quantized in the unit of $2\pi/L$ in the extra-dimension

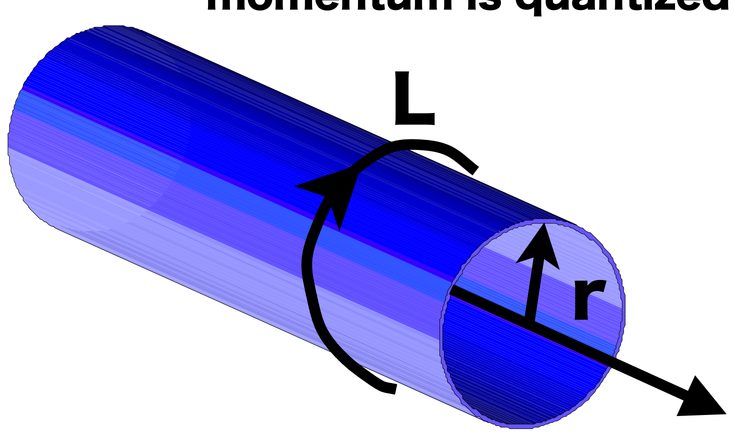

$$\frac{V(r)}{m_1 m_2} = G_3 \sum_{(k_1,\ldots k_n)} \frac{e^{-(2\pi|k|/L)r}}{r} \xrightarrow[r<<L]{} G_3 \frac{1}{r}\left(\frac{L}{2\pi r}\right)^n \int d^n u e^{-|u|}$$

短距離重力

Newtonian　　exotic interaction (Yukawa-type)

$$V_G(r) = V_g(r)\cdot\left(1 + \alpha\exp(-r/\lambda)\right) \qquad \left(V_g(r) = -G\frac{M\cdot m}{r}\right)$$

Newton重力からのズレを探索する

例えばADD model

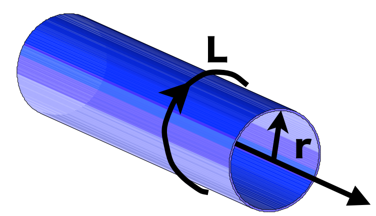

N次元のうち3次元以外はコンパクト化されている

3次元空間における重力

$$F_3(r) = G_3\frac{m_1 m_2}{r^2}$$

N次元空間における重力

$$F_N(r) = G_N\frac{m_1 m_2}{r^{N-1}}$$

r=R*において接続

$$\frac{G_3}{R^{*2}} = \frac{G_N}{R^{*N-1}} \Rightarrow G_3 = \frac{G_N}{R^{*N-3}}$$

$$\frac{V(r)}{m_1 m_2} = G_3\sum_{(k_1,\ldots,k_n)}\frac{e^{-(2\pi|k|/L)r}}{r} \xrightarrow[r<<L]{} G_3\frac{1}{r}\left(\frac{L}{2\pi r}\right)^n\int d^n u\, e^{-|u|}$$

希ガスによる小角散乱

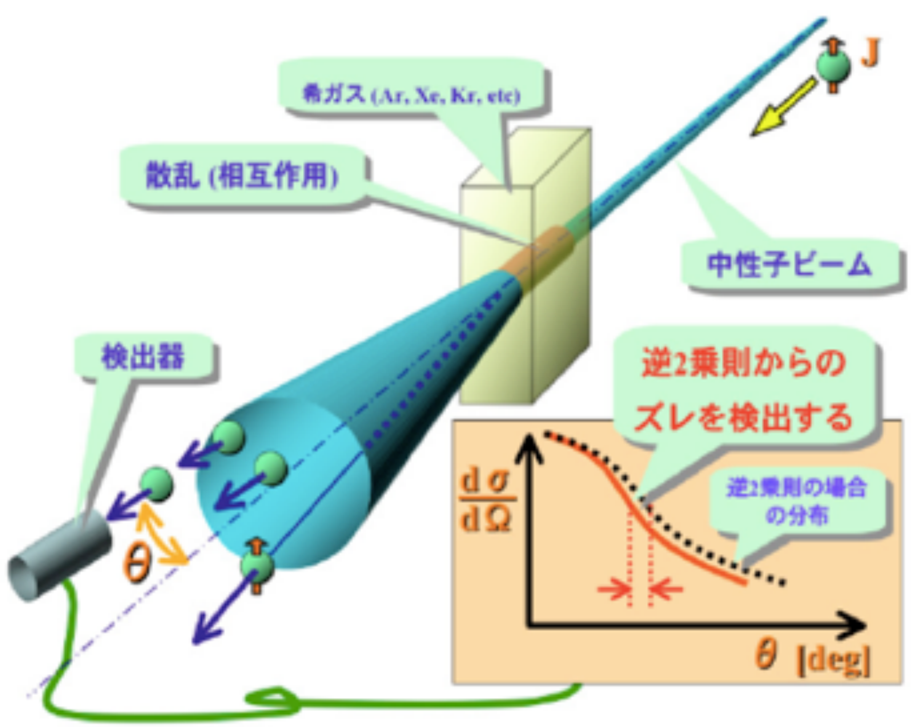

重力を含めた断面積

$$\frac{d\sigma(\theta)}{d\Omega} = \left[a_N + a_{ne}ZF_e(\theta) + a_G F_G(\theta)\right]^2$$

$$\cong a_N^2 + 2a_N a_{ne}ZF_e(\theta) + a_{ne}^2 Z^2 F_e(\theta)^2 + 2a_N a_G F_G(\theta)$$

$a_G \propto \alpha$

$$\frac{d\sigma_G(\theta)}{d\Omega} = 2\cdot\sigma_N^{1/2}\cdot\alpha\cdot\left(\frac{G\cdot m_n\cdot M}{4}\right)\cdot\left(\frac{1}{\frac{1}{m_n c^2}\left(\frac{\hbar c}{\lambda}\right)^2 + 8E_n\sin^2\frac{\theta}{2}}\right)$$

短距離重力

希ガスによる小角散乱

BL05非偏極

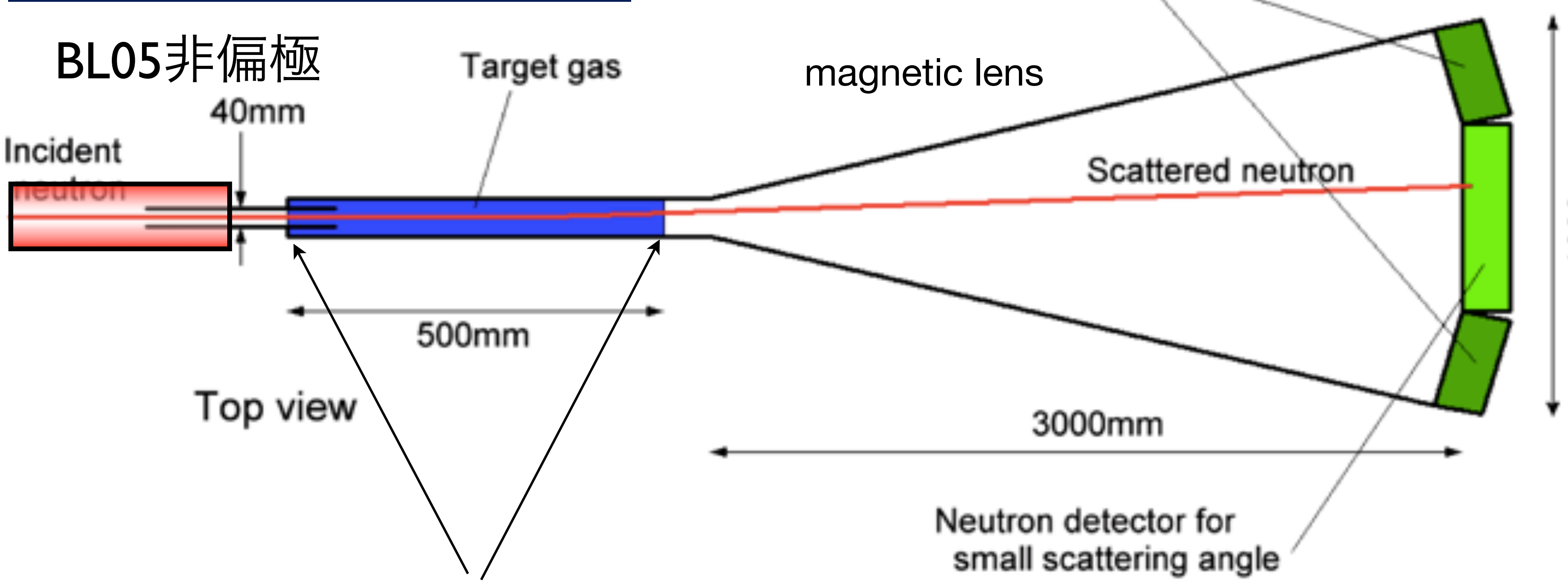

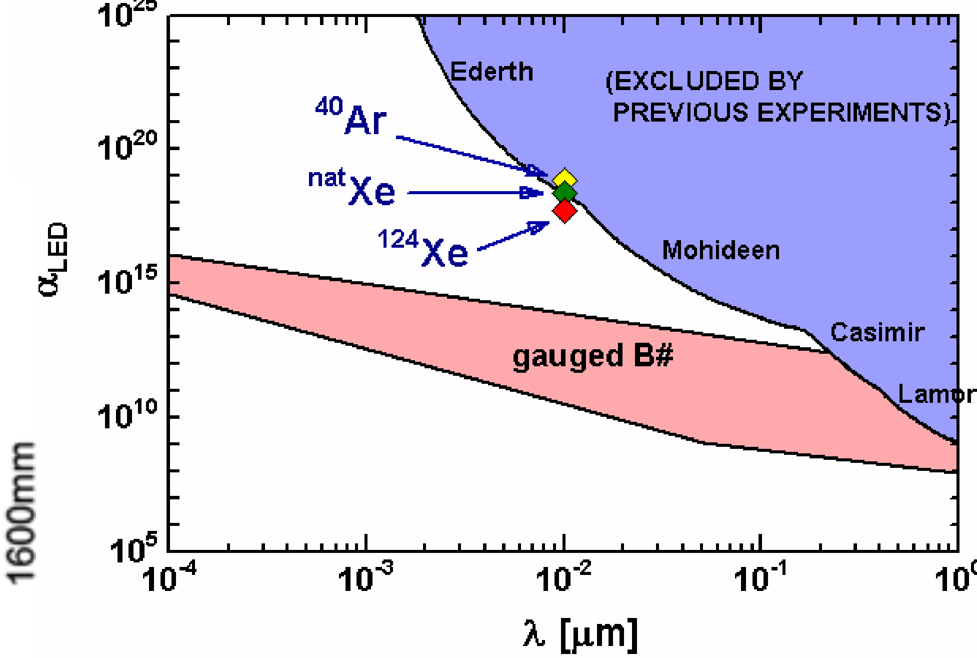

ターゲット容器窓による散乱を抑え、理解する

散乱強度分布をシミュレーション

核データの高精度化（～1%）

$\sigma_N(^{nat}Xe)=2.96$ b
$\sigma_N(^{124}Xe)=0.141$ b

磁気レンズによる集光小角散乱

→小角分解能向上

口径の大きいレンズ

→**2年でα～$10^{17\sim18}$**

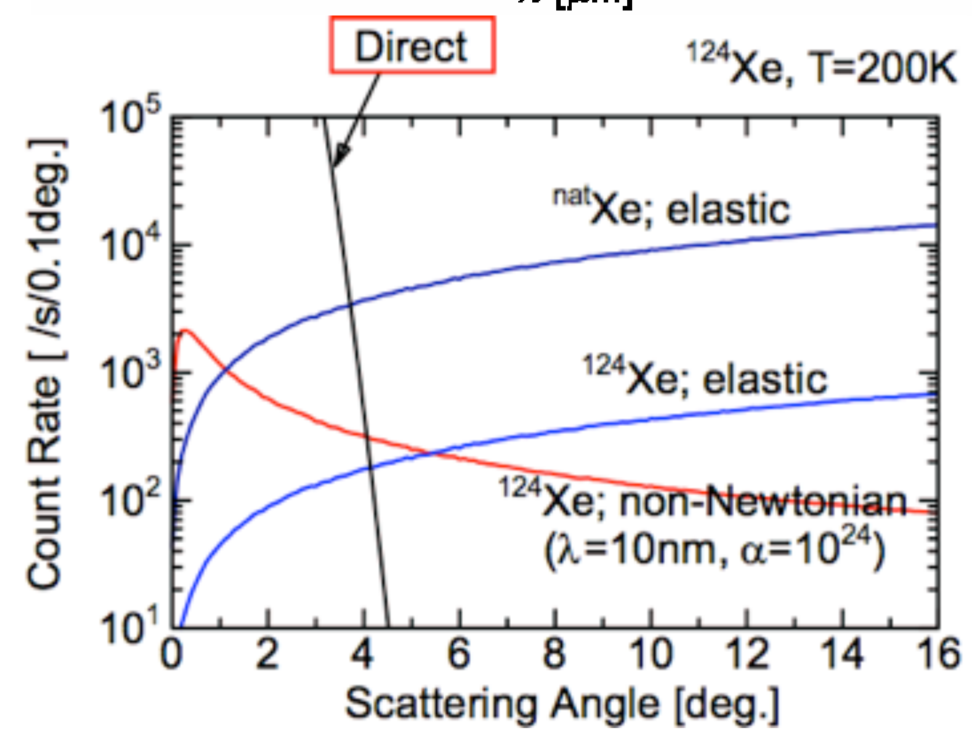

中性子干渉計

干渉計の片経路の重力ポテンシャルを位相シフトから検出

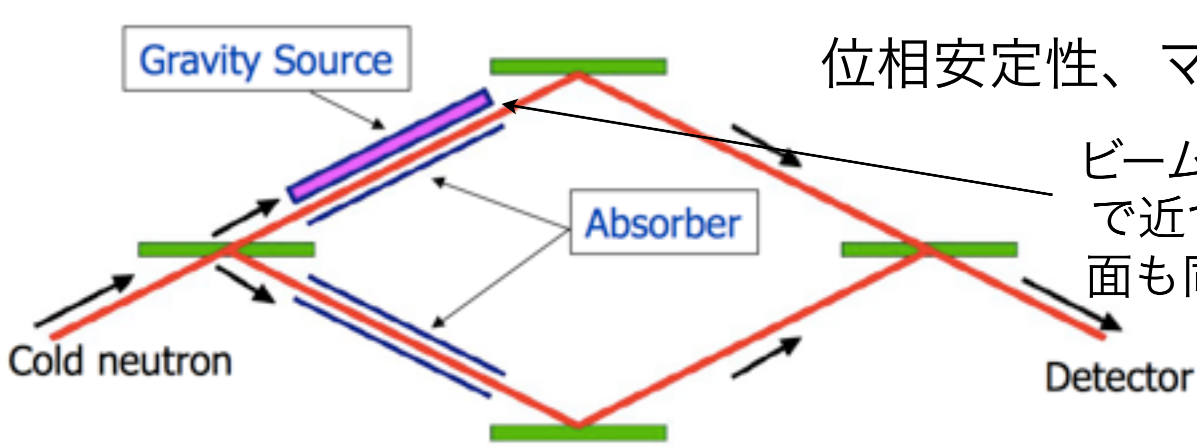

位相安定性、マイクロビームの強度

ビームとのギャップを1μmまで近づけられれば（ビーム断面も同程度）ADD N=3 の検証の可能性がある

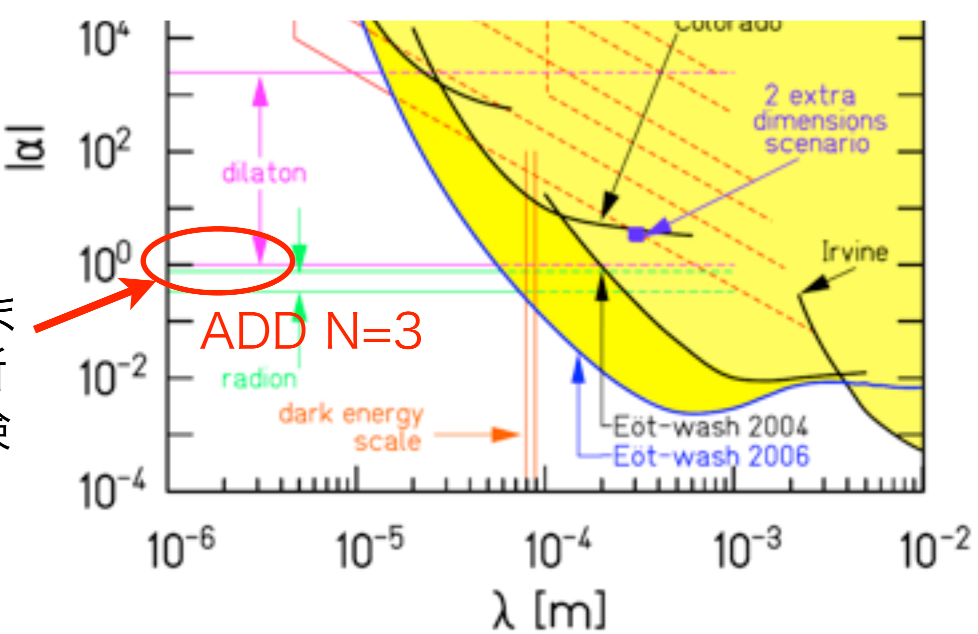

Possible Sensitivity of Multilayer Neutron Interferometer

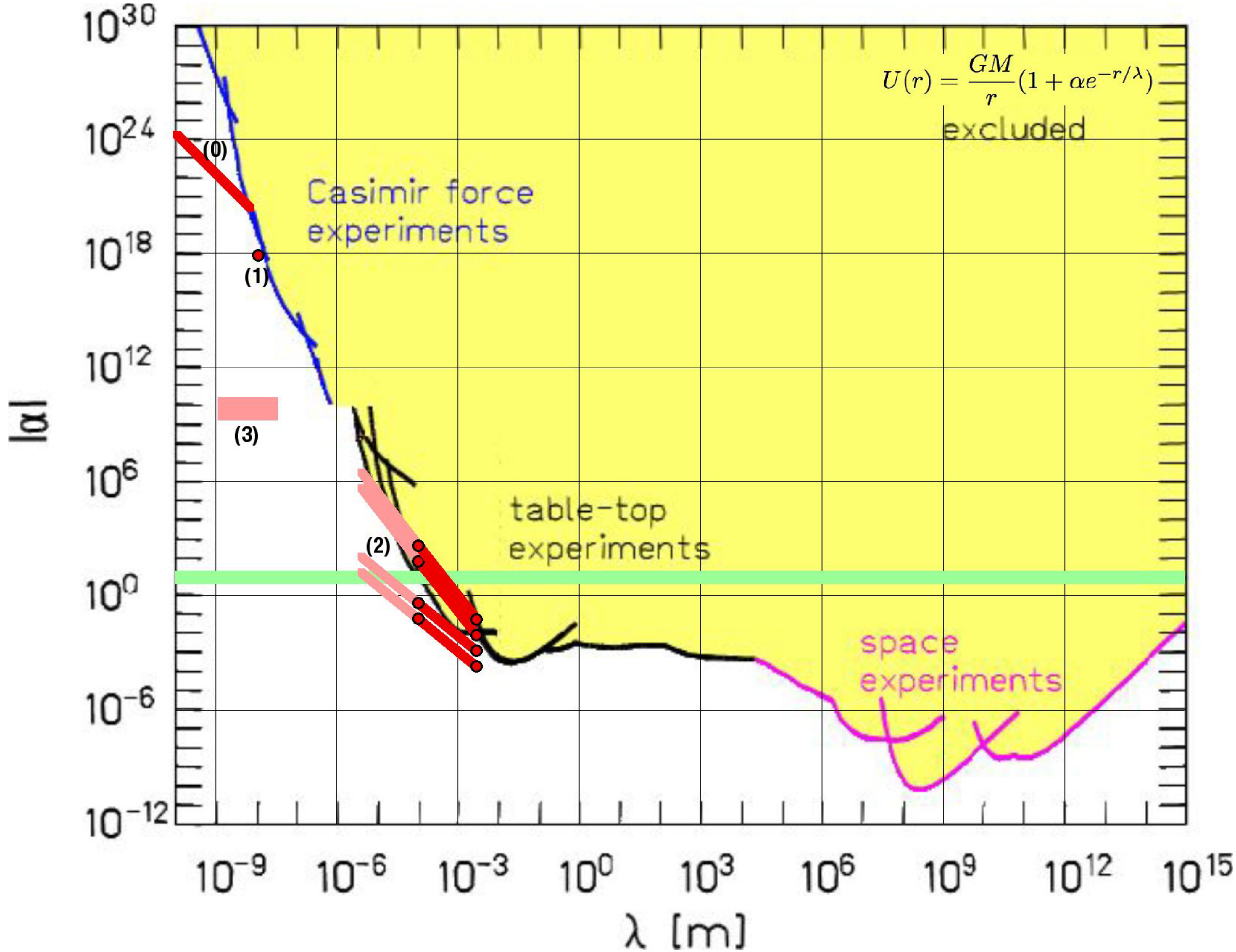

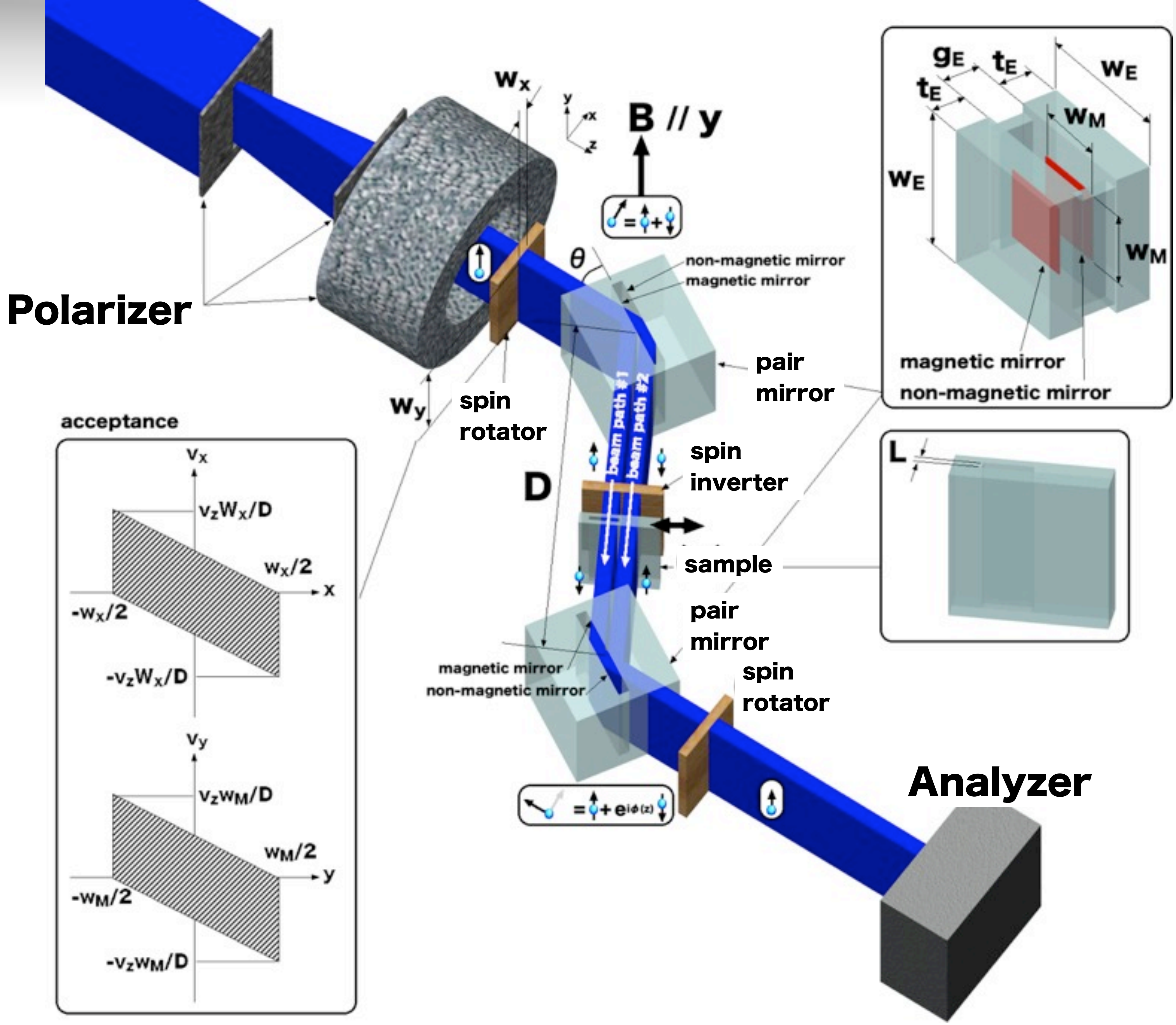
Polarizer
w_x
B // y
θ
non-magnetic mirror
magnetic mirror
w_y
spin
rotator
pair
mirror
acceptance
v_x
$v_z w_x/D$
$w_x/2$
x
$-w_x/2$
$-v_z w_x/D$
v_y
$v_z w_M/D$
$w_M/2$
y
$-w_M/2$
$-v_z w_M/D$
D
beam path #1
beam path #2
spin
inverter
sample
pair
mirror
magnetic mirror
non-magnetic mirror
spin
rotator
Analyzer
g_E
t_E
t_E
w_E
w_M
w_E
w_M
magnetic mirror
non-magnetic mirror
L

ボーズ凝縮体の超高分解能光会合分光によるナノスケールでの重力補正項の探索

Approach : Photo-association

[M. Kitagawa, et al., PRA **77**, 012719(2008)]

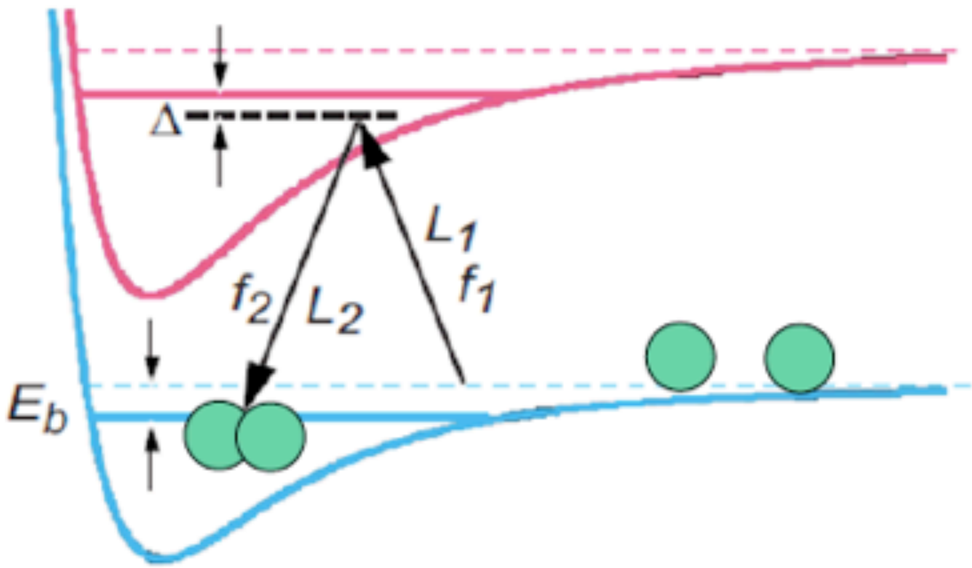

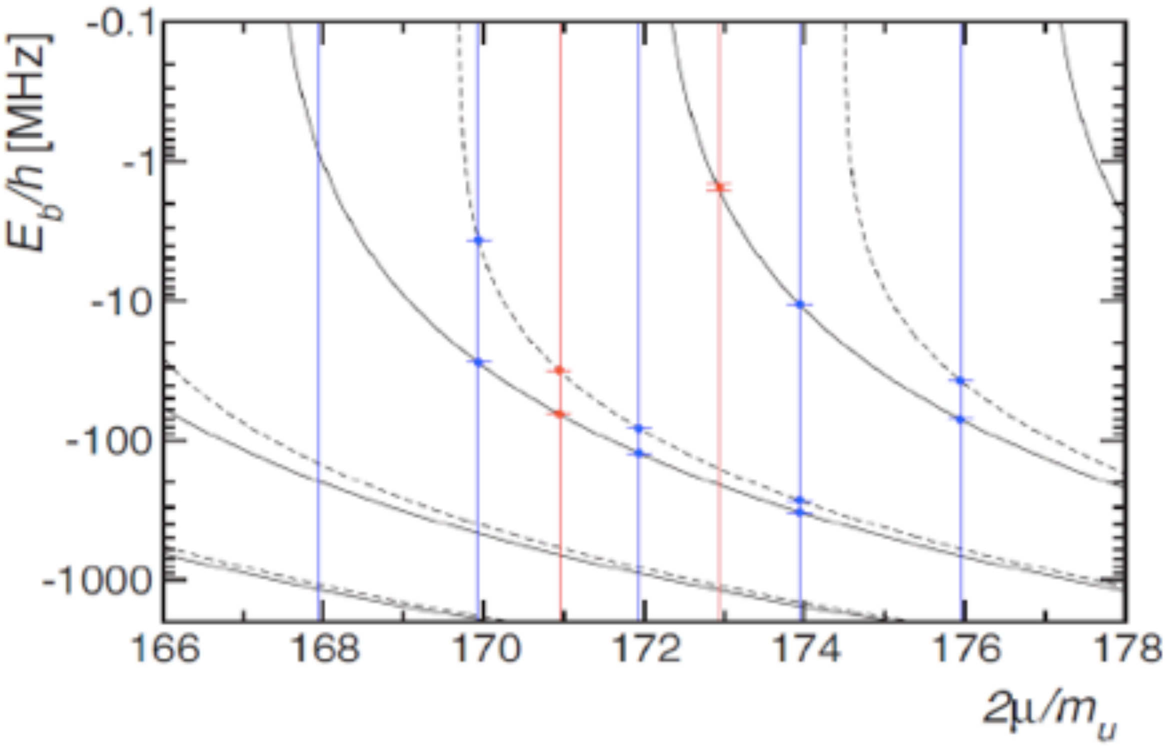

Lenard-Jones-type Potential

$$V(r) = \frac{C_{12}}{r^{12}} - \frac{C_6}{r^6} - \frac{C_8}{r^8} - \frac{GM_1M_2}{r}\left(1+\alpha e^{-r/\lambda}\right)$$

$\Delta f = 1\mathrm{kHz}$

$|\alpha| <\sim 10^{20}$

@1 nm

$C_6=1931.7\ E_h a_0^6$, $C_8=1.93\times10^6\ E_h a_0^8$, $C_{12}=1.3041\ E_h a_0^{12}$

中性子科学 (学際領域)

物質・材料研究

Diffraction

λ=0.1-10nm

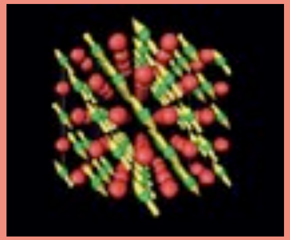

Spectroscopy

ΔE<100meV　　$t>10^{-13}$s

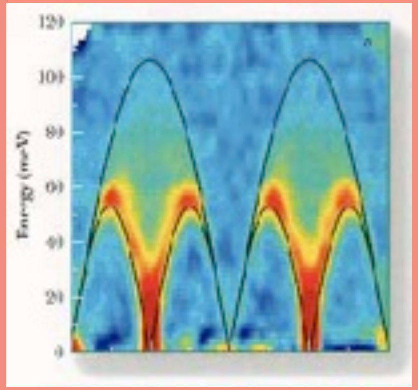

産業応用

Radiography

Residual Stress

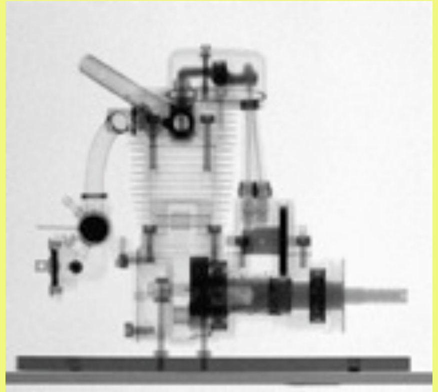

中性子光学

Optics

Detectors

Signal Processing

Electric Dipole Moment

$$\delta_{NEW} = \frac{\Delta O_{NEW}}{O_{SM}} = \frac{\alpha}{\pi}\left(\frac{M}{\tilde{M}}\right)^2$$

Decay

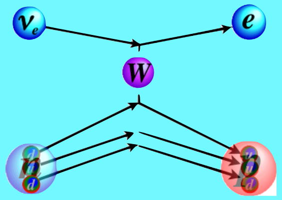

Gravity

基礎物理学

技術革新の原動力

理工連携による静電加速器の更新と量子線研究の展開について

理学研究科・工学研究科

名古屋大学加速器駆動型中性子源(2015)

NUANS
Nagoya University Accelerator-driven Neutron Source

素粒子物理学　精密測定を通じた標準理論を超える新物理研究の基盤

工学的研究　産業製品の非破壊検査

実用材料の評価

鉄鋼材料のミクロおよびメゾスケールでの評価と高性能化

教育　学生が先端研究に直接触れる機会を提供

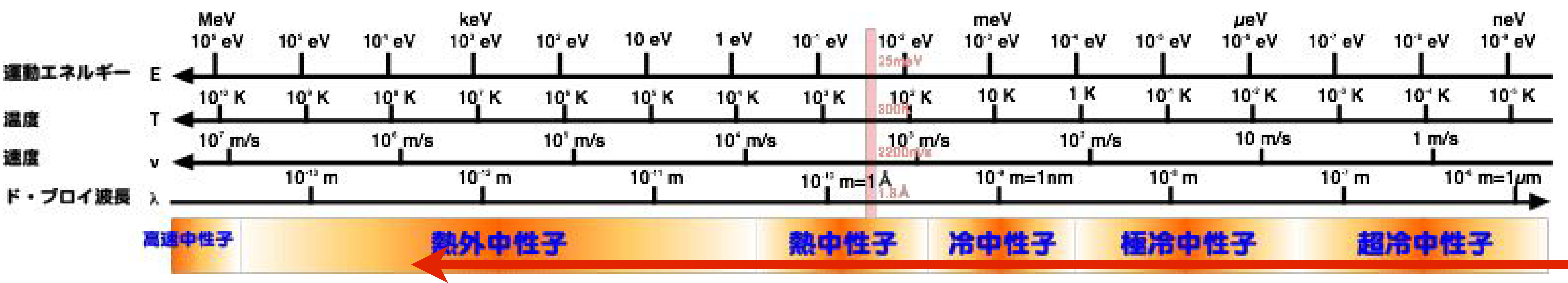

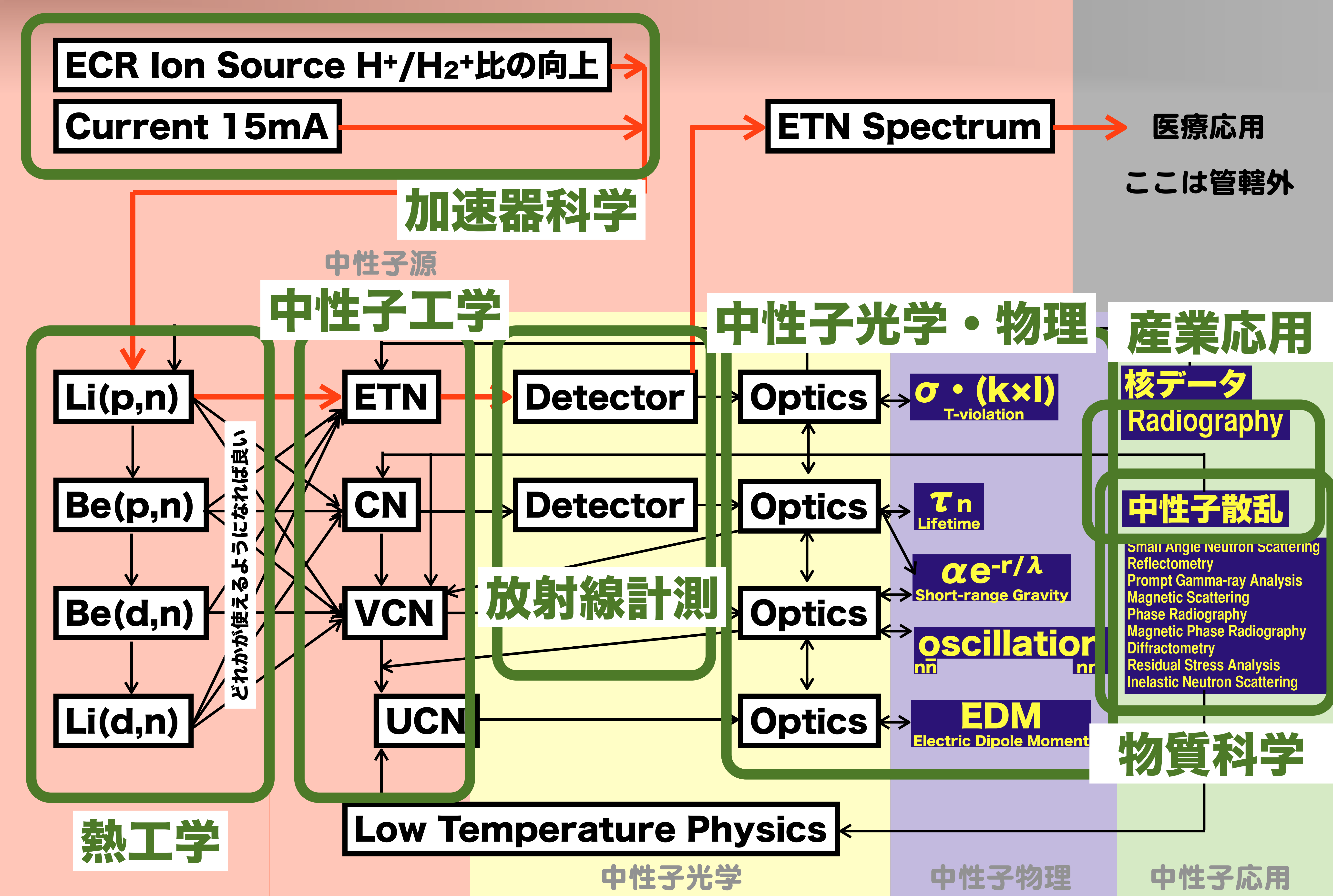

ECR Ion Source H+/H2+比の向上
Current 15mA
加速器科学
ETN Spectrum
医療応用
ここは管轄外
中性子源
中性子工学
中性子光学・物理
産業応用
Li(p,n)
Be(p,n)
Be(d,n)
Li(d,n)
どれかが使えるようになれば良い
ETN
CN
VCN
UCN
Detector
Detector
放射線計測
Optics
Optics
Optics
Optics
σ・(k×I)
T-violation
τn
Lifetime
αe-r/λ
Short-range Gravity
oscillation
nn
nn
EDM
Electric Dipole Moment
核データ
Radiography
中性子散乱
Small Angle Neutron Scattering
Reflectometry
Prompt Gamma-ray Analysis
Magnetic Scattering
Phase Radiography
Magnetic Phase Radiography
Diffractometry
Residual Stress Analysis
Inelastic Neutron Scattering
物質科学
熱工学
Low Temperature Physics
中性子光学
中性子物理
中性子応用

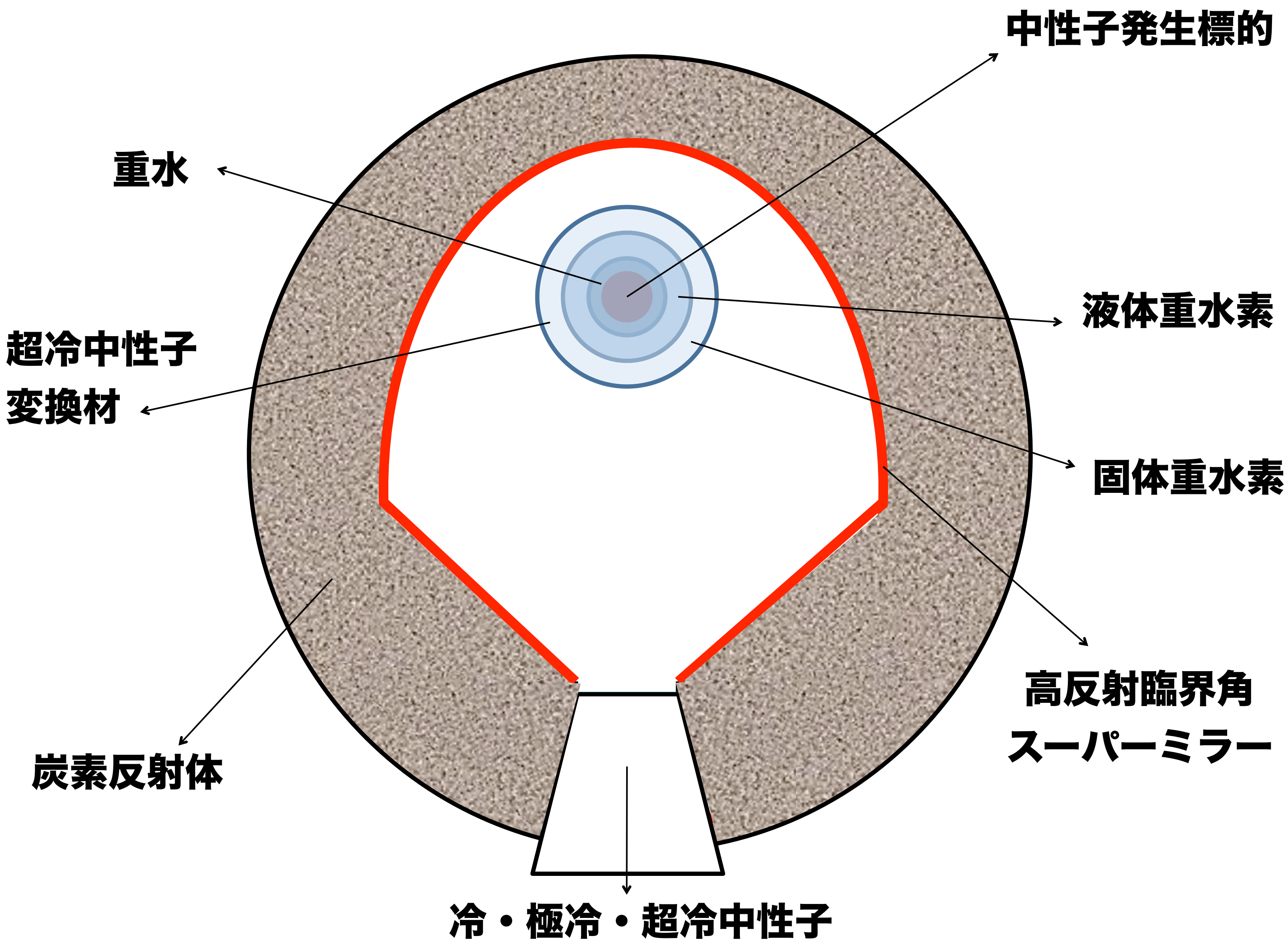
中性子発生標的
重水
液体重水素
超冷中性子
変換材
固体重水素
高反射臨界角
スーパーミラー
炭素反射体
冷・極冷・超冷中性子

寿命、β崩壊角相関

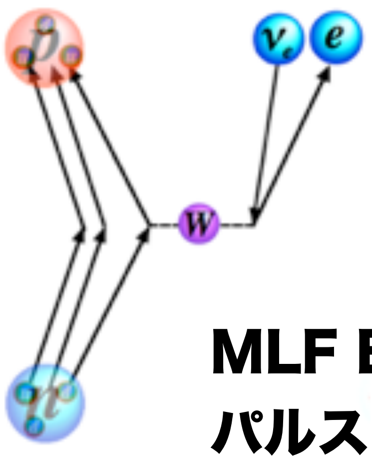

中性子寿命測定の精度向上 <10^{-3}

UCN蓄積法とIn-flight法で6σのずれ

宇宙バリオン密度の観測値がビッグバン元素合成理論と矛盾 (2σ)

MLF BL05 で測定進行中 (現状〜10^{-2})

パルス中性子＋TPCによる入射強度同時測定　**ビーム増強、DAQ・解析高度化で 10^{-3}へ**

崩壊電子非対称度（A項）で CKM Unitarity 検証

ニュートリノ非対称度（B項）の電子エネルギー依存性から新物理

崩壊陽子測定手法の開発

複合核によるTの破れ

s波p波干渉でT非対称が増幅　P非対称では10^6の増幅率

nEDMの上限に対応

$$\left|\Delta\sigma_{\mathrm{T}}^{nA}\right| < 2.5\times10^{-4}[\mathrm{b}]\times\kappa(J)$$

EDMより高感度で新物理探索

増幅率はκ(J)に依存 → κの大きい原子核を探す

MLF BL04 で測定進行中　(n,γ)でκを評価可能

新物理が非対称度に与える効果の理論計算

熱外中性子制御・偏極、標的核種偏極

結晶nEDM

非中心対称性結晶内電場での回折の際のスピン回転を精密測定

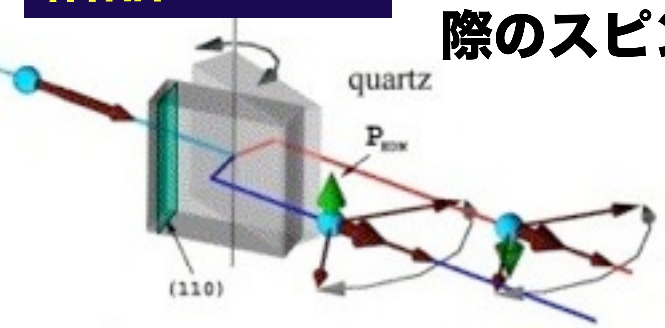

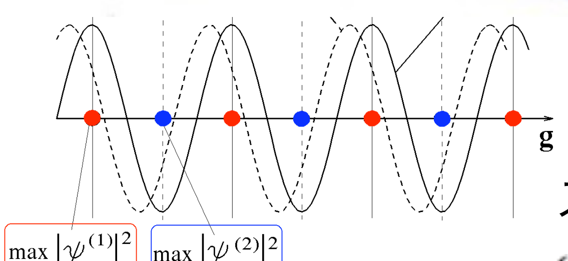

EDM測定感度

$$(\Delta d_n)_{\mathrm{stat}} = \frac{\hbar/2}{\alpha ET\sqrt{N}},$$

E〜10^9 V/cm　T〜$10^{-3\sim-2}$ s

ET はUCN法と同程度

E〜10^4 V/cm　T〜10^3 s

スピン回転

$$\varphi = \varphi_{\mathrm{S}} + \varphi_{\mathrm{EDM}} = \frac{2E\mu_n L v_{\parallel}}{c\hbar v_{\perp}} + \frac{2Ed_n L}{\hbar v_{\perp}}$$

高電場・大型結晶でUCN法の上限に迫る

結晶の作成・評価　SiO_2→BGO→PWO

Schwinger効果評価、磁場環境整備、スピン解析

重力

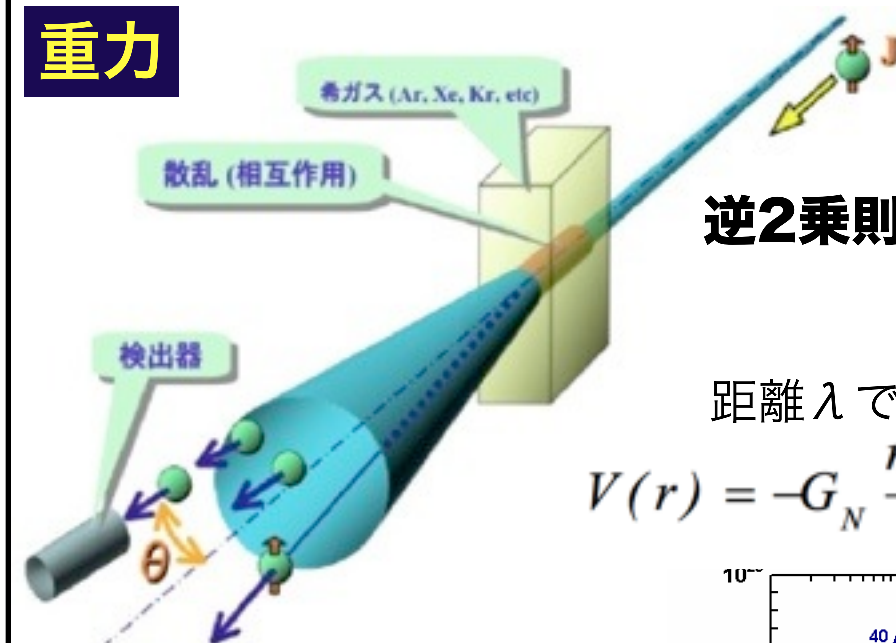

希ガス原子核の重力による散乱の逆2乗則からのずれを探索

距離λで大きさαの短距離力

$$V(r) = -G_N\frac{m_1 m_2}{r}\left(1+\alpha\cdot e^{-\frac{r}{\lambda}}\right)$$

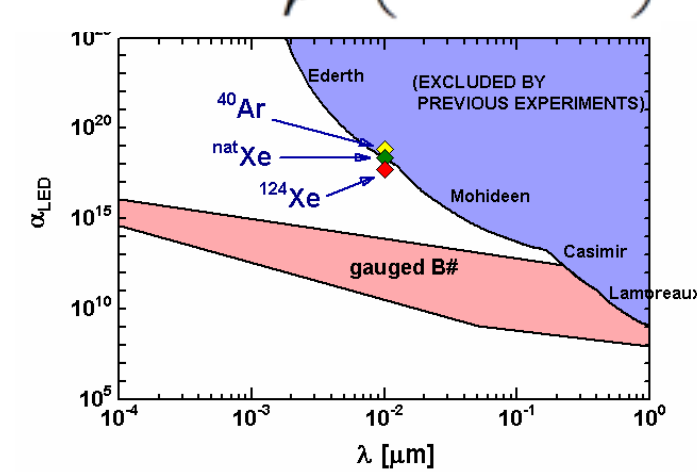

余剰次元などモデル計算

ターゲット容器からの散乱の抑制・評価、ビーム集光

核データの高精度化

etc.

Gravity

Dabbs et al., Phys. Rev. 139 (1965) B756

g_{loc} = 9.7974 m s^{-2}

g = 9.74±0.03 m s^{-2}

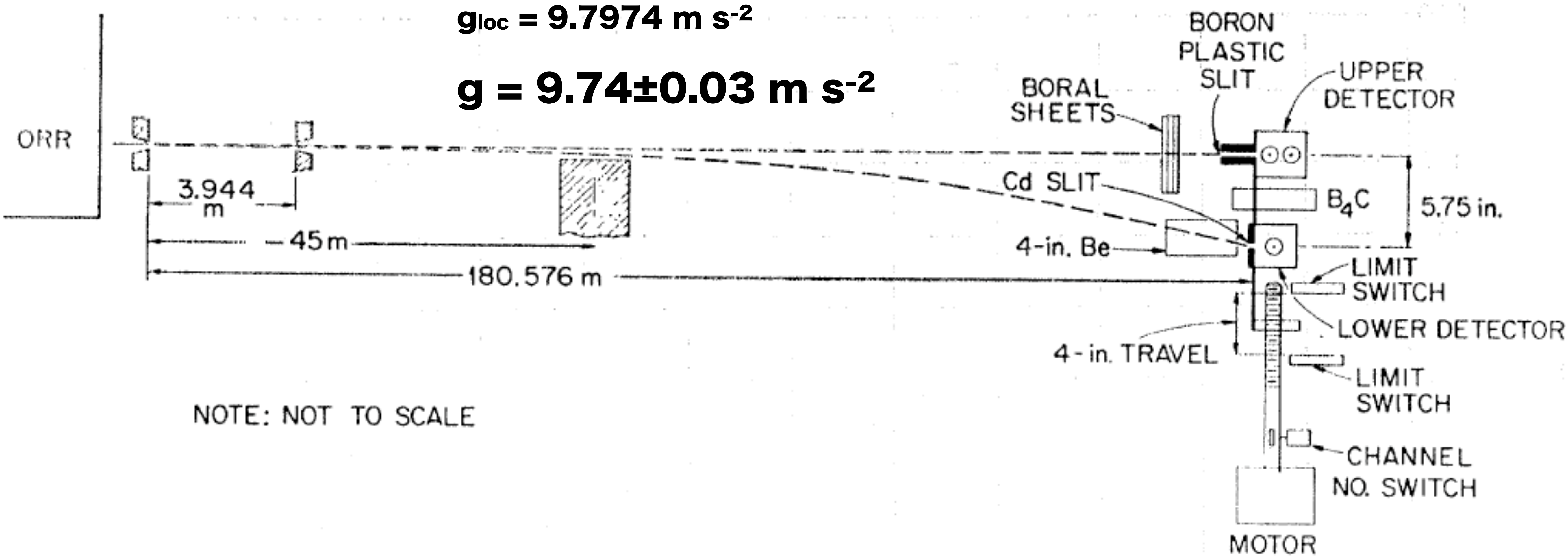

Gregoriev et al., Proc. 1st Int. Conf. Neutr. Phys., Kiev, 1 (1988) 60

g = 9.801±0.013 m s^{-2}

g_{loc} = 9.814 m s^{-2}

McReynolds, Bull. Am. Phys. Soc. 12 (1967) 105

$|\Delta g| < 5\times10^{-13}\, g_0 \qquad g = g_0 + \Delta g\,(\sigma \cdot g)$

Gravity

Collela, Overhauser, Werner, Phys. Rev. Lett. 34 (1975) 1472

λ=0.1445nm

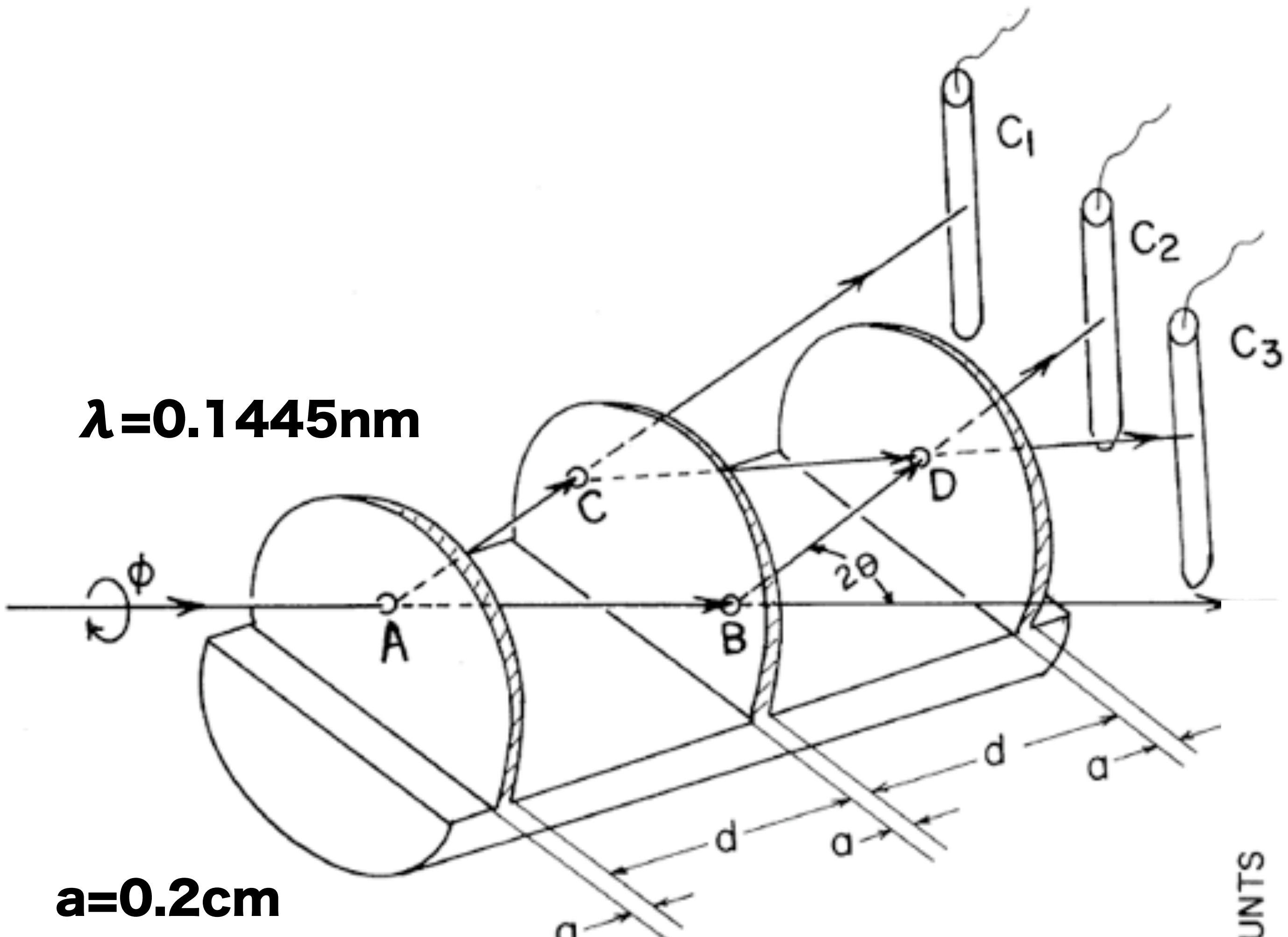

a=0.2cm

d=3.5cm

θ=22.1°

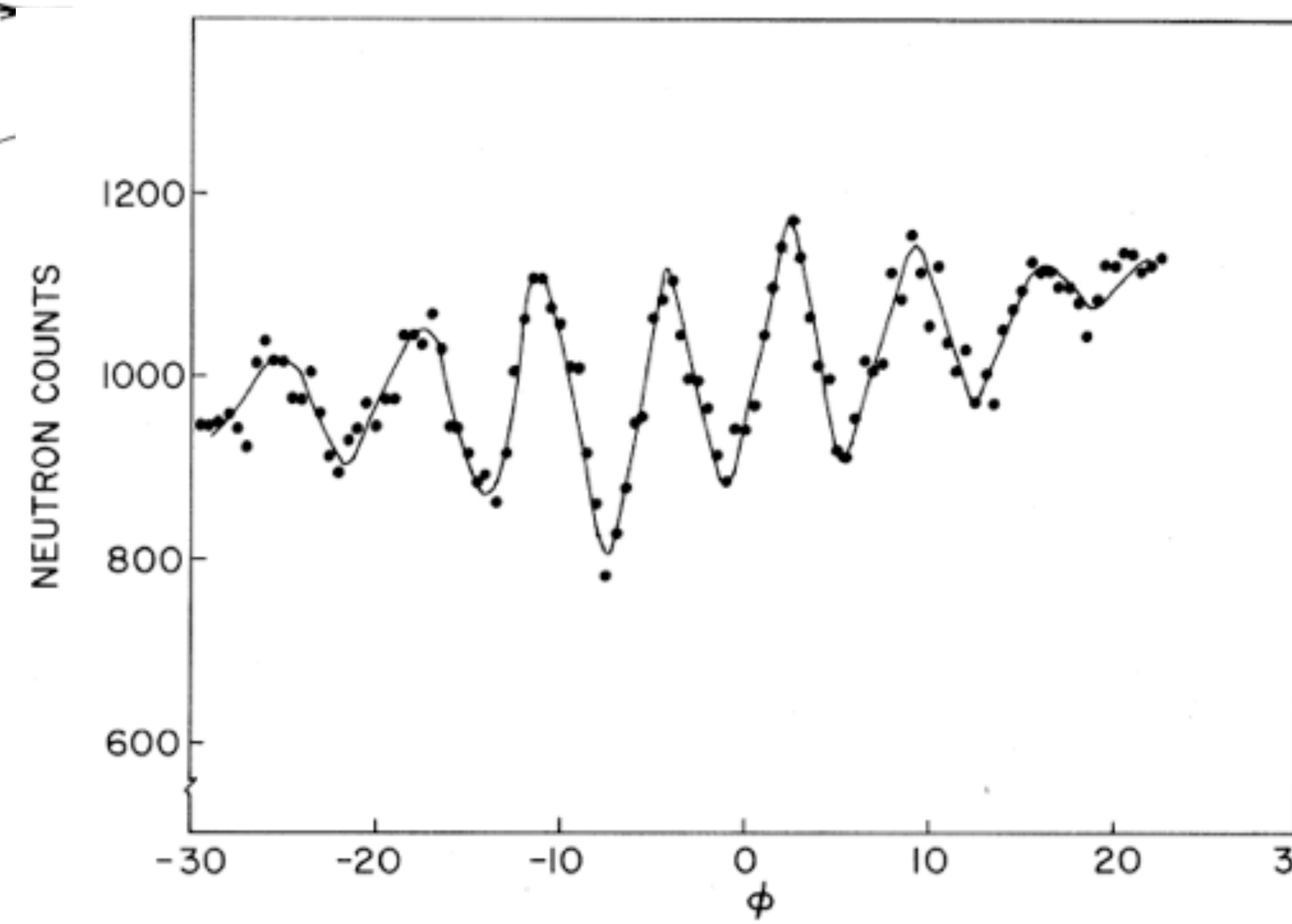

Mass

Greene et al., Phys. Rev. Lett. 56 (1986) 819

$n+p \Rightarrow d+\gamma$ (crystal diffraction)

$m_n = 1.008664919(13)$ amu

$m_n c^2 = 939.56564(28)$ MeV

Spin

1/2 direct observation of Stern-Gerlach effect

C.G.Shull, (1969) Int. Neutron Physics School, Slushta, 1969, p.325, JINR 3-4981, Dubna, 1970

スピノル性 (4π-periodicity)

Kraan, Europhys. Lett. 66 (2004) 164

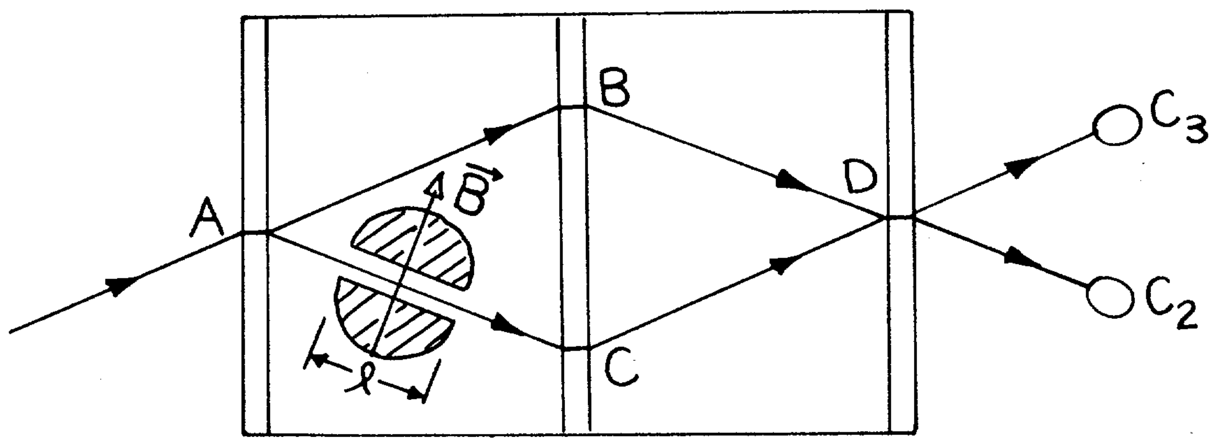

FIG. 1. A schematic diagram of the neutron interferometer. On the path AC the neutrons are in a mag netic field B (0 to 500 G) for a distance l (2 cm).

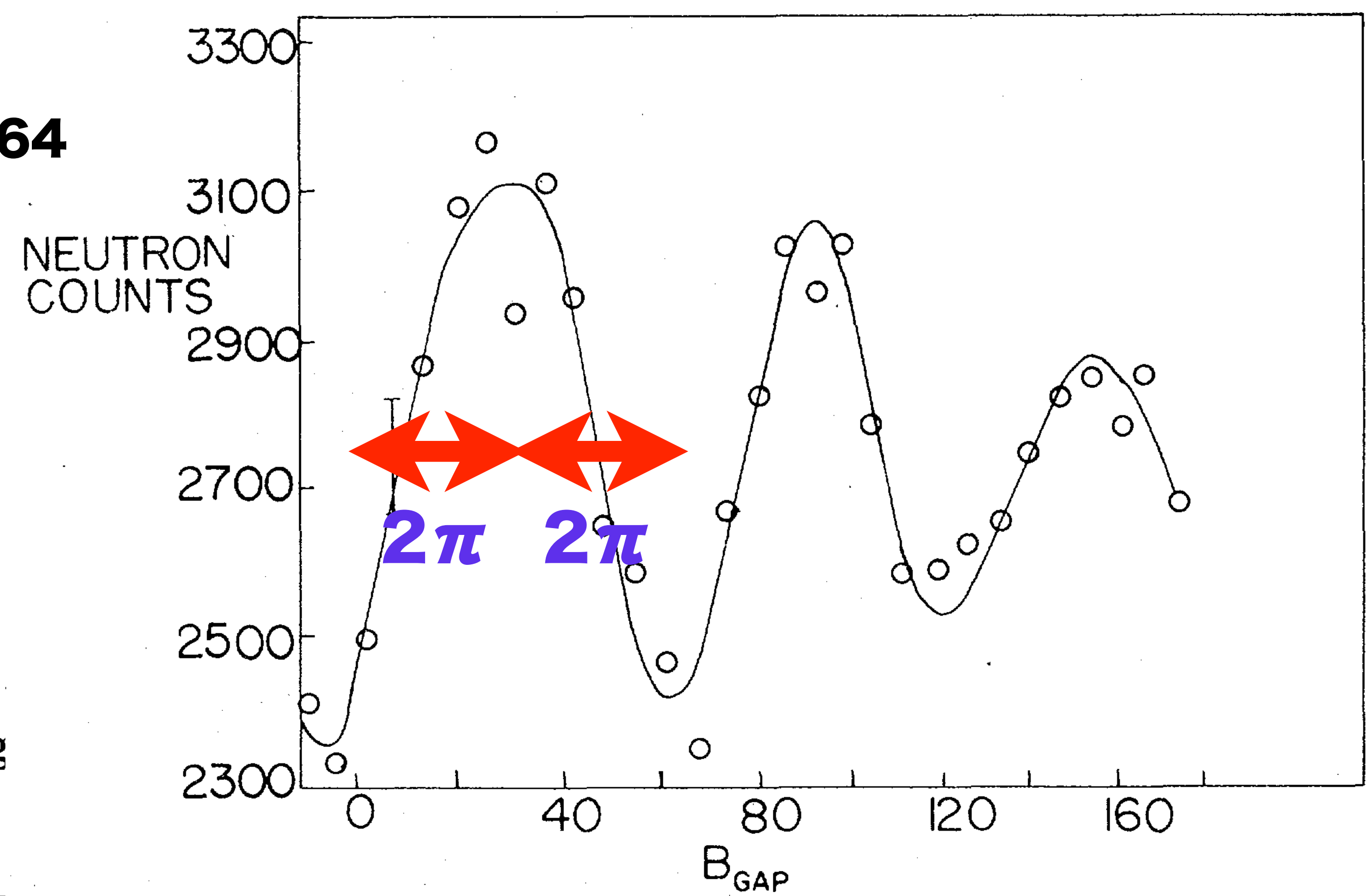

β-decay

$$\frac{d\Gamma}{dE_e d\Omega_e d\Omega_\nu} = \frac{(G_F V_{ud})^2}{(2\pi)^5}(1+3\lambda^2)p_e E_e E_\nu^{\,2}$$

$$\times\left[1+a\frac{\vec{p}_e\cdot\vec{p}_\nu}{E_e E_\nu}+b\frac{m_e}{E_e}+\frac{\langle\vec{J}\rangle}{J}\cdot\left[A\frac{\vec{p}_e}{E_e}+B\frac{\vec{p}_\nu}{E_\nu}+D\frac{\vec{p}_e\times\vec{p}_\nu}{E_e E_\nu}\right]\right]$$

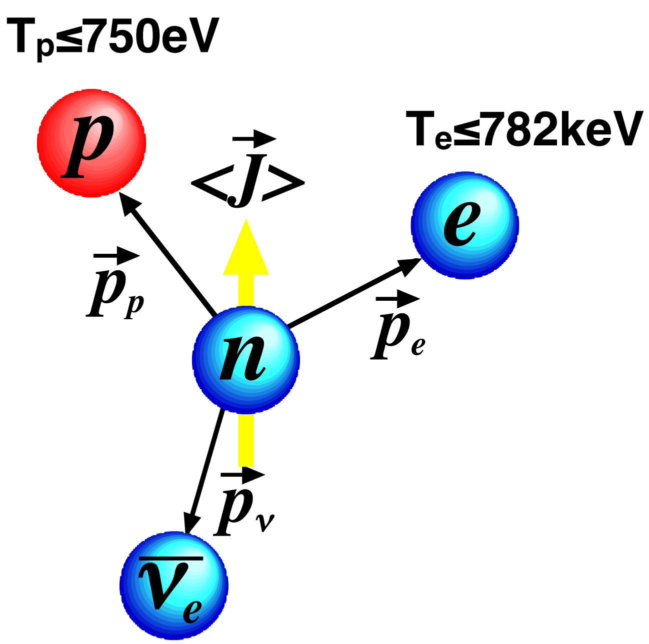

$$V_{ud}^2 = \frac{K/\ln 2}{G_F^2(1+\Delta_R^V)(1+\lambda^2)f(1+\delta_R)\,\tau_n}$$

$|V_{ud}|=0.97418\pm0.00027$

$$\lambda = \frac{G'_A}{G'_V}$$

$G'^2_A = G_A^{\,2}(1+\Delta_R^A)$

$G'^2_V = G_V^{\,2}(1+\Delta_R^V)$

$f(1+\delta_R)=1.71489\pm0.00002$

(PDG2008)

$$\lambda = |\lambda|\,e^{-i\phi}$$

$|\lambda|=1.2695\pm0.0029$

$\phi=(180.06\pm0.07)°$

τ_n	mean lifetime	$\tau_n=885.7\pm0.8$ s
$a=\dfrac{1-\lvert\lambda\rvert^2}{1+3\lvert\lambda\rvert^2}$	electron-neutrino correlation	$a=-0.103\pm0.004$
$A=-2\dfrac{\lvert\lambda\rvert\cos\phi+\lvert\lambda\rvert^2}{1+3\lvert\lambda\rvert^2}$	electron asymmetry	$A=-0.1173\pm0.0013$
$B=-2\dfrac{\lvert\lambda\rvert\cos\phi-\lvert\lambda\rvert^2}{1+3\lvert\lambda\rvert^2}$	neutrino asymmetry	$B=0.9807\pm0.0030$
$D=2\dfrac{\lvert\lambda\rvert\sin\phi}{1+3\lvert\lambda\rvert^2}$	T-odd	$D=(-4\pm6)\times10^{-4}$

Magnetic Moment

$\mu_n = -1.9130427 \pm 0.0000005\ \mu_N$

Schwinger scattering

原子核の電場を横切る際に受ける散乱

相互作用ハミルトニアン

ローレンツ変換により中性子には磁場が見えている

$$H' = -\boldsymbol{\mu}\cdot\boldsymbol{B} = \frac{\mu}{mc}\boldsymbol{\sigma}\cdot(\boldsymbol{E}(\boldsymbol{r})\times\boldsymbol{p})$$

$$\boldsymbol{E}(r) = -\nabla\left(\frac{Ze}{r} - \int d^3r'\frac{e\rho(r')}{|\boldsymbol{r}-\boldsymbol{r}'|}\right)$$

核電場　　電子による遮蔽

Born近似

$$f_{\mathrm{Schw}} = -\frac{m}{2\pi\hbar^2}\int d^3r\, e^{-ik'\cdot r}H'e^{ik'\cdot r} = -\frac{\mu_n}{2\pi\hbar^2 c}\sigma\cdot\int d^3r\, e^{-ik'\cdot r}\boldsymbol{E}(r)\times\left(\frac{\hbar}{i}\nabla\right)e^{ik'\cdot r}$$

$$f_{\mathrm{Schw}}(\boldsymbol{q}) = i\frac{2e\mu_n}{\hbar c}(Z - F(q))\frac{\boldsymbol{\sigma}\cdot(\boldsymbol{k}\times\boldsymbol{q})}{q^2}$$

$$F(\boldsymbol{q}) = \int \rho(\boldsymbol{q})e^{i\boldsymbol{q}\cdot\boldsymbol{r}}d^3r$$

形状因子

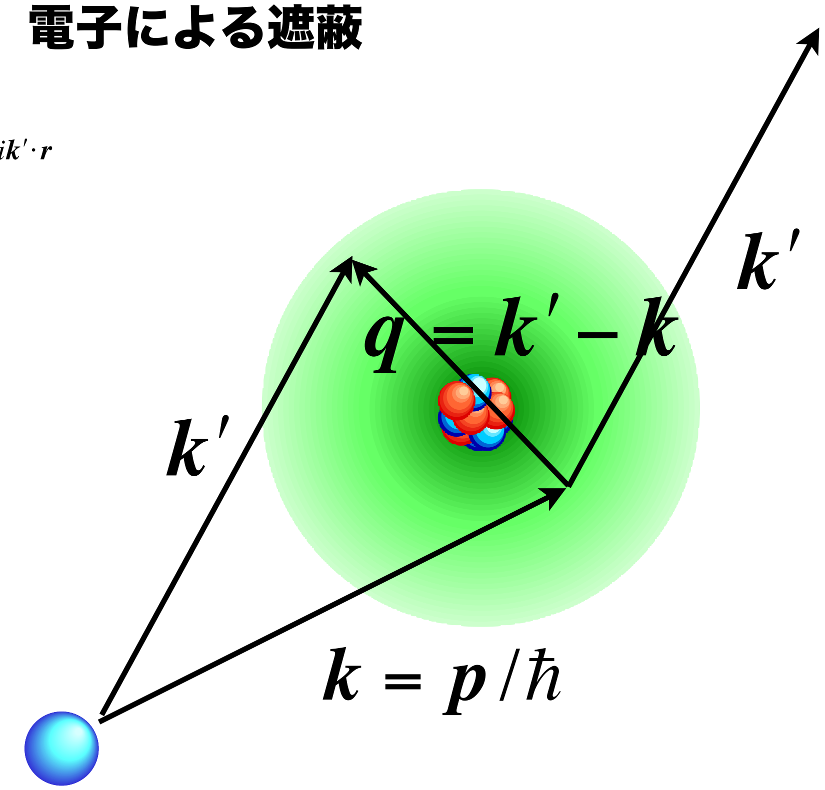

Electric Dipole Moment

$|d_n| < 2.9\times10^{-26}$ e cm (90%CL)

Baker et al., PRL97 (2006)131801

$$\hbar\omega = -2\vec{\mu}_n \cdot \vec{B} - 2\vec{d}_n \cdot \vec{E}$$

P-odd T-odd

T-odd observable
in a static system
→ T-violation

⇕ CPT theorem

CP-violation

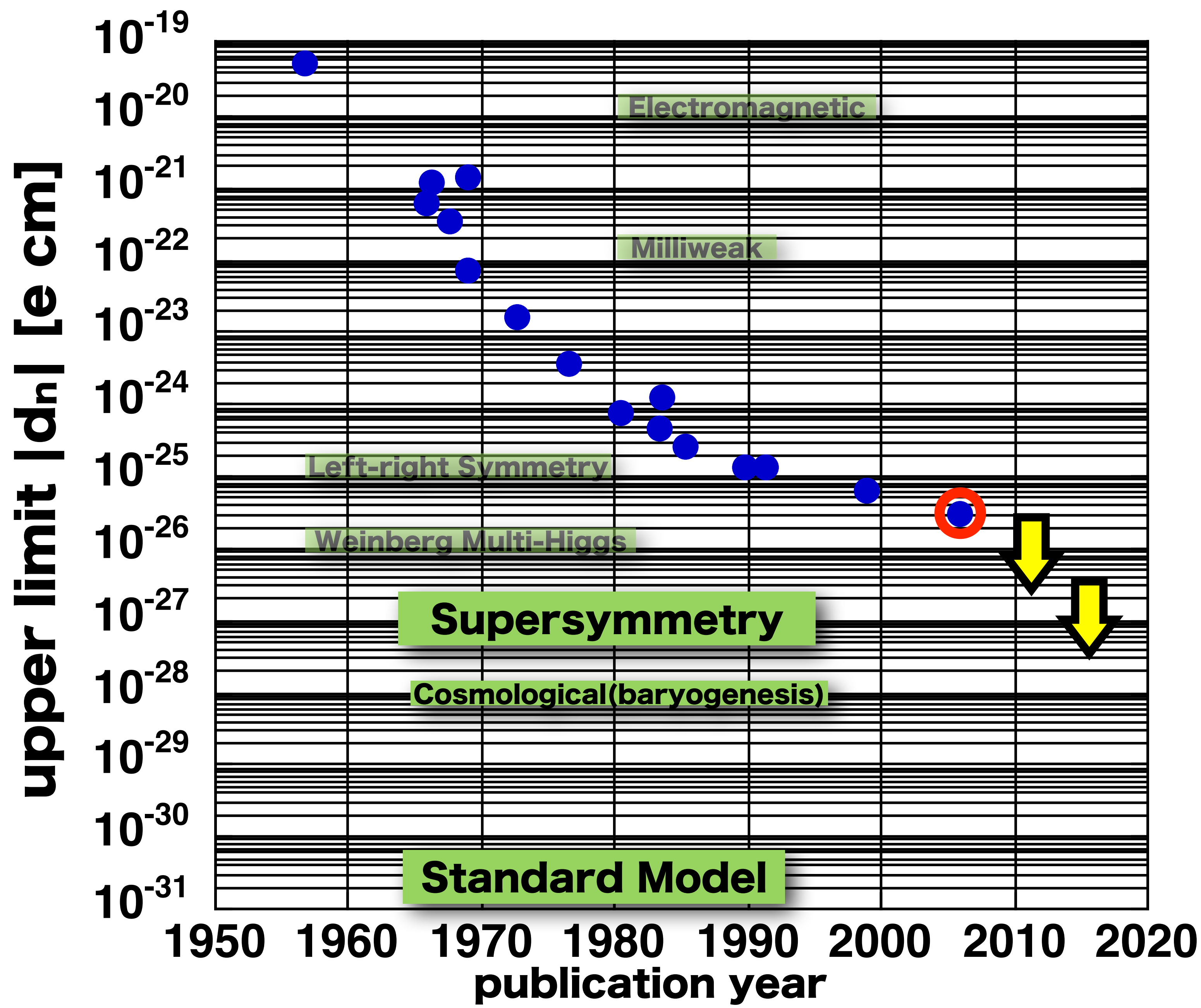

Electric Charge

$q_n = (-0.4 \pm 1.1) \times 10^{-21}$ e

Baumann et al., PRD37(1988)3107

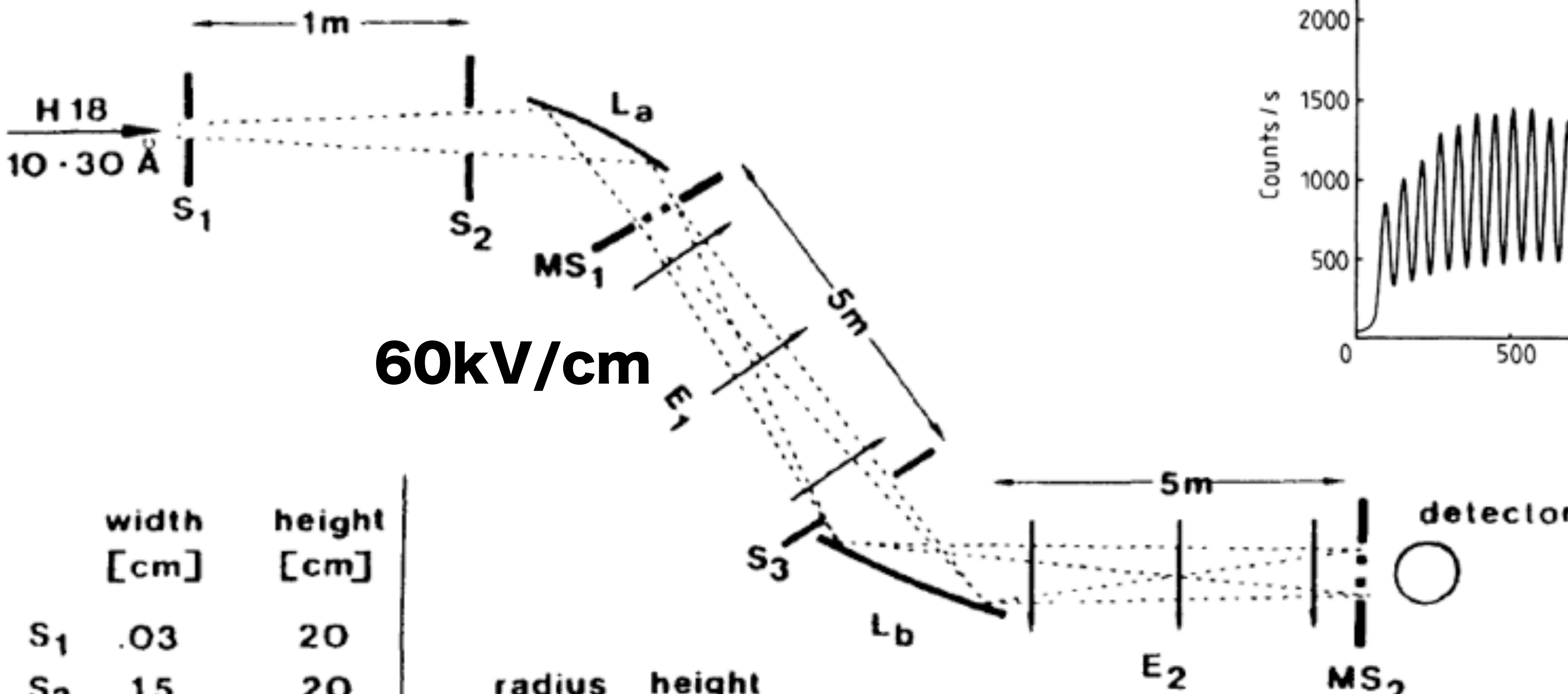

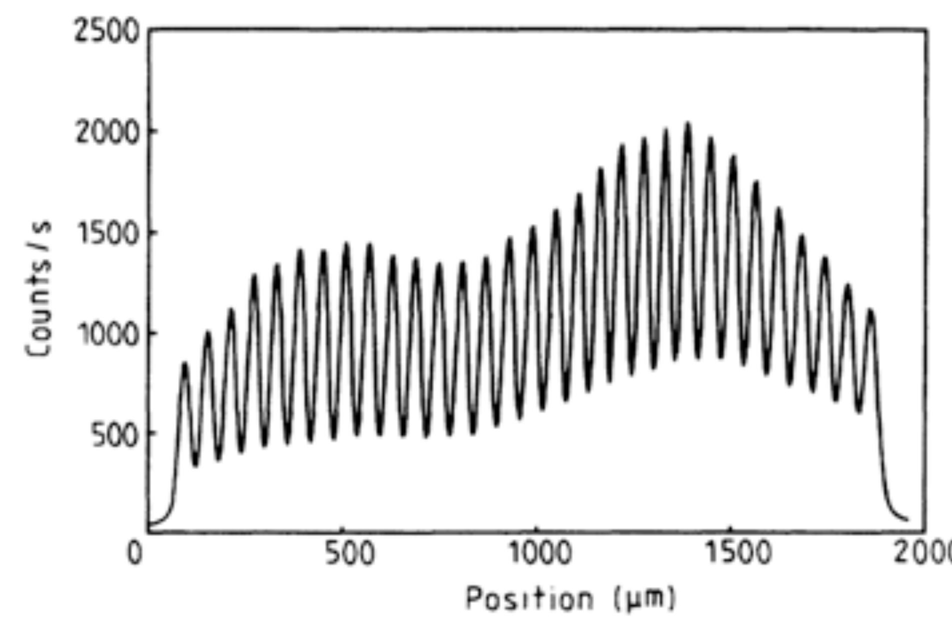

	width [cm]	height [cm]
S_1	.03	20
S_2	.15	20
MS_1	.003	20
S_3	.12	30
MS_2	.002	40

	radius [m]	height [cm]
L_a	80	20
L_b	200	30

$|q_n| < 2 \times 10^{-18}$ e

Littleton and Bondi, Proc. R. Soc., A252(1959)313, A257(1960)442

Conservation Laws and Equality of Charges

Feinberg, Goldhaber, Proc. Nat. Acad. Sci. USA 45(1959)1301

$$\sum_i Q_i = \text{constant in time}$$
$$\sum_i B_i = \text{constant in time}$$
$$\sum_i L_i = \text{constant in time}$$

これらが保存するなら

$$\begin{cases} Q_i' = a_1 Q_i + b_1 B_i + c_1 L_i \\ B_i' = a_2 Q_i + b_2 B_i + c_2 L_i \\ L_i' = a_3 Q_i + b_3 B_i + c_3 L_i \end{cases}$$

これらも保存する

Q_γ=0 because of p+p→p+p+γ

Q=0	Q=Qp	Q=Qn
$\gamma\ (p+p \to p+p+\gamma)$	p	n
$\pi^0\ (p+p \to p+p+\pi^0)$	$\Sigma^+\ (\Sigma^+ \to p+\pi^0)$	$\lambda^0\ (\lambda^0 \to n+\pi^0)$
$K_1^0\ (K_1^0 \to 2\pi^0)$		$\Sigma^0\ (\Sigma^0 \to \lambda^0+\gamma)$
$K_2^0\ (K_2^0 \to \pi^+ + \pi^- + \pi^0)$		$\theta^0\ (\theta^0 \to \lambda^0+\pi^0)$

Electromagnetic Structure

Mean-square Charge Radius

$$\langle r_n^2 \rangle = -0.1161 \pm 0.0022\ \mathrm{fm}^2$$

Electric Polarizability

$$\alpha = (11.6 \pm 1.5) \times 10^{-4}\ \mathrm{fm}^3$$

Magnetic Polarizability

$$\beta = (3.7 \pm 2.0) \times 10^{-4}\ \mathrm{fm}^3$$

Neutron Electron Interaction

$$a_{ne} = (-1.49 \pm 0.05) \times 10^{-3}\ \mathrm{fm}$$

$$\sigma(\theta) = \left| a + Zf\left(\frac{\sin\theta}{\lambda}\right) a_{ne} \right|^2$$

Nucleon Scattering Lengths

neutron-proton scattering length

$$a_{np}=-23.516(13)\ \mathrm{fm}$$

proton-proton scattering length

$$a_{pp}=-17.25(16)\ \mathrm{fm}$$

neutron-neutron scattering length

$$a_{nn}=(-18.5\pm0.4)\ \mathrm{fm} \qquad d(\pi^-,\gamma)2n$$

Antineutron

annihilation

$n\bar{n} \longrightarrow \pi(95\%), K(5\%)$

$(4.8 \pm 0.2)\pi$ (200-250MeV)

total cross-section for all inelastic processes (E_{pbar}=450MeV)

$p\bar{p}$ 105mb $n\bar{p}$ 115mb

cross-section for annihilation process

$p\bar{p}$ 85mb $n\bar{p}$ 75mb

nuclear enhancement

	reaction	annihilation
Cu	1260±90 mb	1040±60 mb
Pb	3000±250 mb	2010±180 mb

Neutron Oscillation

free neutron $\tau_{n\bar{n},\text{free}} > 8.6\times 10^{7}\,\text{s (CL} = 90\%)$

$$L = \bar{\psi} M \psi$$

$$\psi = \begin{pmatrix} n \\ \bar{n} \end{pmatrix} \qquad M = \begin{pmatrix} E_0 & c^2\delta m \\ c^2\delta m & E_0 \end{pmatrix}$$

$$|n_{1,2}\rangle = \frac{1}{\sqrt{2}}\left(|n\rangle \pm |\bar{n}\rangle\right) \qquad m_{1,2} = m_n \pm \delta m$$

$$I(t) = I(0)\sin^2 \frac{c^2\delta m}{\hbar} t$$

in (magnetic) field

$$M = \begin{pmatrix} E_0 + \Delta E & c^2\delta m \\ c^2\delta m & E_0 - \Delta E \end{pmatrix}$$

$$|n_1\rangle = \cos\theta|n\rangle + \sin\theta|\bar{n}\rangle$$
$$|n_2\rangle = \sin\theta|n\rangle - \cos\theta|\bar{n}\rangle$$

$$\Delta E = \mu_n B$$

$$\tan\theta = \frac{c^2\delta m}{\Delta E + \sqrt{\Delta E^2 + (c^2\delta m)^2}}$$

$$m_{1,2} = m_n \pm \sqrt{\frac{\Delta E^2}{c^4} + \delta m^2}$$

$$I(t) = I(0)\frac{c^4\delta m^2}{c^4\delta m^2 + \Delta E^2}\sin^2 \frac{\sqrt{c^4\delta m^2 + \Delta E^2}}{\hbar} t$$

$$\frac{\Delta E\tau}{\hbar} = \frac{\mu_n BL}{v\hbar} < 1$$

bound neutron $\tau_{n\bar{n},\text{bound}} > 1.3\times 10^{8}\,\text{s (CL} = 90\%)$